MONITORING THE LEVELS OF TOXIC METALS OF ATMOSPHERIC PARTICULATE MATTER IN THE RUSTENBURG DISTRICT

Nnenesi Anna Kgabi
BSc Ed., BSc Hons., MSc

Thesis submitted in fulfillment of the requirements for the degree Philosophiae Doctor in Environmental Science at the NORTH-WEST UNIVERSITY

Promoter: Prof. JJ Pienaar (North-West University)
Co-promoter: Prof. M Kulmala (University of Helsinki, Finland)

June 2006

ACKNOWLEDGEMENTS

I am greatly indebted to my promoter (Prof. Jacobus Pienaar) and co-promoter (Prof. Markku Kulmala) for the support and guidance throughout the project. The moral support and encouragement from the staff members in the Faculty of Agriculture, Science and Technology, particularly Prof. Simeon Taole, Mr Solomon Makgamathe, Mrs Ramokone Gopane, Mr Leonard Gopane and Mr Fezile Vuthela are greatly acknowledged. I acknowledge Mr Eric Sjoberg for encouragement and support and for believing in me from the beginning of the project.

The financial support of the Finnish Environmental Institute (SYKE) and the National Research Foundation (NRF) is greatly acknowledged.

The understanding and encouragement from my husband and children, and from my parents are acknowledged. Lastly, thanks to the almighty God, for His divine guidance, protection, wisdom, knowledge, understanding, and for the courage and strength.

EBEN-EZER!!!

DECLARATION

I, Nnenesi Anna Kgabi hereby declare that the Thesis for the degree Philosophiae Doctor in Environmental Science at the North-West University hereby submitted has not previously been submitted by me for a degree at this or any other university, that it is my own work in design and execution, and that all material contained herein has been duly acknowledged.

ABSTRACT

Ambient air quality has been monitored in South Africa for the last four decades using a variety of methods. There is however, no agreed method and system in function to monitor the levels of heavy metals in ambient air in South Africa.

The objective of this study was to determine the concentration levels of toxic metals (Cr, Ni, V, and Pb) of air particulate matter in the mining areas of the North-West Province, and to suggest an air particulate monitoring method and sampling system.

A comprehensive literature study was conducted on aerosol dynamics, the effects of PM on humans and the environment, and the existing monitoring methods used worldwide. The literature review showed that large variations in concentration levels can be observed under different meteorological conditions, and that meaningful source apportionment can be achieved by performing chemical analysis of the trace element component of particulate matter. The South African situation with regard to monitoring of particulate matter herein studied, suggested the need for the development of characterisation methods for particulate matter.

The concentration levels of air particulate matter PM10 were determined using Tapered Element Oscillating Microbalance (TEOM). The hourly concentrations of PM10 were measured in the range from 13.12 to 215.7 $\mu g.m^{-3}$, the daily levels from 10.3 to 151.7 $\mu g.m^{-3}$ and the monthly levels from 22.2 to 131.0 $\mu g.m^{-3}$. The concentrations of the oxides of trace metals were found from analysis by Scanning Electron Microscopy coupled with Energy Dispersive Spectrometry (SEM-EDS), to be in the range of 0.03 – 3.8 $\mu g.m^{-3}$ for Cr, 0.01 – 0.03 $\mu g.m^{-3}$ for Ni, 0.00 – 0.02 $\mu g.m^{-3}$ for V and 0.00 – 0.24 $\mu g.m^{-3}$ for Pb. The monthly concentrations of the toxic trace metals of particulate matter measured using

Inductively Coupled Plasma Mass Spectroscopy (ICP-MS), were in the range of 0.03 – 5.2 $\mu g.m^{-3}$ for Cr, 0.03 – 2.8 $\mu g.m^{-3}$ for Ni, 0.01 – 0.05 $\mu g.m^{-3}$ for V and 0.02 – 0.5 $\mu g.m^{-3}$ for Pb. ICP-MS was shown to be a relevant characterisation tool for particulate aerosols. Sources of metals of particulate matter within the Rustenburg area were successfully apportioned (using correlation and regression analysis, and principal component analysis) in order of decreasing abundance as soil dust, mining industry, traffic and biomass burning, unknown sources, other industries and smelting.

A comparative assessment of the efficiency and relevance of the sampling and analysis methods used in this study was performed. The efficiency of the type of filter media used, the frequency of sampling, the sampling period, the meteorology and the locations of the sampling sites used were assessed.

Recommendations were made that the monitoring procedure and system of air particulate matter in the North-West province and South Africa at large, should not be based only on determining the hourly, daily and annual levels of particulate matter for compliance with air quality standards but should also include determination of the chemical and physical properties of atmospheric pollutants, estimation of the emitting sources, and evaluation of health effects on the exposed community as well as assessment of the environmental impacts. The approved sampling and analysis methods for the province should be comprehensive for both the polluter and the air pollution authorities, and specific and relevant to the type of pollutants within the province.

LIST OF ACRONYMS

Acronym	Description
PM	Particulate matter
PM10	Particulate matter with an aerodynamic diameter of 10 μm and less
PM2.5	Particulate matter with an aerodynamic diameter of 2.5 μm and less
GPC	Gas-to-particle conversion
EF	Enrichment Factor
WHO	World Health Organization
USEPA	United States Environmental Protection Agency
IARC	International Agency for Research on Cancer
EIA	Environmental Impact Assessments
TEOM	Tapered Element Oscillating Microbalance
SEM/EDS	Scanning Electron Microscopy coupled with Energy Dispersive Spectrometry
ICP-MS	Inductively Coupled Plasma Mass Spectroscopy
PCA	Principal Component Analysis
CCN	Cloud Condensation Nuclei
DMPS	Differential Mobility Particle Sizer
CAPCO	Chief Air Pollution Control Officer
SPM	Suspended particulate matter
TSP	Total suspended particulate matter
SE	Secondary electron
BSE	Back scattered electron
PMT	Photomultiplier tube
SAWS	South African Weather Services
APCEL	Asia Pacific Centre for Environmental Law
ETAAS	Electrothermal Atomic Absorption Mass Spectroscopy
ACCU	Automatic Cartridge Collection Unit
NIOSH	National Institute for Occupational Safety and Health

LIST OF FIGURES

LIST OF TABLES

TABLE OF CONTENTS

CHAPTER 1

INTRODUCTION

.....

This chapter gives the background of the research project. The concept of particulate matter, its sizes, sources and classes are discussed. The problem statement, as well as the objectives of this study is outlined. The study area is briefly discussed as part of the background to the problem.

.....

Air pollution is one of the major environmental problems in the North West Province of South Africa, particularly in the mining and mineral smelter areas such as Rustenburg, Madibeng and Klerksdorp. Mining operations and mining dump dust is also a health hazard.

1.1 GENERAL OVERVIEW OF PARTICULATE MATTER

Particulate matter (PM) is a complex mixture of multicomponent particles of which the size distribution, composition, and morphology can vary significantly in space and time (Khlystov, 2001). The particulate matter is composed of tiny, airborne solid or liquid particles other than pure water (Ministry of water, land and air protection, 2002). It includes naturally occurring dust, as well as soot, smoke and other particles emitted by vehicles, power plants, factories, construction and other human activities.

PM is emitted directly from sources such as internal combustion engines and coal combustion, and is also formed in the atmosphere from gaseous precursors. A number of activities are known to generate substantial quantities of particulates in the form of uncontrolled emissions. Such sources include mineral extraction and stockpiling, landfill sites, materials handling

operations and long-term construction operations (Directorate of corporate and environmental services, 2000). Elevated levels of metals (Na, Pb, Cd, and Se) and by-products of petroleum combustion (S, Ni, V) are normally found in the emissions of oil-fuelled plants (Watson & Chow, 2001).

Combustion of fossil fuels is also known to generate particulate matter. PM is mainly composed of carbon species, condensed acidic species and trace elements (Lee *et al.*, 2002). Many metal smelters emit significant amounts of heavy metals into the atmosphere. Lead for instance, occurs in the atmosphere mainly in the particulate form (in the fine particle fraction), but a small part occurs in vapour as organic lead compounds (European environment agency, 1996).

Particulate matter (PM) can be classified as primary and secondary particles. Primary particles are the direct products from combustion processes while secondary particles are a result of the physical and chemical reactions in the atmosphere (Directorate of corporate and environmental services, 2000). Primary particulates are emitted directly into the atmosphere from man-made and natural sources.

The problem of metal concentrations in dust deposition became important with the advent of high temperature processes like smelting and fossil fuel combustion. The major source of crustal elements (e.g. Al, Si, Ca, Ti, and Fe) is the wind-blown dust suspended from construction sites, roads and natural surfaces. Heavy metals originate from a variety of industrial processes such as incineration, manufacturing, and smelting (Pinto & Lester, 1998).

Major components of PM include sulphate, nitrate, ammonium and hydrogen ions, trace elements (including toxic and transition metals), organic material, elemental carbon (or soot) and crustal components (Khlystov, 2001). PM can also consist of at least 160 organic compounds and 20 metals (Ag, As, Ba, Be, Dc, Ce, Cr, Co, Cu, Fe, Mn, Nd, Ni, Pb, Sb, Se, Sr, Ti, V and Zn) (Los Alamos national laboratory, 2003).

Particulate matter (PM) can also be classified according to particle size into fine particulate matter, referred to as PM2.5, and coarse particulate matter or PM10. These two types of particulates differ in chemical composition, source and behaviour in the air. The fine fraction, PM2.5, contains particulates of a diameter of 2.5 micrometers or smaller. PM2.5 is most often generated by combustion processes and by chemical reactions taking place in air (Pinto & Lester, 1998). PM10 does not stay in the air for too long. On the contrary, particulates in the fine fraction PM2.5, can remain in the air for days to weeks and are therefore harmful to humans. They can penetrate deeply into the lungs, and cause lung problems and permanent lung damage. In general, the smaller and lighter a particulate is, the longer it will stay in the air. A fairly dense particulate such as lead dust is likely to stay in the air for a shorter period of time than other particulates. A number of potentially harmful substances have been found in PM2.5. Several studies have shown that toxic trace metals such as nickel, lead and cadmium are more concentrated in PM2.5 than in PM10.

Large gaps exist in understanding the nature, effects, and control of ambient particulate matter. Lack of understanding of the interactions of ambient PM with water limits our ability to estimate their atmospheric lifetimes and transport distances (Khlystov, 2001). Once the particulate matter is emitted into the atmosphere, it ceases to exist as a single particle, but rather exists as an atmospheric aerosol. Aerosols are two-phase systems, consisting of the particles and the gas in which they are suspended (Hinds, 1999; Meszaros, 1981). Aerosols are also referred to as suspended particulate matter, aerocolloidal systems, and dispersed systems. An aerosol particle can be described as a single continuous unit of solid or liquid containing many molecules held together by intermolecular forces and primarily larger than molecular dimensions (> 0.001μm) (Seinfeld & Pandis, 1998).

Aerosols occur in both the troposphere and the stratosphere. Once in the atmosphere, aerosols are transported by prevailing winds and convection, thus the elements contained in aerosols are seldom redeposited on the earth

surface in the same location that they were produced. In the case where air is the gaseous medium in which aerosols of different composition and size are suspended, an aerosol system exists, according to Hidy and Brock, (1970), if (a) the sedimentation velocity of the particles is small; (b) inertial effects during particle motion can be neglected (the ratio of inertial forces to viscous forces is small); (c) the Brownian motion of the particles, due to the thermal agitation of gas molecules is significant, and (d) the surface of the particles is large compared to their volume (Meszaros, 1981).

The sedimentation velocity determines the lifetime of a particle in the system. For a particle with radius *r*, greater than the mean free path of gas molecules, the falling velocity is given by the Stokes equation

$$V_s = \frac{2}{9} \frac{r^2 \rho_p g}{\mu} \qquad (1.1)$$

where *r* is the radius and ρ_p the density of the particle (assumed spherical), μ is the dynamic gas viscosity ($\mu = 1.8 \times 10^{-4}$ poise at temp T = 20°C), and g is the gravitational constant.

The Reynolds number (Re) of particles gives the ratio of inertial forces to viscous forces:

$$\frac{\rho v R}{\mu} = \mathrm{Re} < 1 \qquad (1.2)$$

where ρ is the air density, v is the speed of the particle motion caused by some external force, and R is the radius of the particle (Meszaros, 1981).

Each aerosol species is formed in the atmosphere separately by different processes and they are mixed together to form particles of mixed composition. Aerosols, in general, consist of sulphates, nitrates, sea-salt, mineral dust, organics and carbonaceous components (Sateesh, 2002).

Most aerosol particles in the nucleation mode comprise of sulphuric compounds, and are the result of the oxidation of sulphur containing precursor gases like SO_2, H_2S, CS_2, COS, CH_3SCH_3 and CH_3SSCH_3 to sulphate (SO_4^{2-}) and subsequent condensation into particles (homogeneous gas to particle conversion (GPC)). However, these sulphate particles are highly mobile and subject to coagulation. Much of the sulphate aerosols produced by GPC end up occupying the 0.1 – 1.0μm size range.

Insoluble aerosols act as foreign bodies stimulating defence reactions, e.g. crystalline silica (quartz) which is relatively toxic to cells. Soluble aerosols are easily transferred to blood and other parts of the body, e.g. relatively toxic lead and cadmium. The molecular form (e.g. oxidation state) is very important in metal-containing aerosols (Hameri, 2004).

When aerosols are in low concentration or far from its source, considerable modification of the composition is possible. The degree of enrichment of trace elements in aerosols is given by an enrichment factor EF (Brimblecombe, 1996). The concentration of a given element C_x is related to a reference element

$$EF(Na)_x = \frac{\left(\frac{C_x}{C_{Na}}\right)_{air}}{\left(\frac{C_x}{C_{Na}}\right)_{sea}} \qquad (1.3)$$

for aerosols of marine origin.

$$EF(Al)_x = \frac{\left(\frac{C_x}{C_{Al}}\right)_{air}}{\left(\frac{C_x}{C_{Al}}\right)_{crust}} \qquad (1.4)$$

for aerosols of continental (crustal) origin.

1.2 STATEMENT OF THE PROBLEM

The World Health Organization (WHO) has identified particulate pollution as one of the most important contributors to ill health (World resources institute, 1999). Numerous studies suggest that health-threatening effects can occur at particulate levels that are at or below the levels permitted under national and international air quality standards. According to the WHO, no evidence so far shows that there is a threshold below which particulate pollution does not induce some adverse health effects, especially for the more susceptible populations.

The acids and toxic trace elements found in fine PM have been linked to a few known illnesses in humans and research animals. It has been suggested that the extremely small size of the fine PM promotes efficient entry and adherence to the lungs and the toxicity of the particles are mainly responsible for inflicting damage to the organ (Lee *et al.*, 2002). PM2.5 is considered more critical in PM-related health impacts than PM10 and the secondary particle formation in PM2.5 is extremely complex. The constituents in small particulates also tend to be more chemically active and may be acidic as well, and therefore more damaging.

Adverse health effects reported to be associated with PM can be linked to increased daily and annual mortality rates in adults. These include cardiopulmonary disorders, symptoms of respiratory dysfunction (e.g. wheeze, cough), asthma attacks, pneumonia, bronchitis, and chronic obstructive pulmonary disease (USEPA, 1996a). Cardiovascular mortality was significantly associated with CO, NO_2, SO_2, PM2.5, PM10-2.5 and elemental carbon. Factor analysis revealed that both combustion-related pollutants and secondary aerosols are associated with cardiovascular mortality (Mar *et al.*, 2000).

Fine particulate matter is linked with all sorts of health problems from a runny nose and coughing, to bronchitis, emphysema, asthma, and even death. Heavy metals, chromium and nickel in particular, have been defined by the International Agency for Research on Cancer (IARC) as potential cancer causing agents (USEPA, 1996b).

A better understanding of the chemical constituents of ambient particles is fundamental in bridging the knowledge gap between the air quality and its health effects. Characteristics of airborne particulate matter associated with health hazards are the size distribution and mass concentration.

PM sources vary in importance not only from one mine to another, but also from one time to another at the same mine (Myers, 1998). Less is known about the particle surface composition. There are, therefore, serious concerns about how best to control ambient concentrations of PM.

Ambient air quality has been monitored in South Africa for the last four decades using a variety of methods. There is, however, no agreed method and system in function to monitor the levels of heavy metals in ambient air in South Africa. According to the state of the environment report of the North West Province (2002), the existing data are sourced from project-specific air quality studies, usually undertaken as specialist studies in Environmental Impact Assessments (EIA) or as compliance monitoring by a particular industry (Muller & Mangold, 2002). Due to the problem of data availability, the need for direct quantification of air pollutants in the North West Province is highlighted as a priority issue. There is, therefore, a need for the determination of the concentration levels of toxic metals (chromium, nickel, vanadium, lead) of the particulate matter in the North West Province.

1.3 STUDY AREA

The area chosen for this study is the Rustenburg municipal area located at $25^{0}39'00''S$ and $27^{0}13'59''E$. Rustenburg is one of the biggest mineral

producing districts in South Africa. According to Viljoen & Reimold (1999), South Africa produces 68.3% of the world's chromium ores and roughly 86% of the chrome ores are mined within the Rustenburg mining area. A map showing the villages and mines in the area is given in Figure 1.1.

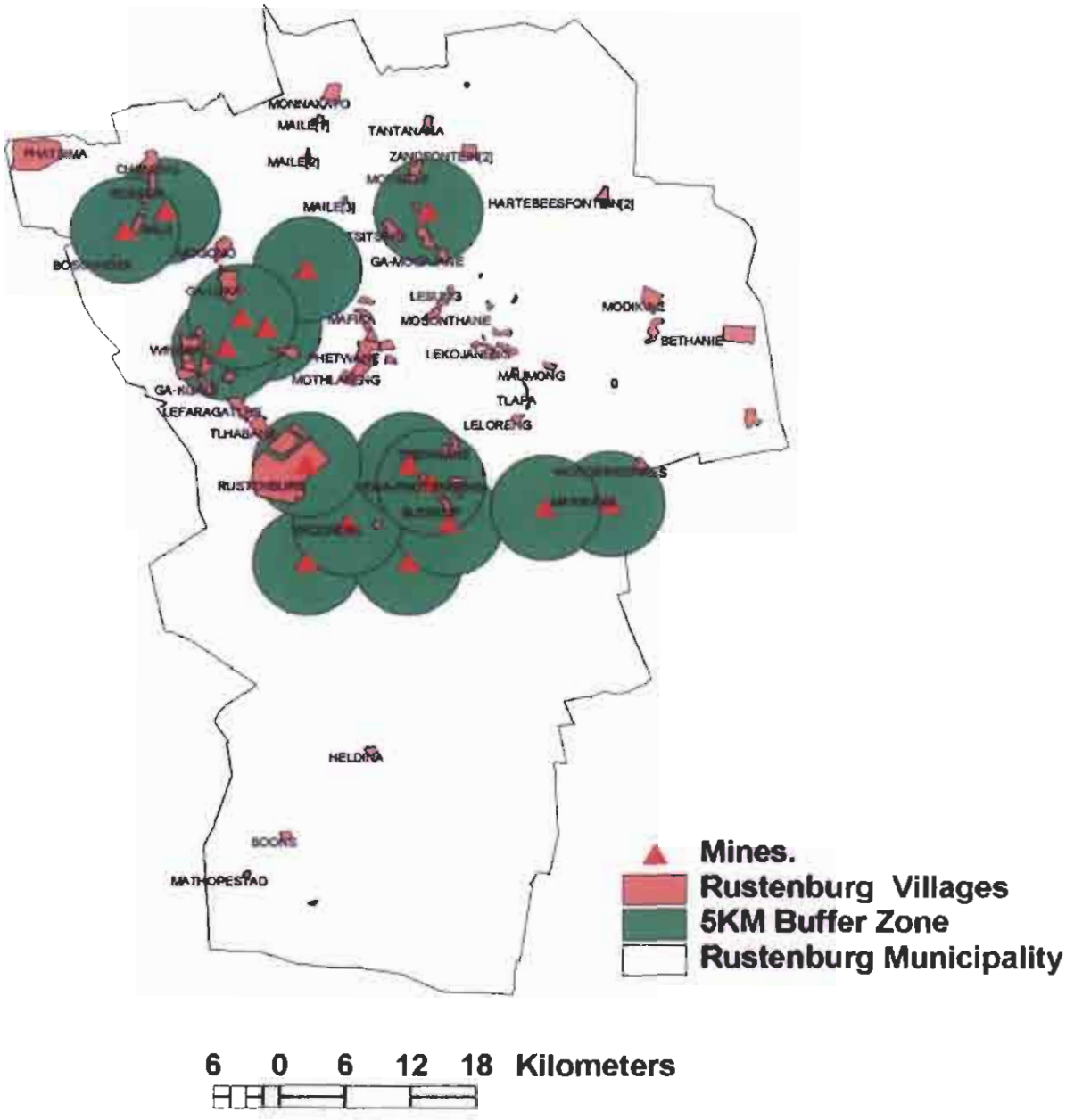

Figure 1.1: *Mines and villages around the Rustenburg municipality*

Most of the villages are just a walking distance (less than 5km) away from the mines. It is therefore expected that the mines and smelters in the area contribute to the emissions into the environment, which affect human health in the area.

The types of mining activities as well as the products mined in this area, as shown in Table 1.1, also give an indication of the type of pollutants that can be found in the area. Mining and smeltering of platinum and ferrochrome is associated with emissions of toxic trace metals that consist mainly of chromium, nickel, vanadium, and lead. These emissions can also be in the form of sulphates and nitrates in the atmosphere.

Table 1.1: *The location of mines and smelters, and the types of mining activities in the Rustenburg area*

Latitude	Longitude	Commodity	Major	Minor
25.703299	27.446100	PGM, Cr, Au, Ni	PGM, Cr, Au, Ni	
25.540600	27.196400	PGM, Cu, Co, Au, Ni	PGM, Cu, Co, Ni	Au
25.666699	27.250000	PGM, Cu, Co, Ni	PGM, Cu, Co, Ni	
25.699999	27.500000	PGM, Cu, Co, Ni	PGM, Cu, Co, Ni	
25.449999	27.350000	V, Fe	V, Fe	
25.681699	27.352200	Pt, Cr, Au, Ni, Cu, Os, Ir	Pt	
25.500000	27.250000	Pt, Cu, Ni, Pd	Pt, Cu, Ni	
25.466699	27.100000	Pt	Pt	Os, Ir, Au, Ni, Cu, Cr
25.449999	27.133299	Pt	Pt	Pd
25.566700	27.183299	Pt, Pd, Ni, Ag, Au	Pt, Pd	Ni, Ag, Au
25.550000	27.216699	PGM, Au, Cu, Ni	PGM	Au, Cu, Ni
25.666699	27.333300	PGM, Pt, Pd, Ru, Au, Rh, Os, Ir, Ni	PGM, Pt, Pd	Ru, Au, Rh, Os, Ir, Ni
25.716699	27.283300	Cr, PGM, Fe, Si	Cr	PGM, Fe, Si
25.716699	27.366700	Cr, PGM, Fe, Si	Cr	PGM, Fe, Si
25.750000	27.333300	Cr, PGM, Fe, Si	Cr	PGM, Fe, Si
25.750000	27.250000	Cr, PGM, Fe, Si	Cr	

1.4 OBJECTIVE OF THE STUDY

The main objectives of this study are to determine the concentration levels of toxic metals (Cr, Ni, V, Pb) of air particulate matter in the mining areas of the North West Province, to suggest an air particulate monitoring method and sampling system and lastly to apportion the sources of toxic metals of air particulate matter in the Rustenburg municipality of the North West province.

Specific objectives of this study include to:

- Determine the mass concentrations of air particulate matter (in micrograms per cubic meter) using Tapered element Oscillating Microbalance (TEOM), which is a continuous real time monitor;
- Collect atmospheric particulate matter on filters for analysis;
- Determine the physical and chemical composition of the samples collected using Scanning Electron Microscopy coupled with Energy Dispersive Spectrometer (SEM-EDS);
- Determine the elemental composition of the collected samples using Inductively Coupled Plasma Mass Spectroscopy (ICP-MS), which is capable of detecting cations in low concentrations of up to a few parts per billion;
- Identify and quantify the sources of toxic metals using correlation and regression, and principal component analysis (PCA).

.....

The problem of scarcity of data on the levels and composition of particulate matter (PM), the need for monitoring methods and standards, and the health hazards of toxic trace metals of PM discussed above, suggest that a literature study be conducted on aerosol dynamics, the effects of PM on man and the environment, and the existing monitoring methods used worldwide.

.....

CHAPTER 2

LITERATURE STUDY

This chapter gives a discussion of the formation and growth of atmospheric aerosols, the properties, the health and radiation effects of aerosols on human beings, monitoring of particulate matter, and some previous studies on monitoring of particulate matter.

2.1 FORMATION AND GROWTH OF ATMOSPHERIC AEROSOLS

The extent to which human beings and the environment are affected by emissions from both natural and anthropogenic sources depends on the formation, growth, size, motion, deposition, and electrical properties of atmospheric aerosols. This section highlights the processes of aerosol formation, growth, and removal in the atmosphere.

Aerosols are usually assigned to one of the following three size categories, which relate to their production mechanisms. These are the aitken particles, or nucleation mode: (0.001 - 0.1 μm radius), the large particles, or accumulation mode: (0.1 - 1 μm radius) and the giant particles, or coarse particle mode: (> 1 μm radius). The terms nucleation mode and accumulation mode refer to the mechanical and chemical processes by which aerosol particles in those size ranges are usually produced. The smallest aerosols, in the nucleation mode, are principally produced by gas-to-particle conversion (GPC), which occurs in the atmosphere. Aerosols in the accumulation mode are generally produced by the coagulation of smaller particles and by the heterogeneous condensation of gas vapour onto existing aerosol particles (NSDL, 2006). These generalities apply best to secondary aerosols (those produced by

precursor gases, condensation and other atmospheric processes) rather than to primary aerosols (those injected into the atmosphere as particles from the surface of the earth).

The formation and growth of atmospheric aerosols have recently received growing experimental and theoretical interest due to climate and health-related effects of fine particles. The increased aerosol concentrations are largely due to secondary particle production, i.e. homogeneous nucleation and subsequent growth from vapours (Lehtinen & Kulmala, 2003).

The freshly formed aerosols become climatically important only if they are able to grow to sizes of 50nm radius and larger. Particles that grow to above 100nm can scatter light very efficiently and thereby have a direct cooling effect on the climate.

Particles formed by the dispersal of surface materials generally have radii larger than 0.1μm. Aitken particles must be produced by condensation of vapours, preceded in many cases by gaseous chemical reactions (Meszaros, 1981). Concentration of Aitken particles is lower in winter than in summer. After sunrise, the aerosol concentration increases. This implies that particles with radii of less than 0.1μm are produced by photochemical reactions.

Due to their Brownian movement, particles with diameters of a few nanometers (nm) coagulate very efficiently with larger particles, which implies that freshly nucleated particles have to grow fairly rapidly past the 10nm limit so as not to be lost in the collision processes (Kulmala *et al.*, 2000a). Such growth is possible only if there is a supersaturated vapour present at concentrations above 10^7 molecules per cubic centimetre of air (Kulmala *et al.*, 2000b).

2.1.1 FORMATION OF AEROSOLS

Nucleation and accumulation account for the formation of most atmospheric aerosols. Aerosols in the nucleation mode are mainly produced by gas-to-particle conversion (GPC), which occurs in the atmosphere. Aerosols in the accumulation mode are generally produced by the coagulation of smaller particles and by the heterogeneous condensation of gas vapour onto existing aerosol particles (Kulmala *et al.*, 2000a).

Most mineral aerosols belong to the coarse particle mode. The residence time of aerosols depends on their size, chemistry and height in the atmosphere. Aerosols between 0.1 – 1.0μm remain in the atmosphere longer than the other two size ranges. Aerosols between 0.001 – 0.1μm are subject to Brownian motion. These particles experience collisions and coagulation that increase their size, thus removing them from the nucleation mode. Aerosols >1μm have higher sedimentation rates than the other two size ranges.

Homogeneous nucleation involves the spontaneous formation of liquid droplets directly from the gas phase, while heterogeneous nucleation occurs with aerosols having sufficient surface area (Seinfeld & Pandis, 1998). High values of supersaturation are needed e.g. S>4 for water. For chemical formation, free radical species act as nuclei upon which other molecules may interact and react chemically e.g. soot. Formation of oxides in a metallic arc may also occur e.g. in welding. Homogeneous nucleation occurs around radii of 1 nm size. Chemical reactions between various gases also result in the GPC mostly catalysed by ultraviolet radiation from the sun. Particles produced by GPC are hygroscopic (water active) and can act as cloud condensation nuclei (CCN) (Seinfeld & Pandis, 1998).

The nucleation of aerosol particles starts typically several hours after sunrise. This indicates that homogeneous nucleation can proceed at night as well, most likely in the chemical reactions of atmospheric gases and water vapour (Meszaros, 1981). During the night, fine and ultrafine aerosols are formed

mostly in catalytic reactions involving some atmospheric gases directly into the atmosphere. Nitrogen dioxide is one of such gas-precursors of aerosol. Nitrates can be formed at night in water droplets via the following sequence of reactions:

$$O_3 + NO_2 \rightarrow NO_3 + O_2, \quad k = 1.2 \times 10^{-13} e^{(-2450/T)} \tag{2.1}$$

$$NO_3 + NO_2 \leftrightarrow N_2O_5, \tag{2.2}$$

$$N_2O_5 + H_2O(aq) \rightarrow 2H^+ + 2NO_3^-, \tag{2.3}$$

The fine and ultrafine aerosols can be generated both in the presence and in the absence of solar radiation.

Particle formation events have been observed to occur quite frequently. However, the fundamental microphysical nucleation process occurring in these events has remained unknown. Mäkelä *et al.* (1997) suggested that the formation events are connected with strong visible and UV radiation and vertical mixing of boundary layer air induced by sunlight, while Kulmala *et al.* (1998a) suggested, in addition to the above, a flip-over of the vertical temperature profile.

The explanations of the ambient particle formation phenomenon usually include photochemical production of an unknown condensational vapour. The vertical mixing of the air particles is assumed either to help the thermodynamics of the nucleation processes as well as the subsequent condensation, or to introduce active precursor gases from the layers of air at different heights in the boundary layer (Seinfeld & Pandis, 1998).

Nucleation of a supersaturated vapour is most widely used in the formation of aerosols by the molecular agglomeration processes. Nuclei may consist either of groups of molecules of condensable vapour (embryos) or 'foreign'

material such as ions or dust ranging in size from a few angstroms (Å) to several microns (Hidy & Brock, 1970).

Supersaturation in a pure gas or a mixture of gases may occur due to physical processes of adiabatic expansion or mixing a cool gas with a warm gas. It may also be achieved by means of a chemical reaction.

Nucleation is a spontaneous condensation process, which is observed when a pure vapour or a component of a gas mixture exceeds the saturation condition in an unconfined space. It can, however, be observed depending on the degree of supersaturation achieved and the nature and concentration of nuclei present in the gaseous medium (Hidy & Brock, 1970).

In a pure vapour, free of dust or ions, for example, the vapour phase will become thermodynamically unstable when supersaturated. The collapse of this instability to a condition of lower energy will not take place until the supersaturation is sufficiently high to ensure that tiny particles of condensed phase will grow in time rather than re-evaporate if formed initially by a molecular scale fluctuation in the vapour.

The formation of particles is a rate process, thus a very rapid expansion, or very rapid cooling by mixing may yield very high apparent supersaturation in a gas, even though many nuclei are present.

2.1.2 GROWTH OF AEROSOLS

Condensation and evaporation involve particle growth at saturation S higher than saturation vapour pressure. The Kelvin effect shows that a curved surface influences the forces acting at the surface molecules.

$$S_{eq} = \exp \frac{4\sigma M}{\rho R D_{eq} T} \qquad (2.4)$$

where S_{eq} is the equilibrium saturation ratio, σ surface tension, M molecular weight, ρ density, D_{eq} diameter of a droplet in equilibrium and T is the temperature. Also $S_{eq} = P/P_s$ where P is the equilibrium vapour pressure at the drop surface and P_s is the equilibrium vapour pressure over a flat surface (Mäkelä *et al.*, 2000). If S in the environment is smaller than S_{eq}, the droplet evaporates or otherwise it grows. Therefore, in certain situations large particles might grow while smaller ones do not. This is applicable to transportation of aerosols in the respiratory tract.

It is important to note that the evolution towards higher particle sizes, seen in the particle size spectra during the particle formation process, is always interpreted as a particles growth process.

Particle growth can be estimated by determining the maximum size of the event mode a few hours from the start of the event and by calculating the growth rate dD_p/dt in $nm.h^{-1}$ from the evolution of maximum size of the event mode. The particle volume growth can be studied by calculating the increase of the total volume concentration of the event mode particles in $m^3.m^{-3}$ and by dividing the total volume increase by the particle number concentration in the nucleation mode, in order to obtain information on the volume change of a single particle.

The total increase in the ultrafine particle volume concentration may be interpreted as a measure of condensation. When the particle formation rate is high, there is more condensation in a given time, i.e. the amount of condensed material is larger (Seinfeld & Pandis, 1998).

The amount of visible light as well as UV-radiation has been seen to correlate with the growth of particles. It could be speculated that an increasing amount of UV-radiation increases the photochemical production of condensable species and thereby increases the particle growth. The particle formation and growth rates were seen to correlate slightly with each other.

Particle formation is usually observed in the late morning as the appearance of 3nm particles at the lower size range of the Differential Mobility Particle Sizer (DMPS) (Mäkelä *et al.*, 1997; Kulmala *et al.*, 2001a). Free-molecular condensation has been described in the past by assuming vapour molecules as point masses (Seinfeld & Pandis, 1998) and using the so-called Fuchs-Sutugin expression for the particle growth rates (Fuchs & Sutugin, 1971). The above approach has errors for particles of less than 10 nm, since it ignores the molecular dimensions in comparison to size and does not account for the particle diffusion coefficient.

The new approach uses the following equation for the collision rate of molecules with particles β_{1i}:

$$\beta_{1i} = 2\pi(d_1 + d_i)(D_1 + D_i) \cdot \frac{Kn + 1}{0.377Kn + 1 + \frac{4}{3\alpha}(Kn^2 + Kn)} \qquad (2.5)$$

which is comprised of the continuum regime condensation rate multiplied by the semi-empirical Fuchs-Sutugin interpolation function (the last term in the equation) (Lehtinen & Kulmala, 2003). The variables d_1 and d_i are the diameters and D_1 and D_i the diffusion coefficients of the condensing molecule and particle in class *i* and 1 respectively. The factor α is the mass accommodation coefficient.

To obtain correct asymptotical behaviour in the small particle limit, the Knudsen number Kn is defined as:

$$Kn = \frac{2\lambda}{(d_1 + d_i)} \qquad (2.6)$$

where the mean free path of the condensation process is:

$$\lambda = \frac{3(D_1 + D_i)}{\sqrt{\overline{C_1}^2 + \overline{C_i}^2}} \qquad (2.7)$$

where C_1 and C_i are the thermal speeds of the molecule and particle respectively. As soon as particles are formed, they grow by condensation to larger sizes, but at the same time their concentration is diminished because of collisions with other particles (coagulation). To get the correct nucleation rate from experimental data, it is essential to know the condensational growth rate in detail.

Coagulation of aerosols

Coagulation affects the size distribution of particles produced in aerosol reactors. It influences the production of particulate pollutants in flames and their elimination by electrostatic precipitators, fibrous filters, cyclones, etc. Coagulation occurs when Brownian motion, differential sedimentation or turbulent flows force two particles or drops into contact and the particles stick to form an aggregate or larger drop (Seinfeld & Pandis, 1998). Agglomeration occurs in solid particles while coalescence occurs in liquid particles.

Brownian motion is a dominant driving force for sub-micron particles. Turbulent flow would be a dominant driving force for particles ranging from 1 to 10 micron and pollutants of this size pose the greatest risk to human health (Koch & Cohen, 2000). Sedimentation will be dominant, after 10 microns. The rate of coagulation depends on both the forces driving the relative motion of the particles and the hydrodynamic, Van der Waals and electrostatic inter-particle interactions.

Brownian motion, (which is a characteristic property of aerosols), can be described as a random motion which is a result of the fluctuations in the impact of gas molecules on the particles. This type of motion is significant for particles of $r < 0.5\mu m$ (Meszaros, 1981). Surface phenomena play an important role in the behaviour of aerosol particles. An important consequence of the Brownian motion of aerosols is the collision and subsequent

coalescence, which is called coagulation and is characterized by the particle loss per unit time:

$$-\frac{dN}{dt} = 8\pi DrN^2 \qquad (2.8)$$

where N is the number of particles per unit volume, t is the time, and D is the diffusion coefficient of particles:

$$D = \frac{kT}{6\pi\mu r}(1 + \frac{Al}{r}) \qquad (2.9)$$

where k is the Boltzmann constant, T is the absolute temperature, A is the Stokes-Cunningham correction and l is the mean free path of gas molecules (Meszaros, 1981). The coagulation equation then becomes:

$$-\frac{dN}{dt} = \frac{4}{3}\frac{kT}{\mu}(1 + \frac{Al}{r})N^2 \qquad (2.10)$$

The above equation shows that the intensity of the particle loss due to thermal coagulation is directly proportional to the square of the particle concentration, while coagulation efficiency increases with decreasing particle radius. Coagulation of small particles at a high concentration is very rapid. The above equation holds for monodisperse aerosols (aerosols composed of particles of uniform size) but the same qualitative conclusion can be drawn for polydisperse systems.

The rate of coagulation when all particles are moving can be determined by calculating the number density of particles in the process of collision (Seinfeld & Pandis, 1998).

The rate of formation and growth of aerosols may have negative effects on human beings and the environment. There is therefore, a need for removal of aerosols from the atmosphere.

2.2 REMOVAL OF AEROSOLS FROM THE ATMOSPHERE

The major processes for removing aerosols from the atmosphere are dry deposition or sedimentation and wet deposition (Laakso *et al.*, 2003). Dry deposition is the transport of gaseous and particulate species from the atmosphere onto surfaces in the absence of precipitation. Wet deposition combines all natural processes by which the aerosol particles are scavenged by atmospheric hydrometeors (cloud and fog drops, rain, snow) and are deposited to the earth's surface. Figure 2.1 shows the two processes of aerosol removal from the atmosphere.

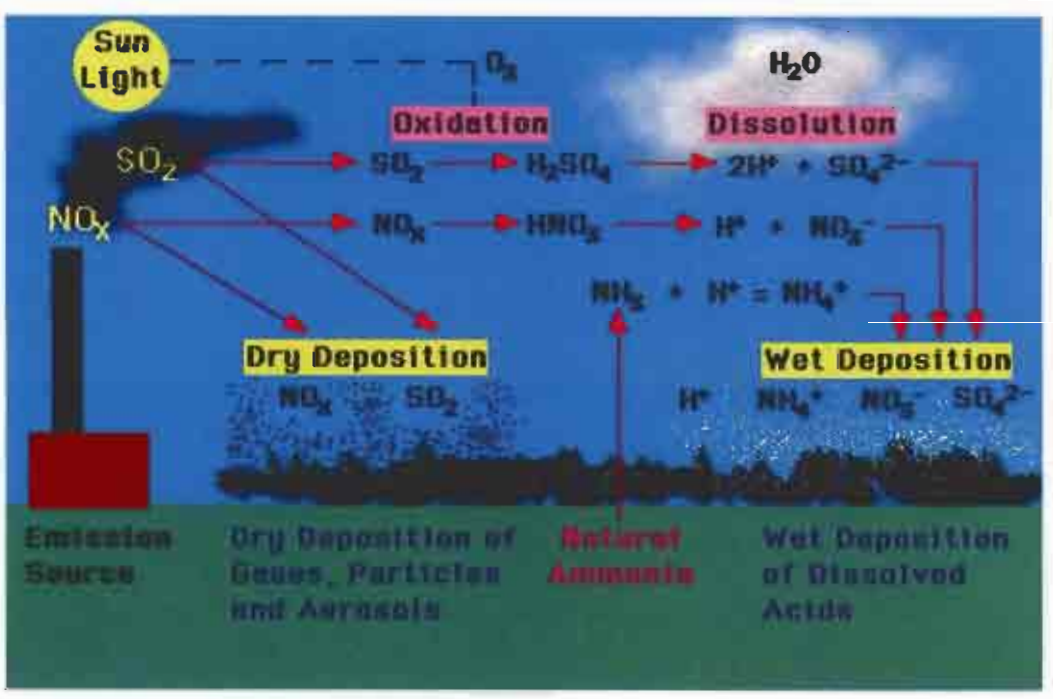

Figure 2.1: *A sketch of wet and dry deposition of aerosols*

Dry deposition occurs when gases or particles contact a surface and stick to or react with the surface in the absence of precipitation. Dry deposition process depends on atmospheric stability, chemical properties of the depositing particles and the specific properties of the contacting surface. Sedimentation (dry deposition) involves the fall of aerosols under gravity. The fall velocity and diffusion coefficient are the basic parameters which determine the removal rate. In calm atmospheric conditions, when the gravitational force

is balanced by the opposing force due to a viscous drag caused by air, the falling particles attain a terminal velocity.

Wet deposition is an important aerosol particle removal mechanism in the atmosphere. In the submicron range, particles are removed either by cloud processing, below-cloud scavenging or coagulation (Seinfeld & Pandis, 1998). The following steps are important for successful removal of aerosols by wet deposition: the species must be removed from the atmosphere and delivered to the surface, the aerosol/gas species must be brought into the presence of condensed water, the species must be scavenged by the hydrometeors and then be removed from the atmosphere and delivered to the surface. Figure 2.2 shows the wet deposition process as explained by Seinfeld and Pandis (1998).

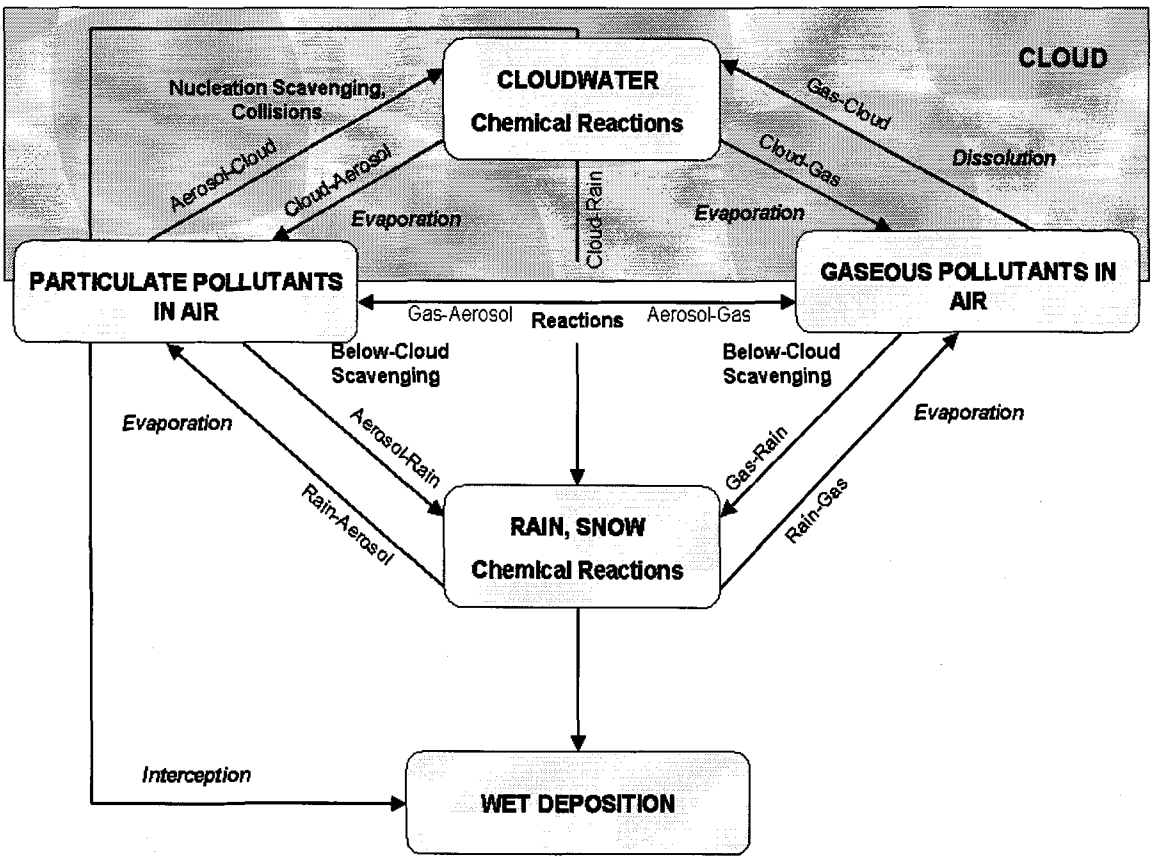

Figure 2.2: *A sketch describing the wet deposition of atmospheric aerosols Seinfeld and Pandis (1998).*

The main phenomena affecting collision efficiency between falling droplets and aerosol particles are inertial impaction, Brownian diffusion, phoresis caused by thermal or concentration gradients, turbulent effects and electrical forces. For particles smaller than 1μm, Brownian diffusion is the main removal mechanism (Laakso *et al.*, 2003).

It is evident that the formation, growth and removal of atmospheric aerosols is dependent on the size of particles, the radiation and the time of day, which may be linked to different natural and anthropogenic processes, as well as the geographic location. Information on the properties of aerosols is thus important for the control and/or monitoring of atmospheric aerosols.

2.3 PROPERTIES OF AEROSOLS

All aerosols are two-component systems having special properties that depend on the size of the particles and their concentration in the suspended medium. Aerosol properties influence the production, transport, and ultimate fate of atmospheric particulate pollutants. The toxicity of inhaled particles depends on their chemical and physical properties, thus an understanding of aerosol properties is required to evaluate airborne particulate hazards.

2.3.1 SIZE OF AEROSOLS

The size of aerosol particles is usually given as the radius of the particle, assuming that the particle has a spherical shape. The size categories are: the Aitken particles or nucleation mode (0.001 - 0.1 μm), large particles or accumulation mode (0.1 - 1μm), giant particles or coarse mode (> 1 μm) (Seinfeld & Pandis, 1998).

Particle size is important in all aspects of aerosol behaviour. The spherical shape is usually used for simplicity, that is, because of the one dimension geometric diameter. The commonly used diameter is the aerodynamic

diameter. Size distributions include particle number between sizes d + dd represented as:

$$dn = n(d)\,dd, and \int_o^\infty n(d)\,dd = N \quad (2.11)$$

where n(d) is the number frequency distribution function and N is the total number of particles.

Mass distribution m(d)

$$dm = m(d)dd, \quad \text{and} \quad \int_o^\infty m(d)dd = M \quad (2.12)$$

Cumulative distributions

For numbers less than d: $Cn(d) = \int_o^d n(d)\,dd$ (2.13)

For mass less than d: $Cm(d)\int_o^d m(d)\,dd$ (2.14)

Frequency distributions can be obtained by differentiating cumulative distributions e.g. the log normal distribution (Seinfeld & Pandis, 1998):

$$m(d) = \frac{M}{d\sqrt{2\pi}\ln\sigma g}\exp -\frac{(\ln d - \ln d_m)^2}{2(\ln\sigma g)^2} \quad (2.15)$$

where σ_g is the geometric standard deviation, and can be defined as:

$$\sigma_g = \frac{d_{84\%}}{d_m} \quad (2.16)$$

where $d_{84\%}$ is the diameter below which 84% of the particles lie and d_m is the median diameter. Log normal size distribution is associated with a single aerosol generation process. For more aerosol generation processes e.g. the mining environment where aerosols can be formed due to coarse dust from extraction processes and fine diesel particles, multimodal distributions are

applicable. Particles within specific size fractions are associated with different types of health effects.

The size distribution function describes how aerosol number (or area or volume) is distributed with respect to size (Sateesh, 2002). The size distribution mainly depends on the production mechanism (source). Aerosols formed by gas to particle conversion are in general smaller in size and those produced by mechanical disintegration are larger. The size distribution determines the lifetime of each species in the atmosphere.

Table 2.1: *Global source strength, lifetime and burden* (Seinfeld & Pandis, 1998)

Source		**Aerosol Type**	**Flux (Tg/yr)**	**Lifetime (d)**	**Burden (mg/m^2)**
Natural	Primary	Dust (desert)	900 - 1500	4	19 – 33
		Sea salt	2300	1	3
		Biological debris	50	4	1
	Secondary	Sulfates from biogenic gases	70	5	2
		Sulfates from volcanic SO_2	20	10	1
		Sulfates from Pinatubo	40	400	80
		Biogenic organics	20	5	0.6
Total			3400 - 4000		27 – 41
Man-made	Primary	Dust (soil+desert+industry)	40 - 640	4	1 – 14
		Black carbon	14	7	0.6
		Organic carbon in smoke	54	6	1.8
	Secondary	Sulfates from SO_2	140	5	3.8
		Organics from hydrocarbons	20	7	0.8
Total			270 – 870		8 – 21

Aerosols of different size ranges are important for different atmospheric processes. The size distribution $f(r)$ is defined as:

$$\frac{1}{N}\frac{dN}{dr} = f(r) \qquad (2.17)$$

where N is the total number concentration and dN is the same parameter for particles with a radius between *r* and *r* + *dr*

$$\int_o^x f(r)dr = 1 \qquad (2.18)$$

The volume concentration (aerosol volume per unit volume of air) distribution is given by:

$$\frac{1}{V}\frac{dV}{dr} = f(r) \qquad (2.19)$$

The size distribution function gives an indication of the volume of particulate material in the atmosphere, and is often given as the number of particles over a given size range that is to be found in a cubic centimetre of air. Figure 2.3 relates the different concentration distributions to the size of aerosols.

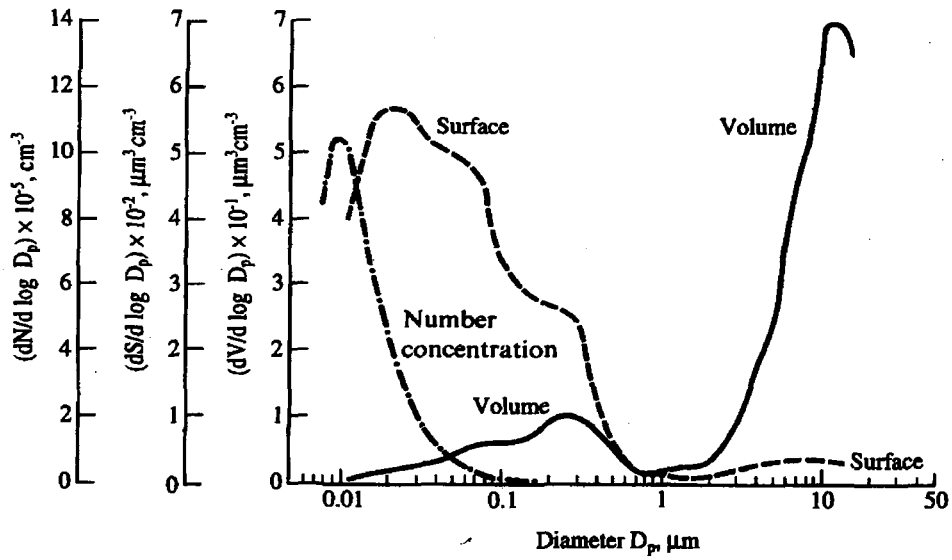

Figure 2.3: *A typical sketch showing the volume, surface, and number-concentrations of different particle sizes (Brimblecombe, 1996)*

Removal of large particles is easily achieved since they may just fall out. Smaller particles may just coagulate. Particles with long residence time (e.g. $r < 0.3$ μm) appear to accumulate in air (Brimblecombe, 1996).

The size distribution of aerosol particles also varies as a function of relative humidity because of the presence of water-soluble material in the particulate matter. Considering a particle with radius r_o, initially in an environment containing no water vapour (in a dry state), if the relative humidity of the particle's environment is increased, the radius initially remains the same, disregarding the adsorption process, which is of little importance (Meszaros, 1981).

2.3.2 MOTION OF AEROSOLS

Particle motion describes the gas-particle relation and characterises the particle diameter with regard to the medium in which it is suspended. In the free molecular regime, the sub-micrometer particles, especially $r < 0.1$μm, are affected by the motion of individual gas molecules. The continuous regime comprises of larger particles that can be treated as being submersed in a continuous gaseous medium (characterised by a Knudsen number > 1). The intermediate size particles can usually be treated by an adjustment of equations from the continuum regime (requires Cunningham slip correction factor), which characterises the transition (or slip) regime (Morawska, 2004).

The motion of aerosol particles may occur as a result of external forces (gravity, electrical). A drag force arises because of the difference between the velocity of the particle and that of the fluid.

The gas diffusion coefficient (D) is the result of the Brownian motion and results in net movement from regions of higher to regions of lower concentrations. It is important always to correct for temperature, pressure, volume, etc. when measurements are conducted for conditions different to standard (Morawska, 2004).

$$D = -\left(\frac{3\sqrt{2}\pi}{64Nd_{molec}^2}\right)\sqrt{\frac{RT}{M}} \qquad (2.20)$$

where N is the number of gas molecules per unit volume, d_{molec}, the molecular collision diameter, R is the gas constant, D, diffusion in the concentration gradient, T, the temperature and M is the molecular weight of the gas molecules. Assuming that the motion of the aerosol particle consists of statistically independent successive displacements which yields the Brownian diffusivity (particle diffusion coefficient) D, then according to Seinfeld & Pandis (1998), flux density J, can be given as

$$J = -D\frac{\partial N}{\partial x} \qquad (2.21)$$

An aerosol particle suspended in a fluid undergoes irregular random motion due to bombardment by surrounding fluid molecules. Particle diffusion likewise connected to Brownian motion, is dependent on the size and shape of the aerosol particle, resulting in slower diffusion of larger particles than smaller ones.

Table 2.2: *Comparison of the distance an aerosol particle travels due to Brownian motion and gravity in 1s (Seinfeld & Pandis, 1998)*

Particle Size	**Brownian Motion**	**Gravity**
1 μm	Diffuses 4 μm	Falls 200 μm
0.1 μm	Diffuses 20 μm	Falls 4 μm. Although over time scales of hours, its total displacement is governed by gravity.
0.01 μm	Diffuses 1000 times it falls under gravity.	Needs several weeks for gravity to equal random Brownian motion

2.3.3 ELECTRICAL PROPERTIES OF AEROSOLS

Aerosols are important from the point of view of aerosol electricity. A fraction of air molecules is electrically charged (small ions) as a result of ionisation radiation (Meszaros, 1981). Electrical properties influence particle behaviour, especially during sampling, filtration and also deposition into the lungs (Hameri, 2004). Aerosol populations can either be neutral or charged, but individual particles may be highly charged. Aerosol exposed to charges of both polarities for sufficient time can be analysed using the Boltzmann equilibrium charge distribution, which is typical for long-lived atmospheric aerosols.

Air ion implies all airborne particles that are electrically charged and serve as a basis of air conductivity (University of Helsinki, 2004). Air ions comprise a large variety of charged particles of different chemical composition, mass and size, from molecular clusters up to large aerosol particles (Dolazalek *et al.,* 1985; Tammet, 1998a).

The formation of cluster ions is also dependent on the thermodynamical properties of the clusters and the environment. If the cluster ions grow to a critical size, about 1 – 2 nm, then spontaneous nucleation follows (Raes & Janssens, 1985; Yu & Turco, 2000). The cluster ions behave like kernels of condensation of nucleating vapours, converting them from the gas phase to the aerosol phase (University of Helsinki, 2004).

Two concurrent processes, ion-induced nucleation (Yu & Turco, 2000) and homogeneous nucleation (Provincial Health Office, 1993), are considered as possible ultrafine aerosol formation routes in atmospheric air. Aerosol ions just like ordinary aerosol particles above 1.6 nm, experience all the processes known from aerosol physics: growth and vapour condensation, coagulation, wet and dry removal (deposition), and propagation in the atmosphere (Hidy, 1984; Hoppel *et al.,* 1990).

Electrical properties of air are determined by the electrical mobility of ions formed (Meszaros, 1981). Electrical mobility of an ion is defined as coefficient of proportionality between the drift velocity v and the applied electric field strength E by the formula

$$K = vE \tag{2.22}$$

For weak fields and low concentrations of ions, K is related to the diffusion coefficient of ions by the Einstein equation

$$D = kTKq^{-1} \tag{2.23}$$

where k is the Boltzmann constant, q is the ion charge, and T is the absolute temperature (Mason & McDaniel, 1988).

Mobility depends on both the properties of an ion (size, mass, charge and structure) and of the environment in which the ion moves (University of Helsinki, 2004). There is no general law relating mobility of ion to ion-size or mass. The Stokes-Millikan empirical equation is used when the particle size is comparable to or larger than, the mean free path of the gas molecules (about 60nm in air at STP).

The electrical conductivity of the atmosphere, which is inversely proportional to the aerosol particle content in the air, has been used as and indicator of particulate pollution.

2.4 EFFECTS AND MONITORING OF PARTICULATE MATTER

Effects of PM can be noticed in the entire ecosystem, including humans and their environment. The atmospheric impacts of particulate matter occur mainly in the form of reduced visibility (associated with stack plumes and winter smog), thermal air pollution or ambient heat retention. Thermal air pollution is

common in urban areas where industrial waste heat and urban surfaces, e.g. tar, can result in urban heat island (Muller & Mangold, 2002).

Other effects on the environment include corrosion of buildings and artefacts, damage to plants, as well as health hazards to animals. This study, however, focuses on the health and radiation effects of PM mainly because they affect human beings directly, and they can be used in setting guidelines for the particulate matter within the province.

2.4.1 HEALTH EFFECTS OF TOXIC TRACE METALS

Exposure to ambient particulate matter has been associated with a range of adverse health effects including: premature mortality, aggravation of existing respiratory conditions, changes to lung tissues and structures, and altered respiratory defence mechanisms. These responses to exposure are a function of the exposure concentration, the duration of the exposure, and the amount absorbed in the body (i.e., dose over time) (Gulflink, 2002). People exposed to higher concentrations of air particulate matter for long periods increase their chances of serious health effects such as cancer, damages to the immune system, neurological damages, reproductive problems (i.e. reduced fertility), development problems and respiratory problems. Health effects of PM associated with endocrine disruption include reduced fertility, birth defects and breast cancer (Provincial Health Office, 1993).

Prolonged exposure to nickel and chromium cause lesions of the skin and mucous membranes, possible cancer of nose or lungs - bronchogenic carcinoma, whilst lead causes behavioural changes, kidney damage and periphery neuropathy characterised by decreased hand-grip strength (Heckmann Building Products, 2000). Chromium and nickel have been identified by the International Agency for Research on Cancer as potential cancer causing agents.

Skin contact with certain hexavalent chromium compounds can cause skin ulcers. Breathing high levels of hexavalent chromium can cause irritation to

the nose, such as nose bleeds, runny nose, ulcers and holes in the nasal septum. Some people are extremely sensitive to hexavalent chromium and trivalent chromium. Allergic reactions consisting of severe redness and swelling of the skin have been noted (Environmental Health Criteria, 1988).

Humans are constantly exposed to nickel in various amounts because it is ubiquitous. With respect to occupational exposures, the main routes of toxicological relevance are inhalation and to a lesser extent, skin contact. In the producing industry, soluble nickel compounds are more likely to be found in hydrometallurgical operations. Generally, exposures in the producing industry are in the form of moderately soluble and insoluble nickel compounds. Exposures in the nickel-using sectors vary according to the products handled and include both soluble and relatively insoluble forms of nickel (Heckmann Building Products, 2000).

Nickel sulphate aerosols may cause irritation to the upper respiratory tract and respiratory sensitisation, to the eyes as well as irritation to the skin. Nickel sensitivity may result in allergies, skin rashes and/or asthma. Soluble nickel compounds are not carcinogenic themselves. They can cause cell inflammation and cell proliferation. They may also act as enhancers of other compounds such as insoluble nickel compounds, which may present health hazards since insoluble nickel compounds are known to be carcinogenic (National Toxicology Program, 1994).

Vanadium is an important alloying element and is added to a variety of steels. The major effects from breathing high levels of vanadium are on the lungs, throat and eyes. Workers who breathe in vanadium for short and long periods of time sometimes have lung irritation, coughing, chest pain, sore throat, runny nose and wheezing. These effects usually stop soon after the exposure is ended (Department of Health and Ageing, 2005).

Lead is present in the atmosphere in the particle form. Non-ferrous smelters, lead gasoline additives and battery plants are the most significant contributors to the atmospheric lead emissions. Particulate lead can be inhaled or ingested

from food, water, soil or dust. It then accumulates in the body in the soft tissue, blood and bones. Lead can also affect the nervous system, kidneys, liver and other organs. According to Schlecht and O'Connor (2004) too much exposure to lead may cause problems such as: anaemia, kidney disease, reproductive disorders and mental retardation.

The concentration of lead in the blood is a good indicator of exposure to lead from all sources, and adverse health effects tend to increase in severity with increased blood lead level. USEPA standards for blood lead level of 0.15 $\mu g.ml^{-1}$ (mean value for children) can be achieved at an ambient air lead level of 1.5 $\mu g.m^{-3}$ (Rajakopal, 2005). The most sensitive body systems to the effects of lead are the haematopoietic system. In addition, lead has been shown to affect the normal functions of the reproduction, endocrine, hepatic, cardiovascular, immunological and gastrointestinal systems.

Respiratory deposition

An understanding of how and where particles deposit in our lungs is necessary to evaluate properly the health hazards of aerosols. While filtration occurs in a fixed system at a steady flow rate, respiratory deposition occurs in a system of changing geometry, with a flow that changes with time and cycles in direction.

The respiratory system can be divided into three regions: the head airways region (nose, mouth, pharynx, larynx), also called extrathoracic or nasopharyngeal region, where air is humidified; the lung airways or tracheobronchial (airways from trachea to the terminal bronchioles) region; the pulmonary or alveolar region, where gas exchange takes place. These regions differ in structure, airflow patterns, function, retention time, and sensitivity to deposited particles (Hinds, 1999).

The respiratory system of a normal adult processes 10 – 25 m^3 (12 – 30 kg) of air per day. The surface area for gas exchange is 75 m^2, and is perfused with more than 2000 km of capillaries. Once deposited, particles are retained in

the lung for varying times, depending on their physiochemical properties, their location within the lung, and the type of clearance mechanism involved. During actual breathing, the airflow rate is continuously changing and reverses direction twice during each cycle. However, the air velocities given in Table 2.3 are based on steady flow.

The most important deposition mechanisms are impaction, settling, and diffusion and are given in Table 2.4. Interception and electrostatic deposition are not always important. The extent and location of particle deposition depend on particle size, density, shape, airway geometry and the individual's breathing pattern.

For healthy adults, during inhalation, the incoming air negotiates a series of direction changes as it flows from nose (mouth) to the alveolar region. Each time the air changes direction, the suspended particles continue a short distance in their original direction because of their inertia. Thus some particles deposit on the airway surfaces by inertial impaction. The mechanism is limited to deposition of large particles that are close to the airway walls. Nonetheless, it causes the most aerosol deposition on a mass basis.

Deposition by impaction typically occurs at or near the first carina. The probability of deposition by impaction depends on the ratio of particle stopping distances to airway dimensions at velocities associated with a steady inhalation of 3.6 m^3/h (1.0 l/s) for selected airways, and is high in the bronchial region. Table 2.3 gives the main regions of the lung affected by entry and deposition of aerosols of different sizes.

TABLE 2.3: *Characteristics of selected regions of the Lung[a] (Hinds, 1999)*

AIRWAY	GENERATION	NUMBER PER GENERATION	DIAMETER	LENGTH (mm)	TOTAL CROSS SECTION	VELOCITY[a] (mm/s)	RESIDENCE TIME[b] (ms)
Trachea	0	1	18	120	2.5	3900	30
Main bronchus	1	2	12	48	2.3	4300	11
Lobar bronchus	2	4	8.3	19	2.1	4600	4.1
Segmental bronchus	4	16	4.5	13	2.5	3900	3.2
Bronchi with cartilage in wall	8	260	1.9	6.4	6.9	1400	4.4
Terminal bronchus	11	2000	1.1	3.9	20	520	7.4
Bronchioles with muscle in wall	14	16,000	0.74	2.3	69	140	16
Terminal bronchiole	16	66,000	0.60	1.6	180	54	31
Respiratory bronchiole	18	$0.26X10^6$	0.50	1.2	530	19	60
Alveolar duct	21	$2 X 10^6$	0.43	0.7	3200	3.2	210
Alveolar sac	23	$8 X 10^6$	0.41	0.5	72,000	0.9	550
Alveoli		$300X 10^6$	0.28	0.2			

[a]Based on Weibel's model A; regular dichotomy of average adult lung with volume 0.0048 m^3 [4800 cm^3] at about three-fourths maximal inflation. Table adapted from Lippmann (1995). [b]At a flow rate of 3.6 m^3/hr [1.0 L/s].

Deposition by settling occurs mostly in the smaller airways and the alveolar region. This is mainly because of the low flow velocities and the small airway dimensions. This mechanism is most important in the distal airways (those farthest from the trachea). Hygroscopic particles grow as they pass through these water-saturated airways, thus the increase in size favours settling and impaction in the distal airways (Hinds, 1999). Table 2.4 shows the deposition mechanisms for standard density particles in the lungs.

Table 2.4: *Relative Importance of Settling, Impaction, and Diffusion Mechanisms for Deposition of Standard Density Particles in Selected Regions of the Lung (Hinds, 1999)*

AIRWAY	STOPPING DISTANCE[a]			SETTING DISTANCE[b]			Rms DISPLACEMENT[c]		
	AIRWAY DIAMETER (%)								
	0.1 μm	1μm	10 μm	0.1 μm	1μ m	10 μm	0.1 μm	1 μm	10 μm
Trachea	0	0.08	6.8	0	0	0.52	0.04	0.01	0
Main bronchus	0	0.13	10.9	0	0	0.41	0.03	0.01	0
Segmental bronchus	0	0.31	27.2	0	0	0.22	0.05	0.01	0
Terminal bronchus	0	0.17	14.9	0	0.02	2.1	0.29	0.06	0.02
Terminal bronchiole	0	0.03	2.8	0	0.18	15.6	1.1	0.22	0.06
Alveolar duct	0	0	0.23	0.04	1.7	150	3.9	0.79	0.23
Alveolar sac	0	0	0.07	0.12	4.7	410	6.7	1.3	0.40

Stopping Distance[a] at airway velocity for a steady flow of 3.6 m^3/hr [1.0 L/s.
Settling Distance[b] = settling velocity H residence time in each airway at a steady flow of 3.6 m^3/hr [1.0 L/s]. [c]Rms Displacement during residence time in each airway at a steady flow of 3.6 m^3/hr [1.0 L/s].

Inhalability of particles

The entry of particles into the mouth or nose can be thought of as a sampling process that includes isokinetic and still-air sampling; however, the human head is a blunt sampler with a complex geometry (Vincent, 1989). The efficiency of particle entry into the nose or mouth can be characterized by the aspiration efficiency, inhalability, or inhalable fraction (*IF*), the fraction of particles originally in the volume of air inhaled.

The inhalable fraction, which is usually less than one, depends on particle aerodynamic diameter and the external wind velocity and direction. The equation for the inhalable fraction and inhalable fraction sampling criterion *IF* (d_a) is:

$$IF(d_a) = 0.5\ (1 + \exp(-0.06\ d_a))\quad \text{for}\, U_o < 4m/s \qquad (2.24)$$

where d_a is the aerodynamic diameter in μm. For ambient air velocity U_o greater than 4m/s, IF is given by Vincent *et al.* (1990):

$$IF\ (d_a, U_o) = 0.5\ (1 + \exp\ (-0.06\ d_a)) + 10^{-5}U_o^{2.75}\exp\ (0.055d_a) \qquad (2.25)$$

Nasal inhalability IF_N can be approximated according to Hinds *et al.* (1998) as:

$$IF_N(d_a) = 0.035 + 0.965\exp\ (-0.000113\ d_a^{2.74}) \qquad (2.26)$$

2.4.2 RADIATION EFFECTS OF AEROSOLS

Aerosols affect the amount of solar radiation reaching the surface of the earth. This is called climate forcing or radiative forcing. The unit of radiative forcing is typically weber per square meter (Wb/m^2). Aerosols both absorb and scatter solar radiation. Many external factors force climate change. These radiative forcings arise from changes in the atmospheric composition, alteration of surface reflectance by land use, and variation in the output of the sun. Except for solar variation, some form of human activity is linked to each (IPCC, 2001).

Direct radiative influence in the visible region involves the scattering and absorption of visible radiation by aerosols, which produces climate forcing by changing the planetary albedo (reflectance of the planet). Most of the light extinction caused by aerosols is due to scattering. Particles in the 0.1 - 1.0 μm size range are especially active in this regard, as their radii are comparable to the wavelengths of visible solar radiation (NSDL, 2006).

Figure 2.4 shows the radiative impact as a function of aerosol sources to illustrate the uncertainties on aerosol studies and climate change. The rectangular bars represent estimates of the contributions of these forcings,

some of which yield warming, and some cooling. The indirect effect of aerosols shown is based on the size and number of cloud droplets.

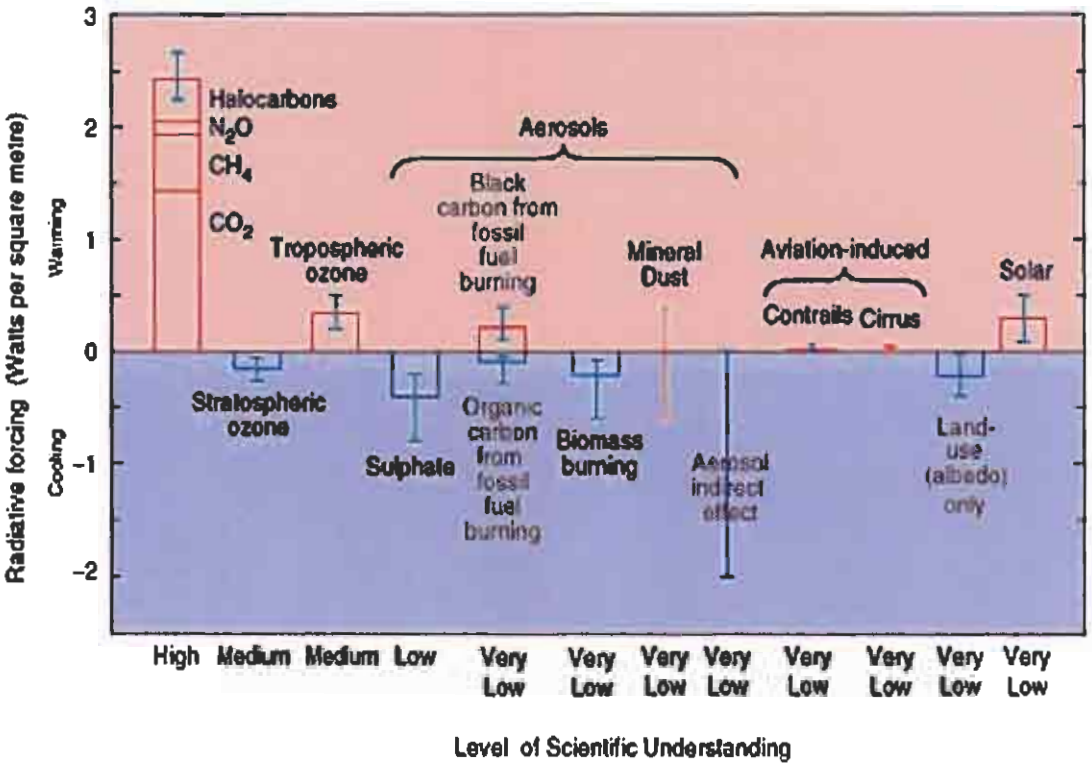

Figure 2.4: *The radiative forcing as a function of aerosol sources (IPCC, 2001).*

Indirect Radiative forcing aerosols can act as CCN for formation of clouds. An increase in the concentration of aerosols results in increased concentration of cloud droplets, which leads to an increase in the albedo (or reflectance) of clouds. This causes a decrease in the visible solar radiation reaching the earth's surface.

Scattering of solar radiation causes light extinction and particles in the 0.1 – 1.0 μm size range usually scatters solar radiation. This is due to their radii that are comparable to the wavelengths of visible solar radiation. Scattering of light in this size range is usually called Mie scattering since it is characterized by the Mie theory. Chemical composition of aerosols determines their complex (they contain real and imaginary parts) refractive

index. Particle refractive index is an important parameter while determining the radioactive effects (Sateesh, 2002). The real part determines the scattering properties and the imaginary part, the absorption characteristics. Particles originating from combustion processes usually have high absorption properties and hence a high imaginary part of the refractive index.

Optical depth is a measure of transmittance of a vertical atmospheric column of a unit cross-sectional area. Optical depth is a result of the combined effect of scattering and absorption in a vertical column. Major contributors of this extinction (a measure of attenuation) in the atmosphere are aerosols and air molecules. The optical depth due to aerosols only (aerosol optical depth) is obtained by subtracting the contribution due to air molecules from the total atmospheric optical depth, which is known with reasonable accuracy.

Particulate matter reduces visibility by attenuating the light from objects and illuminating the air causing the contrast between the objects and their backgrounds to be reduced. Not only does it affect visibility, but it also hastens the erosion of building materials and the corrosion of metals (Brimblecombe, 1996). Visibility is limited by difficulties in perceiving the contrast difference between two distant objects (Brimblecombe, 1996). The decrease in contrast is responsible for the haziness we observe in particle-laden atmospheres.

In the infrared region, the presence of aerosols increases the surface reaching infrared radiation and decreases the outgoing infrared radiation. A fraction of the reduction in visible solar radiation at the surface (due to aerosols) is offset by the increase in infrared solar radiation. Most aerosols are concentrated near the surface (within 3 km) hence the absorbing aerosol component heats the lower atmosphere.

Soot aerosols, due to their high absorption effects, contribute largely to the reduction of solar flux at the surface, whereas sulphate and nitrate aerosols, due to their scattering effects, contribute largely to the solar radiation reflected back to space.

The health and radiation effects discussed above emphasise the need for a proper system for monitoring particulate matter. It is thus imperative for one to understand the current situation in South Africa, and the North West province in particular, with regard to monitoring system, standards, limits and methods.

2.5 MONITORING OF PM

Monitoring usually refers to the tracking of concentration trends over time. Ambient monitoring is carried out for a variety of reasons, including assessment of environmental problems and evaluation of interventions. The choice of parameters should be based on the sources in the area and on the receptors and impacts of concern. The monitoring plan should set out the rationale for selecting the number and location of monitoring stations, the monitoring frequency, and the sampling methods and should include a quality control plan.

Ambient air quality monitoring activities can be broadly classified into two categories, scientific investigation (research) and compliance monitoring. For scientific research, the meteorological parameters that need to be measured during the sampling period include temperature, relative humidity, precipitation, wind speed and direction, UV intensity, and solar intensity (Khlystov, 2001).

Continuous monitoring methods are available for many of the most important air pollutants, but the value of the additional data obtained needs to be weighed against the cost and complexity of such systems.

2.5.1 CONTINUOUS MONITORING

There are several state-of-the-art technologies that are commercially available for automated continuous monitoring of PM. These include opacity monitors; light scattering technologies, beta gauge, acoustic-energy monitoring,

triboelectric technology and tapered-element oscillating microbalance (TEOM) (Baron & Willeke, 2001).

The tapered-element oscillating microbalance (TEOM) is the only device that measures the mass of PM2.5 directly, but it is sensitive to humidity and temperature and requires periodic changes in down times of one half hour to two hours after each filter change. The existing technologies use inertial impactors or dichotomous samplers as particle size separators that only approximate PM size. For both of these technologies, sizing is based on the aerodynamic properties of particles and the diameter of a unit density sphere. However, because of difference in properties of PM, particles that are larger and lighter than the reference sphere get through while some smaller, heavier particles may be settled out and lost.

Monitoring of both PM mass and chemical composition is important for identification of the emission source, determination of compliance with the set air quality standards, and development of effective control programs. Chemical analysis of the organic fraction of airborne PM is very costly and difficult because of compounds. Therefore a special technique is needed for the analysis of PM.

2.5.2 THE SITUATION IN SOUTH AFRICA

The constitution of South Africa (Act No. 108 of 1996) specifies an environment, which is not harmful to human health, as a basic human right. Despite having all the environmentally protective laws in place: The National Environment Act (Act. No. 107 of 1998), Environment Conservation Act (Act No. 73 of 1989), Occupational Health and Safety Act (Act No. 85 of 1993), and Atmosphere Pollution Prevention Act (Act No. 45 of 1965), South Africa currently does not have established air quality standards in place nor an overall approach that includes such elements as air monitoring, emission inventories, and regular monitoring requirements (Lents & Nikkila, 2003).

Dust emanating from depositions in excess of 20 000 cubic meters is subject to directions from the Chief Air Pollution Control Officer (CAPCO). As with scheduled processes and smoke, dust control is regulated without reference to statutory air quality standards. Table 2.5 shows the guideline values for ambient air quality in South Africa.

Table 2.5: *Guideline values for ambient air quality in South Africa*

Concentration In Parts Per Billion (ppb)					
Pollutant	**Instant Peaks**	**1 Hour Average**	**24 Hour Average**	**1 Monthly Average**	**Annual Average**
Sulphur Dioxide (SO_2)	600	300	100	50	30
Ozone (O_3)	250	120			
Nitrogen Oxide (NO)	1 400	800	400	300	200
Nitrogen Oxides (NO_x)	900	600	300	200	150
Non-Methane Hydrocarbons	700	400			

Total Suspended Particulate (high Volume Sampler)

- 24 Hour Average = 300 micrograms per cubic meter
- Annual Average = 100 micrograms per cubic meter

Inhalable Particulate Matter (PM10)

- 24 Hour Average = 180 micrograms per cubic meter
- Annual Average = 60 micrograms per cubic meter

Smoke (from CSIR Soiling index) ($\mu g.m^{-3}$) approximately 5 times the soiling index

- 24 Hour Average = 250 micrograms per cubic meter = approx 50 $S.m^{-3}$
- Annual Average = 100 micrograms per cubic meter = approx 20 $S.m^{-3}$

Dust Fallout (deposition) classification for a monthly average

- Slight = less than 0.25 grams per square meter per day

- Moderate = 0.25 to 0.50 grams per square meter per day
- Heavy = 0.50 - 1.20 grams per square meter per day
- Very heavy = greater than 1.20 grams per square meter per day.

Maximum Lead (Pb) Concentration

- Monthly average - 2.5 micrograms per cubic meter.

Implementation of the guidelines tabled above is even more difficult since there are no standardised sampling and monitoring procedures. In the North West Province, each industry has a method of sampling and analysis of particulate matter, and most of them just monitor the levels of particulate matter and are not interested in the composition thereof. The situation thus calls for a study leading to a suggestion on suitable sampling and analysis methods, as well the procedure for a complete monitoring program.

2.6 OTHER STUDIES ON MONITORING OF ATMOSPHERIC PARTICULATE MATTER

The South African situation (scarcity of data) as portrayed in Section 2.5.2 above, suggests that the previous studies conducted worldwide be used as a basis for establishing a sampling and monitoring system for the North West Province.

2.6.1 STUDIES ON CONCENTRATION LEVELS OF PARTICULATE MATTER

Studies have been conducted worldwide on determination of the levels of particulate matter, and variations have been observed from one area to another. These include a study conducted by Solomon *et al.* (2000b) at Meadview, USA, where the annual PM10 average of 9.2 $\mu g.m^{-3}$ was observed for the measurements done from May 1998 to May 1999. A higher level of 38.4 $\mu g.m^{-3}$ was observed during the months January and February 1999 at Rubidoux site in the United States of America, and Tolocka *et al.* (2001)

observed a PM10 annual average of 13.9 $\mu g.m^{-3}$ at the Shenandoah National Park in the USA, during May 1998 to May 1999.

PM characteristics of seven selected regions (Germany, Spain, Sweden, Austria, United Kingdom and Netherlands) within the European Union (EU) were analysed and compared. Results of levels and speciation studies of PM10 and PM2.5 (with at least one year of data coverage from 1998 to 2002) at regional, urban background and kerbside sites were assessed. Based on the examples selected, PM10 levels (annual mean) ranged from 19 to 24 $\mu g.m^{-3}$ at regional background sites, from 28 to 42 $\mu g.m^{-3}$ at urban background, and from 37 to 53 $\mu g.m^{-3}$ at kerbside sites (Querol *et al.* 2004).

A study was also conducted in the Western Cape Province of South Africa, and an annual average level of 33 μgm^{-3} was obtained in 1999 at the Goodwood site in Cape Town (Granger, 2003).

Seasonal variations in the levels of particulate matter are evident worldwide. A study conducted by Paoletti *et al.,* 2002, where analysis of airborne particulate samples, to evaluate the PM concentration, showed a seasonal variation of the PM mean concentration that ranged from 56 $\mu g.m^{-3}$ ±50% in the winter season to 41 $\mu g.m^{-3}$ ±30%, in the summer season.

Aerosol samples of PM2.5 and PM10 were collected in Beijing during both summer and winter seasons from 2002 to 2003 synchronously at three sampling sites, i.e. (1) a traffic site, located in the campus of the Beijing Normal University (BNU) between the 2nd and 3rd ring roads, (2) an industrial site near the Capital Steel Company (CS), and (3) a residential site, Yihai Garden (YH), located near the South 4th ring road. The mean PM10 concentrations observed at the three sites BNU, CS and YH were 172.2(±101.9) and 184.4(±130.5), 170.0(±66.7) and 287.7(±155.7), 150.1(±56.9) and 292.7(±172.7) for summer and winter respectively (Sun *et al.,* 2004).

Seasonal variations are normally deduced from monthly PM levels and these include the 248 $\mu g.m^{-3}$ and 320 $\mu g.m^{-3}$ levels for June and July observed during a study conducted in Gaborone, Botswana in 2002, which exceeded the monthly PM10 guideline of 200 $\mu g.m^{-3}$ set by the Botswana government (Mmolawa, 2004).

The meteorology of an area influences both the hourly, daily and seasonal variations of PM. This has been evident in several studies including the one by Kukkonen *et al.,* 2005, where detail analysis in four selected episodes involving substantially high concentrations of PM10 that occurred in Oslo on 4-10 January 2003, in Helsinki on 3-14 April 2002, in London on 18-27 February 2003 and in Milan on 14-19 December 1998 was performed. All four the episodes addressed were associated with areas of high pressure (Oslo, Helsinki and London) or a high-pressure ridge (Milan). The best meteorological prediction variables were found to be the temporal evolution of the temperature inversions and atmospheric stability and, in some of the cases, wind speed. Strong ground-based or slightly elevated temperature inversions prevailed in the course of the episodes in Oslo, Helsinki and Milan, and there was a slight ground-based inversion also in London; their occurrence coinciding with the highest PM10 concentrations. The 24-hour levels of PM10 measured were in the range of 10 – 220 $\mu g.m^{-3}$ for the Oslo study sites, 20 – 230 $\mu g.m^{-3}$ for Helsinki study sites, 0 – 130 $\mu g.m^{-3}$ for London sites, and 10 – 380 $\mu g.m^{-3}$ for Milan.

Research aimed at determining which meteorological variables most influence ozone and PM in the South-western USA and examining patterns of underlying pollutant trends due to emissions was conducted by Wise and Comrie, 2005. Ozone and PM data were analysed over the time period 1990–2003 for the South-west's five major metropolitan areas: Albuquerque, NM; El Paso, TX; Las Vegas, NV; Phoenix, AZ; and Tucson, AZ. Results indicate that temperature and mixing height most strongly influence ozone conditions, while moisture levels (particularly relative humidity) are the strongest predictors of PM concentrations in all five cities examined. Meteorological variability typically accounts for 40–70% of ozone variability and 20–50% of PM

variability. Long-term trends in PM concentrations were relatively constant in all five cities analysed but contained coincident extremes unrelated to meteorology (Wise & Comrie, 2004).

Daily PM10 concentrations have been used to assess acute as well as chronic effects of PM worldwide. In a study conducted by Chaulya (2004a), the average 24hour PM10 concentrations ranged between 40.8 and 171.9 $\mu g.m^{-3}$, and a study carried out in Edinburgh by Heal *et al.* (2005), showed the mean daily PM10 and PM2.5 for a year of measurement as 15.5, 8.5 and 6.6 $\mu g.m^{-3}$. The PM2.5 data were well within possible future limit values proposed by the European Commission Clean Air For Europe programme.

The levels of PM can be very high at a specific time of day mainly due to natural or anthropogenic activities. Average 24-hour concentrations as high as 302 μgm^{-3} were observed by Fiala (2000) at the Branik site in the Czech Republic in 1999.

Both PM10 and PM2.5 concentrations in Seoul were measured as 47 and 79 μgm^{-3} respectively, which were found by Mishra *et al.* (2004a) to be about twice as high as their Busan counterparts (i.e. 19 and 34 $\mu g.m^{-3}$) than. The higher particulate concentrations in Seoul may reflect the relative dominance of anthropogenic sources (industry and traffic) compared to Busan or Jeju.

The fact that the levels of PM can be affected by both the natural and anthropogenic sources implies that the levels can vary according to the time of day. Munishi (2002) observed peak concentrations of NO_2 and PM in the morning and evening hours.

The levels mentioned in all the studies above are, however, very low compared to the average concentrations ranging from 592 to 1, 211 $\mu g.m^{-3}$ observed at Dar es Salaam (Msafiri, 2004).

2.6.2 COMPOSITION OF PARTICULATE MATTER

Studies on the composition of particulate matter use a variety of analytical methods. The studies presented in this section are mainly based on the determination of toxic metals in the air particulate matter.

The geographical distribution patterns of atmospheric lead (Pb) were investigated by Mishra *et al.* (2004a) using the data sets acquired from three locations in Korea during the wintertime period (December 2002). As these sites were selected to represent different levels of anthropogenic activities in Korea, Pb concentrations of each site were found in the highly variable range of 8.42–96.7 at Jeju, 35–238 at Busan, and 38.7–401 at Seoul.

A study conducted by Fiala (2000) in the Czech Republic at Sokolov and Všechlapy yielded ICP-MS concentrations of 3.5 to 3.7 $ng.m^{-3}$ and 15.8 to 57.8 $ng.m^{-3}$ for Ni and Pb respectively.

The levels of oxides of Al, Ca, Si, Na, Cl, S, O, with Fe in a study conducted by Chong et al. (2002) suggests the presence of aluminosilicates with traces of sulfate or sulfite, and chloride, while in a study conducted at the Upstate Medical University (2003), the presence of oxides of P, Cl suggests a Pb phosphate mineral (Pb-P-Ca and/or Cl). The presence of SO_x was also considered as an indication of the levels of sulphur dioxide, sulphuric acids, ammonium sulfate, ammonium bisulfate, and the presence of metal oxides (Upstate Medical University, 2003) which may exist in the form of sulphate aerosols in the atmosphere.

The Ca levels obtained at four study sites (Atlanta, Rubidoux, Shenandoah National Park, and Meadview) by Baron and Willeke (2001) between May 1998 and May 1999 in the USA, ranged from 0.03 to 0.16$\mu g.m^{-3}$.

2.6.3 SOURCE APPORTIONMENT STUDIES

Several studies conducted to identify sources of toxic trace metals of PM were successful in apportioning sources based on previous studies as well as different models. Various researchers have associated traffic sources with Zn, Cu, and Pb. A study conducted by Arslan (2001) showed that zinc might come from lubricating oils, tyres of motor vehicles and zinc in carburettors. A reasonable correlation between Zn, Cu and Pb supports the idea that vehicular traffic movement and industrial activities were the source of heavy metals in the area.

According to Jiries (2001) Zn and Cu may be derived from mechanical abrasion of vehicles as they are used in the production of brass alloy and come from brake linings, oil leak sumps and cylinder head gaskets. The high concentration of copper found may be associated with electrical and mechanical working. In a study conducted in an industrial area of Taejon, Korea, Pb was also found to be strongly correlated with crustal elements (Ba, Sb, Co, Fe, etc.) and fuel combustion (V). Strong correlations were also noticed among Pb, Fe, Zn, and Ti from a study conducted in Los Angeles by Chow *et al.,* (2003).

The co-presence of both Pb and Zn and moderate correlations between Pb and V observed by Mishra *et al.,* (2004b) in Seoul indicates that the contribution from fuel combustion is significant.

Principal component analysis has been used by several researchers including Sun *et al.,* (2004). The first factor that explained most of the variance (60.5%) observed during this study contained As, Zn, Pb, Ni, Cd, and Cu, representing the combined sources of industry and motor vehicle emission. In a study conducted by Pacyna (1998), metallurgical processes could produce the largest emissions of Cu, Ni, and Zn while according to Lee *et al.,* (1999) exhaust emissions from road vehicles could also contain various amounts of Cu, Zn, and Ni. The second factor showed high loadings for Fe, Mn, Mg, Ca, Ti, Al, and Na, and explained 17.8% of the total variance. This factor was

clearly associated with mineral aerosols that would likely originate from re-suspended road dust.

Al-Momani (2003) identified crustal material as the only source of Al. It is therefore logical to use Al as a tracer of crustal material. A strong correlation (a value near 1) between Al and any other element suggests crustal material as a major source of that particular element.

Metal smelting and fuel combustion were also identified by Nriagu, (1989) as a source of non-crustal volatile metals in the atmosphere. According to Held, *et al.,* (1996) the elements Zn and Mn can be used as tracers for smelting sources, K can be used for biomass burning, Cl for sea salt, sulphate for anthropogenic sources, and Al, Si, Ti for soil dust. Zn, excess Mn, Cu and Ni are unambiguous signals of anthropogenic smelting.

The co-presence of high Al, Mg, Si, Ca mixed with K, Fe, Mn, Zn indicates the contribution of a metal smelting source to particulate aerosols in this study, according to Begum *et al.* (2004), while the occurrence of Cr with Co or Ni indicates the anthropogenic origin of particulate aerosols (Mishra et al., 2004b).

Various studies have shown that the shape, size and colour of the particles can be used to identify the emission sources. Greyish particles of variable shapes and sizes, which are predominantly geological elements such as silica, iron, manganese and aluminium, have been identified in different studies. White particles of variable sizes and shapes as well are mostly chromium. The chromium particles arising from combustion are characterized, in most cases, by a spherical shape due to fundamental melting processes that occur during their formation (Anwari *et al.,* 1992). Crustal material suspended by the wind and particles generated during the processing of soil and industrial processing of minerals have irregular shapes indicative of the minerals being processed (Li *et al.*, 2000).

Spherical particles shown by some of the morphologies are normally associated with particles that have been formed in a high-temperature furnace. These are typically alumino-silicates, often with significant concentrations of iron that come from pyrites and other iron-containing minerals in coal. Elemental analysis indicates that a large portion of the spherical particles contain elevated concentrations of carbon, oxygen, and silicon and lesser quantities of magnesium, sodium, aluminum, sulfur, calcium, and silicon (Li *et al.,* 2000).

The method used by Resane (2004) to detect Cr(VI) in the Rustenburg area yielded concentrations ranging from 1.9 to 15.9 $ng.m^{-3}$, which is alarming since the US EPA suggests that 8 $ng.m^{-3}$ of soluble Cr(VI) species in air is associated with cancer risks (Resane, 2004).

It is clear from the literature study that large variations in concentration levels could be observed under different meteorological conditions. The literature has also shown that meaningful source apportionment can be achieved by performing chemical analysis of the trace element component of particulate matter. This information will be taken into account in the discussion of the results obtained during this study. The South African situation with regard to monitoring of particulate matter suggests the need for the development of characterisation methods for particulate matter.

CHAPTER 3

METHODOLOGY

In this chapter, the description and advantages of each of the methods used for sampling and analysis of particulate matter during this study are discussed. The principle of operation and the main components of each method are also discussed.

3.1 SAMPLING OF PM

Sampling refers to the collection of data that are representative of a system. In some cases, the data can be measured directly (temperature is an example), but often the representative sample has to be analysed or tested to determine the value of individual parameters. Important questions are the design of the sampling scheme and the protocols for the collection, storage, and transport of samples. The choice of sampling methods should always be made on the basis of an evaluation of factors such as reliability, accuracy, ease of operation, and cost.

The major prerequisite in selecting a sampling system is to determine what size ranges of particles are to be monitored and the method of analysis (if applicable). Selection of the analytical method is very important because it dictates the type of filter media and the compatible sampling system to be used. Several filter types are available, and the specific filter used depends upon the desired physical and chemical characteristics of the filter and the analytical methods used.

3.1.1 SELECTION OF FILTERS

In almost all sampling procedures, the samples of particulate matter are collected on some form of a filter. It is therefore important to note the basic characteristics and properties of filters in order to select the type of filter needed for sampling of air particulates. The basic characteristic of the types of filter material used in high volume sampling are outlined in Table 3.1, while useful filter properties are described in Table 3.2. Several characteristics are important in the selection of filter media and these include: particle sampling efficiency (filters should remove more than 99% of suspended particulate matter (SPM) drawn through them, regardless of particle size or flow rates), mechanical stability (filters should be strong enough to minimize leaks during sampling and wear during handling), chemical stability (filters should not chemically react with the trapped SPM), temperature stability (filters should retain their porosity and structure during sampling), blank correction (filters should not contain high concentrations of target compound analytes) (Baron & Willeke, 2001).

VISUAL FILTER INSPECTION

After purchased, all filters must be visually inspected for defects, and defective filters must be rejected if any are found. The following are specific defects to look for: Pinhole, a small hole appearing as a distinct and obvious bright point of light when examined over a light table or screen, or as dark spot when viewed over a black surface. Loose material, which includes any extra loose material or dirt particles on the filter must be brushed off before the filter is weighed. Discoloration, any obvious visible discoloration might be evident of a contaminant. Filter nonuniformity, any obvious visible non-uniformity in the appearance of the filter when viewed over a light table or black surface might indicate gradations in porosity across the face of the filter. A filter may also have imperfections not described above, such as irregular surfaces or other results of poor workmanship.

Table 3.1: *Characteristics of filter medium* (Baron & Willeke, 2001).

Cellulose Fiber (Cellulose Pulp)
▪ Low ash ▪ Maximum temperature of 150^0C ▪ High affinity for water ▪ Enhances artifact formation for SO_4^{2-} and NO_3 ▪ Good for x-ray/neutron activation analysis ▪ Low metal content
Quartz Fiber (Quartz spun with/without organic binder)
▪ Maximum temperature up to 540^0C ▪ High collection efficiency ▪ Non-hydroscopic ▪ Good for corrosive atmospheres ▪ Very fragile ▪ Difficult to ash: good with extraction
Synthetic Fiber (Teflon® and Nylon®)
▪ Collection efficiency > 99% for 0.01 μm particles ▪ Low artifact formation ▪ Low impurities ▪ Excellent for X-ray analysis ▪ Excellent for determining total mass of a non-hydroscopic nature ▪ Nylon fiber good for HNO_3 collection
Membrane Fiber (Dry gel of cellulose esters)
▪ Fragile: requires support pad during sampling ▪ High pressure drop ▪ Low residue when ashed

Table 3.2: *Summary of useful physical properties of various filter media (Seinfeld & Pandis, 1998)*

Filter And Filter Composition	Density mg/cm^2	pH	Filter Efficiency %
Teflon® (Membrane) $(CF_2)_n$ (2 μm Pore Size)	0.5	Neutral	99.95
Cellulose (Whatman 41) $(C_6H_{10}O_5)_n$	8.7	Neutral (Reacts with HNO_3)	58% at 0.3 μm
Glass Fiber (Whatman GF/C)	5.16	Basic pH - 9	99
"Quartz" Gelman Microquartz	6.51	pH - 7	98.5
Polycarbonate (Nuclepore) $C_{15}H_{14} + CO_3$ (0.3 μm Pore Size)	0.8	Neutral	93.9
Cellulose Acetate/Nitrate Millipore $(C_9H_{13}O_7)_n$ (1.21 μm Pore Size)	5	Neutral (Reacts with HNO_3)	99.6

3.1.2 FILTRATION

Filtration is a simple, versatile, and economic means for collecting samples of aerosol particles. Fibrous filters are the most economical means for achieving high-efficiency collection of submicrometer particles at low dust concentrations. Table 3.3 gives some common aerosol sampling filter materials. The most important types of filters for aerosol sampling are fibrous and porous membrane filters (Hinds, 1999).

Besides collection efficiency and pressure drop, the selection of a filter for aerosol sampling may depend strongly on the analytical method to be used. Glass fiber and cellulose ester filters are much less affected by moisture and age while polycarbonate, polyvinyl chloride, and Teflon filters are the least affected. If aerosol particles are to be analysed by chemical methods, the interferences caused by the filter material or contaminants in the filter should be taken into consideration.

Table 3.3: *Characteristics of some common aerosol-sampling filter materials*

Filter	Type	Material	Thickness (mm)	Pore Diameter (μm)	Solidity	Pressure Drop[a] (kPa)	Efficiency[a,b]	Filter Quality[a,b] (kPa^{-1})
Whatman	Fiber	Cellulose	0.19	3-20	0.35	2.5[c]	72[c]	0.52
41	CPM[d]	Polycarbonate	0.01	0.8	0.85	5.9	92[e]	0.39
Nuclepore	Fiber	Polystyrene	1.5	0.7	0.04	2.9	99.5	1.10
Microsorban	Fiber	Glass	0.23	0.1-4	0.10	2.0[c]	99.93[c]	3.70
MSA 1106B	Membrane	Cellulose	0.15	0.8	0.19	9.5[c]	99.98[c]	0.93
Millipore AA		Ester						

[a] *At U_0 = 0.27 m/s [27 cm/s].* [b] *For d_p = 0.3 μm.* [c] *From Lippmann (1995).*
[d] *CPM = capillary pore membrane.* [e] *Estimated.*

3.1.3 SAMPLERS

TAPERED ELEMENT OSCILLATING MICROBALANCE (TEOM)

TEOM series 1400a monitor incorporates the patented tapered-element oscillating microbalance technology to measure particulate matter mass concentration continuously. The monitor can be configured with a variety of sample inlets to measure PM10, PM2.5, PM1 or total suspended particulate (TSP) concentrations (Rupprecht & Patashnick, 2002).

TEOM series 1400a monitor is composed of two major components namely the TEOM sensor unit and the TEOM control unit. The sensor unit contains the mass measurement hardware that continuously monitors the accumulated mass on the systems exchangeable filter cartridge. The TEOM device can calculate the mass concentration of the sample stream in real time by maintaining a flow rate of 3 L/min through the instrument and measuring the total mass accumulation on the filter cartridge.

The TEOM series 1400a monitor is a true 'gravimetric' instrument that draws ambient air through a filter at a constant rate continuously weighing the filter and calculating near real time (10 minute) mass concentration. The Figure 3.1 below is a sketch showing the main components of a TEOM.

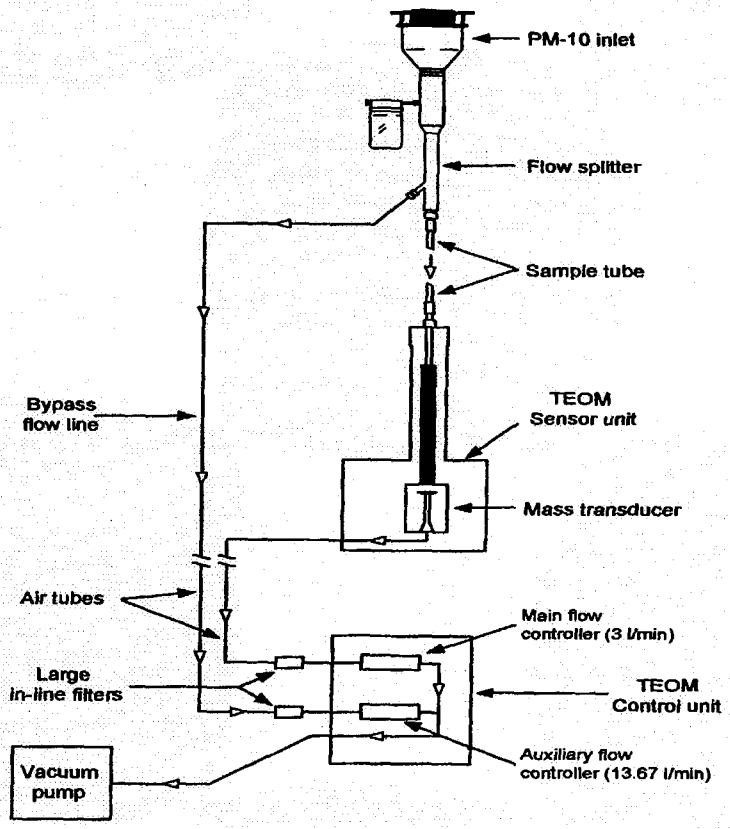

Figure 3.1: *Schematic diagram of TEOM*

The TEOM mass transducer weighing principle is the same as that of a laboratory microbalance in that the mass detected by the sensor is the result of the measurement of a change in a parameter (frequency in TEOM) that is directly coupled via a physical law.

The tapered element is a hollow tube clamped on one end and free to oscillate at the other end, which is found at the heart of the mass detection system. An exchangeable filter cartridge is placed over the tip of the free end. The sample stream is drawn through this filter paper, then down the tapered element (Center for Environmental Research Information, 1999).

The tapered element oscillates precisely at its natural frequency and a precision electronic counter measures the oscillation frequency with a 2-

second sampling period. The tapered element is in essence a hollow cantilever beam with an associated spring rate and mass and if the additional mass is added, the frequency of the oscillation decreases. In a spring mass system, the frequency follows the equation:

$$F = \left(\frac{K}{M}\right)^{0.5} \tag{3.1}$$

Where F = Frequency (radians /second)

K = Spring rate

M = Mass

K and M are in consistent units and the relationship between mass and change in frequency can be expressed as:

$$dm = k_o\left(\frac{1}{f_1^2} - \frac{1}{f_0^2}\right) \tag{3.2}$$

Where dm = Change in mass

k_0 = Spring constant (including mass conversion)

f_0 = Initial frequency (Hz)

f_1 = Final frequency (Hz)

$$k_0 = \frac{dm}{\left(\frac{1}{f_1^2} - \frac{1}{f_0^2}\right)} \tag{3.3}$$

The calibration constant k, of an instrument can be easily determined by measuring the frequencies with and without a known mass (pre-weighed filter cartridge).

3.2 ANALYSIS OF PARTICULATE MATTER

Analysis of samples is a critical step; the value of the results of the monitoring depends greatly on the degree of confidence that can be assigned to the analysis. The two methods used for analysis of particulate matter in this study are Scanning Electron Microscopy coupled with Energy Dispersive Spectrometry (SEM/EDS) and Inductively Coupled Plasma Mass Spectroscopy (ICP-MS).

3.2.1 SCANNING ELECTRON MICROSCOPY

Scanning Electron Microscopy (SEM) is a technique commonly used to examine the microstructure of bulk specimens (Chung *et al.,* 2001). The technique is a valuable imaging tool, which resolves specimens to very fine details and can be used to determine the elemental composition of specimens. SEM provides topographical and elemental information at magnifications of 10 times to 10^5 times with virtually unlimited depth of field (Skoog *et al.,* 1998).

Applications of SEM include materials evaluation which involves grain size, surface roughness, porosity, particle size distributions, material homogeneity, intermetallic distribution and diffusion, failure analysis which gives results on contamination location, mechanical damage assessment, electrostatic discharge effects, and micro-crack location, quality control screening which involves dimension verification, film and coating thickness (Skoog *et al.,* 1998).

In the SEM analysis, a source of electrons is used to illuminate the sample; the electrons are accelerated down the column passing through electromagnetic lenses and apertures to form a fine probe at the surface of the specimen in the chamber area. The beam is scanned across the surface of the specimen by means of scan coils and appropriate detectors collect signals. The output of detectors modulates the brightness of a cathode ray tube. The area scanned on the cathode ray tube is larger than the area on the

sample thus magnification is achieved and information from the sample is built up as a two-dimensional image.

COMPONENTS OF SEM

The main components of a scanning electron microscope, which include the electron gun, the electromagnetic lenses, the scan coils and detectors, are shown in Figure 3.2.

The electron gun, which is a stable source of electrons, is held at negative potential relative to the earth potential and the electrons are emitted from the filament by thermionic emission (Goldstein *et al.*, 2003). The anode is at the base of the gun chamber and is held at the earth potential. Electrons accelerate from the high negative potential of the filament towards the anode, through a hole in the anode which allows electrons to move down the column to the specimen.

Electromagnetic lenses are used to focus electrons in the microscope. The lenses demagnify the source of electrons to form a much smaller diameter probe incident on the sample. The electromagnetic lens is essentially a coil of wire around a metal cylinder (solenoid). The magnetic field for the coil is given by the equation

$$H = NI \qquad (3.4)$$

where H is the magnetic field, N is the number of turns of the coiled wire, I is the current. The diversion of the electron path caused by these lenses depends on the magnetic field, the velocity and the direction.

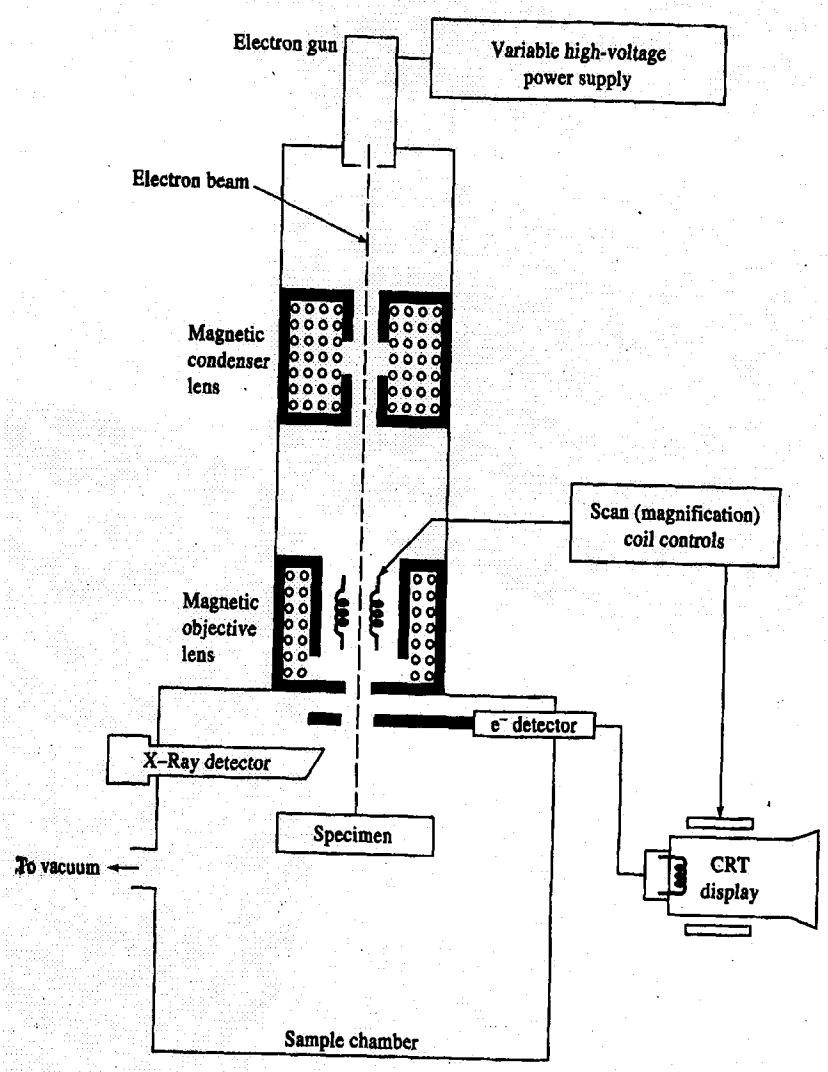

Figure 3.2: *A typical sketch showing the different components of an SEM*

The two main types of lenses used in the SEM are the condenser lens(es) and the objective lens. The condenser lens is the first lens and it controls the intensity of the electron beam. The electron beam converges and passes through a focal point. The position of the focal point moves up and down with H (Skoog *et al.*, 1998). The condenser lenses also affect the number of electrons in the beam for a given objective aperture size.

The objective (final) lens focuses the electron beam on to the specimen whilst preventing the interference between secondary electrons and the emitted X-

rays. The strength of the objective lens changes the distance between the pole piece and the plane onto which the electrons are focused.

The deflection scan coils are situated above the objective lens and are used to raster the electron beam on the surface of the specimen. Scanning occurs when a current is applied to each of the vertical and horizontal scan coils, and the probe is deflected to cover a rectangular area on the specimen. The gun shift coils and tilt coils are used to align the gun while the image shifting coils are used to move the image (Chung *et al.*, 2001).

The main types of detectors used in the SEM are the scintillator type detector, also known as the secondary electron detector (SE) and the solid-state type detector, also known as the backscatter electron detector (BSE). The BSE, which is usually mounted close to the specimen and is split into four quadrants; is very thin, thus allowing simultaneous X-ray microanalysis.

The standard detector used in scanning electron microscopy is a combined secondary and backscatter detector; known as the Everhart-Thornley detector, which consists of a Faraday cage, light pipe and photomultiplier tube (PMT). The scintillator produces light when struck by electrons, the light pipe transports light from the scintillator to the PMT. The PMT amplifies light and converts it to an electrical signal (Skoog *et al.*, 1998).

The most common mode of the Everhart-Thornley detector is with a positive bias of around 500V on the Faraday cage, which deflects the trajectories of the secondary electrons emitted from the sample into the detector.

PROPERTIES OF SEM

The SEM has important properties, which should always be considered so as to get reliable results. These include the working distance, depth of field, resolution, and magnification.

Working distance is the distance between the lower pole piece of the objective lens and the position of the specimen at which the electrons are focused onto the specimen.

The depth of field (DOF) is the range (distance) above and below the plane of focus which appears to be in focus. The DOF is inversely proportional to the angle of electron beam (aperture angle) and hence can be enhanced by reducing the final lens aperture and lowering the specimen (i.e. increasing the working distance). The depth of field characterizes the extent to which image resolution degrades with distance above or below the plain of best focus (Chung *et al.,* 2001). A microscope with greater depth of field can image 3-dimensional samples better.

Resolution in the SEM is determined by the spot size. Small spots give high resolution. Beam divergence also affects resolution since the spot size increases with increasing working distance.

Resolution in the light microscope is limited by the wave nature of light according to the Abbe's equation:

$$d = 0.612 \lambda / n \sin \Phi \qquad (3.5)$$

where d is the resolution, λ is the wavelength, n is the index of refraction, and Φ is the aperture angle (Goldstein *et al.*, 2003).

Magnification is a function of the sample area that is scanned. The scanning area increases with the working distance whilst magnification decreases with the working distance.

TYPES OF SIGNALS PRODUCED IN THE SEM

The main types of signals produced in SEM are energy secondary emission, Auger electron generation, characteristic X-ray emission, Bremstrahlung, backscattered electron emission and cathodoluminescence. Each type of

signal originates within a specific volume of interaction, for example, secondary electrons, backscattered electrons and X-rays.

Secondary electrons are the smallest in volume and they determine both the spatial resolution and depth from which analysis can be achieved. These electrons are emitted due to inelastic scattering of an energetic electron with outer valence electrons when backscattered electrons exit the sample, often some distance away from the beam spot. Secondary electron imaging shows the topography of surface features of a few nm across. Films and stains as thin as 20 nm produce adequately contrasted images (Skoog *et al.,* 1998).

Backscattered electrons give information about the composition and surface topography of the specimen. Electrons re-emitted through the surface of the material as incident electrons strike the bulk specimen. Backscattered electron-imaging shows the spatial distribution of elements or compounds within the top micron of the sample (Skoog *et al.,* 1998).

X-rays can be produced of the inelastic scattering of the incident electrons with matter. The processes involved are the characteristic X-ray emission and continuum X-ray emission. The X-ray microanalysis specifically gives information about the elemental composition of the specimen, in terms of both the quantity and distribution. The microanalysis of the sample results in structural, compositional and chemical information about the sample.

Energy Dispersive X-ray Spectroscopy (EDS) identifies the elemental composition of materials imaged in a SEM for all elements with an atomic number greater than boron (Chong *et al.,* 2002). The characteristic X-rays detected by the X-ray spectrum are sorted out in terms of energy and the peaks on the spectrum correspond to the elements present in the sample. The relative intensities on the spectra represent abundances of the elements present. The lines and therefore the elements, are identified by reference to a database stored in the computer memory.

In quantitative analysis the amount of a particular element present in the analysed volume of a specimen is determined. The intensities of X-ray lines from the specimen are compared with those from standards of known composition. The composition of the analysed volume is then calculated by applying matrix corrections. It is important that the analysed volume should be homogeneous and representative of the specimen.

3.2.2 INDUCTIVELY COUPLED PLASMA MASS SPECTROSCOPY

ICP-MS is a powerful and rapidly developing technique for multi-element determinations at very low levels in solution or liquid samples. The primary goal of ICP is to get elements to emit characteristic wavelength specific light, which can then be measured. The detection limits can be at single parts per trillion or below for about 40 to 60 elements in solution and a dynamic range of 10^4 to 10^8 . In ICP-MS, a conventional inductively coupled plasma (ICP) source is used to produce the primary ions, which are then analysed in a quadrupole mass spectrometer with a mass range up to 300 and unit resolution across the range (Skoog *et al.,* 1998).

A typical ICP-MS instrument as shown in Figure 3.3 consists of a sample introduction system (a nebulizer and spray chamber), an inductively coupled plasma source, a differentially pumped interface, ion optics, a mass spectrometer, and a detector.

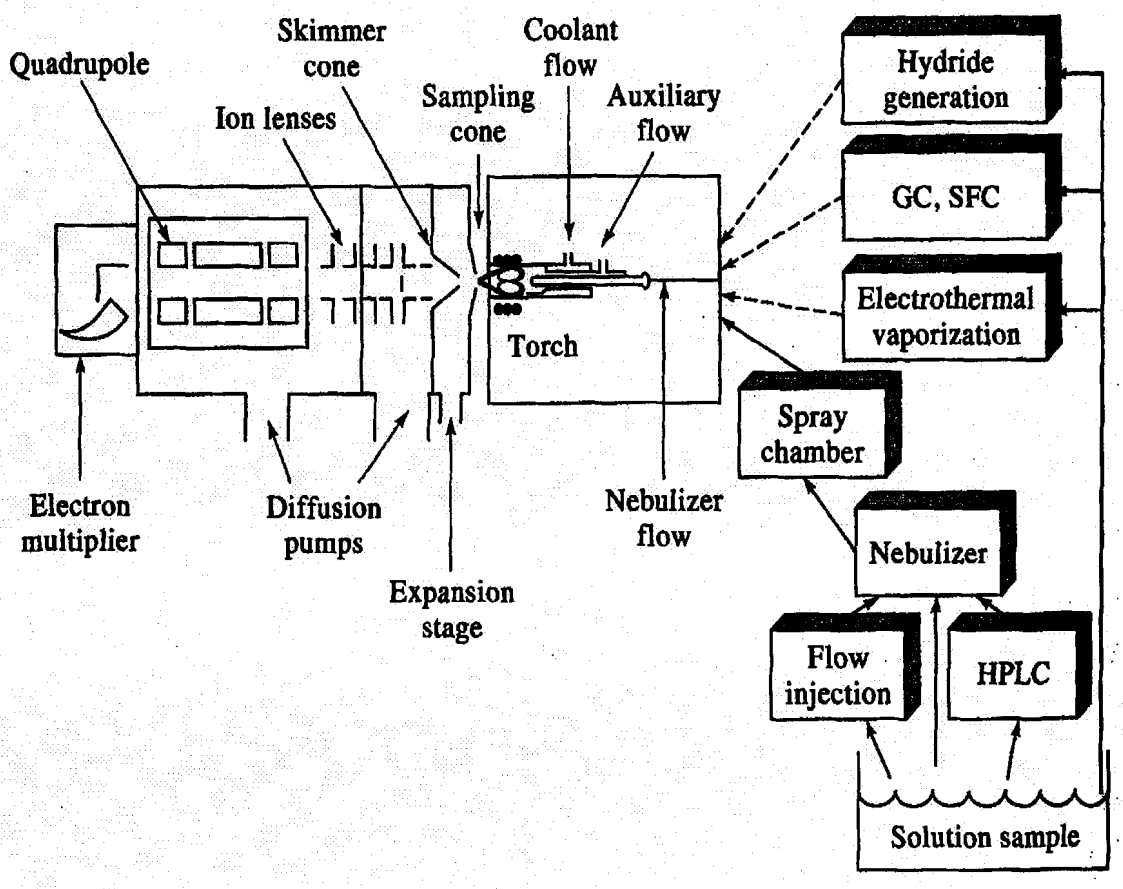

Figure 3.3: *Typical schematic diagram of an ICP-MS*

THE ION SOURCE: ICP

The ion source used in this technique is the inductively coupled plasma (ICP). ICP is a flowing, partially ionised gas (typically Ar), which is sustained in a quartz torch that consists of three tubes. A conventional inductively coupled plasma (ICP) source is used to produce primary ions, which are then analysed in a quadrupole mass spectrometer with a mass range of up to 300 and a unit resolution across the range (Herbst, 1984).

Argon is the most commonly used plasma gas because it is generally inexpensive, inert, and mono-atomic; and produces a relatively simple background spectrum. The plasma has an annular (or doughnut) shape

because most of the radio frequency current is carried in a thin skin on the outside of the plasma.

SAMPLE INTRODUCTION

The role of the sample introduction systems is to convert a sample into a form that can be effectively vaporized into free atoms and ions in the ICP. A peristaltic pump is typically used to deliver a constant flow of sample solution (independent of variations in solution viscosity) to the nebuliser.

Several different kinds of nebulisers are available to generate the sample aerosol, and several different spray chamber designs have been used to modify the aerosol before it enters the ICP.

Gases can be directly introduced into the plasma, for example after hydride generation. Electro-thermal vaporization or laser can introduce solids.

The Spray Chamber

Aerosols that are too large to be vaporised effectively in the plasma (>20 μm diameter) are eliminated in the spray chamber. The spray chamber also limits the total amount of solvent liquid aerosol and vapour that enters the plasma. The aerosol existing in the spray chamber enters the hot, atmospheric pressure plasma gas (typically argon).

Spray chambers were designed mostly empirically for use with conventional pneumatic nebulisers during the development of ICP optical emission spectrometry. The main purpose of the spray chamber was thought to be to remove large droplets that would not have sufficient time to be completely vaporized during their 1 to 2-msec travel in the plasma, although what size was too large was not directly known until recently.

A spray chamber is also necessary to limit the amount of solvent that enters the ICP (less than about 20 ml/min of aqueous aerosol and 30 mg/min of

water vapour). When water aerosol and vapour loading are higher, the plasma is cooled and molecular oxide formation increases.

The Nebuliser

Pneumatic nebulisers are the most commonly used to generate aerosols for ICP-MS. Typically, the nebuliser gas flow rate is 0.5 to 1.0 l/min at a pressure of 50 psi or less.

In the concentric nebuliser, a ring through which gas passes at a sonic velocity surrounds the liquid-carrying tube. The average drop size of the aerosol depends on the gas flow rate, ring orifice area, inner diameter of the sample-carrying capillary, and thickness of the wall of the centre capillary (Chung *et al.*, 2001).

In the cross-flow nebuliser, the gas is introduced through an orifice at a right angle to the solution carrying tube. Shear produced by differences in the gas and liquid velocities breaks the liquid up into filaments that relax to form droplets.

The size of the aerosol drops in the initial (primary) aerosol depends on the design of the nebuliser, the nebuliser gas flow rate, and, to a lesser extent, the sample uptake rate.

The Interface

The main reason for the success of the ICP-MS technique has been the development of a suitable interface. The interface allows the coupling of the ICP source (at atmospheric pressure) with the mass spectrometer (at high vacuum) while still maintaining a high degree of sensitivity (Chung *et al.*, 2001).

MASS SPECTROMETER

Most ICP-MS instruments are based on quadrupole mass spectrometers. The mass spectrometer acts as a filter, transmitting ions with a pre-selected mass or charge ratio. These transmitted ions are then detected with a channel electron multiplier.

Mass analysers can be of the double focusing or quadrupole type. The quadrupole analyser consists of four straight metal rods positioned parallel to and equidistant from a central axis. By applying direct current (DC) and radio frequency (RF) voltages to opposite pairs of the rods it is possible to have a situation where the DC voltage is positive for one pair and negative for the other. In a similar way, the RF voltage on each pair is then 180 degrees out of phase, i.e. they are opposite in sign, but with the same amplitude (Skoog *et al.,* 1998).

Ions entering the quadrupole are subjected to oscillatory paths by the RF voltage. By selecting the appropriate RF and DC voltages only ions of a given mass or charge ratio will be able to traverse the length of the rods and emerge at the other end. Other ions are lost within the quadrupole analyser. If their oscillatory paths are too large they will collide with the rods and become neutralised. The transmitted ions are then detected with a channel electron multiplier. Extensive use of computer control and optimised geometry means that a full elemental analysis can be made in one scan, with measurement times of about 10s per element, even for concentrations as low as the ppb level (Rouessac and Rouessac, 2000).

For multi-element analysis, RF and DC voltage scanning is required. Scanning, and hence data acquisition, can be carried out in several modes. The possibilities are as follows: a single continuous scan, peak hopping, multi-channel scanning.

ICP-MS has the ability to separate weak signal intensity at mass M from an adjacent major peak, i.e. at M+ 1 or M-l. This is termed abundance sensitivity.

This is an important factor in ICP-MS when ultra trace analysis is being carried out against a background of a major element impurity (or the sample matrix) the proverbial needle (ultra trace element of interest) in a haystack (sample matrix).

DETECTORS

Several different detectors have been used in ICP-MS instruments. These include the Channeltron electron multipliers, Discrete dynode electron multipliers, Daly detectors and Faraday collector detectors.

The counting rate in the detection system is 2 - 4 x 10^6 pulses per second and is determined such that the detector may only sustain a maximum current flow, and the response time or 'dead time' of the detector and electronics (which is the time during which an avalanche of electron occurs) of the detector is blind or dead for a new pulse. If the time interval between the arrivals at the detector of two ions is shorter than the dead time, the second ion is detected.

The alinearity caused by the dead time can be corrected mathematically using the equation

$$N' = \frac{N}{(1 - ND)} \qquad (3.6)$$

where N' is the true or estimated count rate, N is the observed count rate, D is the dead time. The correction can be carried out by the ICP-MS software (Bradford & Cook, 2004).

If an electron absorbs sufficient energy, equal to its first ionisation energy, it escapes the atomic nucleus and an ion is formed. In the ICP the major mechanism by which ionization occurs is thermal ionisation. When a system is

in thermal equilibrium, the degree of ionisation of an atom is given by the equation:

$$\frac{n_i n_e}{n_a} = 2\frac{Z_i}{Z_a}\left(2\pi mkT/\eta^2\right)^{3/2}\exp\left(-E_i/kT\right) \qquad (3.7)$$

where n_i, n_e and n_a are the number of densities of the ions, free electrons and atoms respectively, Z_i and Z_a are the ionic and atomic partition functions respectively, m is the electron mass, k is the Boltzmann constant, T is the temperature; η is Planck's constant and E_i is the first ionisation energy.

INTERFERENCES

Matrix-dependent effects result from the presence of an excess salts in the plasma source and lead to a loss in sensitivity. In addition, blockages in the nebuliser can result in erratic signal generation from high-solid-content samples, while mass discrimination can also occur (Vaughan and Horlick, 1986).

The occurrence of matrix interferences can result in signal enhancement or depression with respect to the atomic mass. An example of an isobaric interference would be mass 58, where nickel (67.8% abundance) and iron (0.31% abundance) both occur. For nickel 60 (26.23), no interfering element occurs. Another element of interest is atomic mass 51 where vanadium (99.76%) and no interfering element occurs. With chromium 52 (83.76) an interfering element does not occur.

.....

It follows from the discussion that the selected sampling and analysis methods (TEOM, SEM/EDS and ICP-MS) have several advantages and disadvantages. These methods, however, contribute to a better understanding of aerosol composition and characteristics. It is worth noting that the efficiency

of these methods depends, among other things, on proper operating procedures and quality control.

.....

CHAPTER 4

EXPERIMENTAL PROCEDURE

This chapter gives a brief description of the sampling sites used, and the actual sampling and filter analysis procedures, as well as the statistical analysis procedures followed during the study.

The experimental procedure for this study involved sampling of particulate matter using TEOM and analysis using SEM-EDS and ICP-MS. The theory of these methods was discussed in Chapter 3.

4.1 SITE DESCRIPTION

Sampling of PM was done at three sites namely Site A with latitude $25^0$43′03,0′′E and longitude $27^0$23′57,8′′S, Site B with latitude $25^0$40′01,3′′E and longitude $27^0$16′38,5′′S, and Site C with latitude $25^0$30′15′′E and longitude $27^0$5′45′′S. These sites are representative of well-defined environments, exposure situations or source activities like remote areas, urban background, traffic and industry. The map in Figure 4.1 shows the exact location of Sites A, B and C within the Rustenburg district.

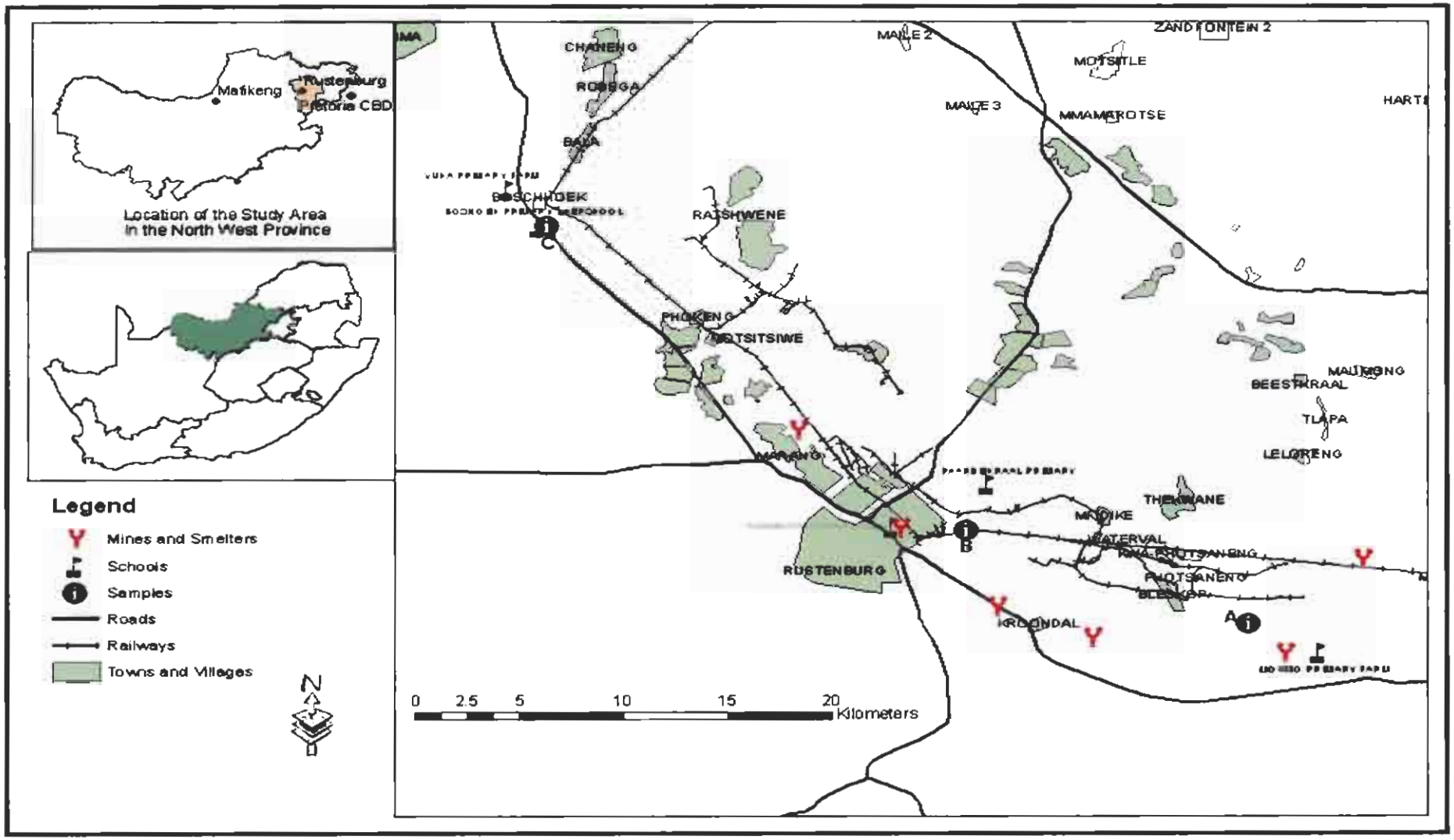

Figure 4.1: *A map showing sampling Sites A, B and C in the Rustenburg District*

4.2 SAMPLE COLLECTION

The sampling equipment used for this study is the tapered element oscillating microbalance (TEOM Series 1400A), which is composed of a control unit and a sensor unit. The PM samples were collected onto teflon-coated boroscilate fiberglass filters. The ambient sample stream was allowed to pass through the PM10 inlet at a flow rate of 16.7 L/min, which was then isokinetically split into a 3L/min sample stream that was sent to the instrument's mass transducer and a 13,7L/min exhaust stream. The TEOM device can calculate the mass concentration of the sample stream in real-time by maintaining a flow rate of 3 L/min through the instrument and measuring the total mass accumulation on the filter cartridge.

The sample stream is preheated to 50°C before entering the mass transducer so that the sample filter always collects the sample under the conditions of very low, and therefore relatively constant humidity.

The TEOM series 1400a monitor must be operated with a filter installed in the mass transducers. A filter must be installed before applying the power to the instrument. TEOM filters must not be handled with fingers, the filter exchange tool provided with the instrument must be used, and the tool must be clean and free of any contaminations.

The door of the TEOM sensor must be opened for the shortest time possible to minimise temperature changes in the system. The TEOM filters must be preconditioned to avoid excessive moisture build-up prior to their use in the system. Two holders on the right side of the mass transducer (inside) must be used to store the next two TEOM filters to be used. TEOM filters generally exhibit a filter loading percentage of 15% at a main flow rate of 3 L/min and less at lower flow rates and this filter loading is displayed on the monitor's main screen.

4.3 ANALYSIS OF FILTERS

The ESEM FEI QUANTA 200, coupled with the OXFID ENCA 200 EDS, was used during the analysis of samples. The requirements for sample analysis by SEM are that the sample has to be stable under vacuum conditions, it has to be conductive to allow electron beam irradiation, and lastly the substrate of sample should fit well into the sample stage. The samples were analysed at high vacuum, with a voltage of 15kV and the working distance of 10mm. A dead time of forty percent, which corresponds to a live time of 100 seconds, was used during the analysis of samples.
The filters were fixed onto sample studs to ensure good electrical connection between the specimen and the microscope stage. The samples were not coated. The filters were scanned several (10) times (1 scan per 10 second) to ensure that a representative portion of the sample is covered. No extraction was performed.

Peaks were identified manually by entering the atomic symbol and then scrolling through the periodic table. The other way of identifying peaks is with auto ID, where the auto key is used to find peaks and label them. The quantifying function of the computer programme was used to determine the peak intensities and the resulting intensities were converted to percentage weight.

The samples collected on filters were also analysed using the Agilent ICP-MS 7500c with the operating conditions and measurement parameters given in Table 4.1. The procedure for ICP-MS analysis involved weighing of the filters, digestion, dilution, and measurements. Air particulates collected on filters were extracted into a dilute nitric acid solution by sonication with heating. The extraction solution was stored at room temperature until analysis by ICP-MS.

Table 4.1: *Operating conditions and measurement parameters for ICP-MS*

Rf power	1.6kW
Rf Matching	1.64V
Carrier gas flow rate	1.09L/min
Wash time	5s
Rinse time	60s
Replicates	3
Sample uptake rate	55s
Sample stabilization	45s

A relatively new system, by which most of the interferences can be resolved, uses a quadrupole-, hexapole- or octapole-collision (reaction) cell. The cell is flushed with a reaction or buffer gas and the argon (polyatomic) ions are neutralised and/or eliminated. The lower levels of interferences observed in the high-pressure quadrupole reaction cell are the results of more collisions that lead to thermal equilibrium. Table 4.2 shows the isotopic abundances and the theoretically possible interferences.

Table 4.2: *Measured isotopes, isotopic abundances and potential Interferences (Vaughan and Horlick, 1986)*

Isotope Mass	Element	Isotope Abundance (%)	Interferences		Method Detection Limit (µg/L)	Reason For Use Of Isotope
			Isobaric	Polyatomic Ions		
53	Cr	9.5	Fe	HSO, ArC, HClO, ClO, ArOH, ArNH, SO	5	For high C and low Cl
60	Ni	26.4		CaO, CaOH, MgCl, NaCl		
51	V	99.8		HSO, ArC, ClO, ClN, ArNH, ArN, SO, SN	1	Abundance
57	Fe	2.1		CaO, ArO, ArOH, CaC, CaN, CaOH, MgO_2, ArF	50	Abundance and background
29	Si	4.7		CO, N_2, BO, SiH, AlH, COH, N_2H	10	
43	Ca	0.14	Sr^{2+}	MgO, BO_2 , AlO, CaH, CNO, SiO, CO_2	100	Low background, least interference
66	Zn	27.9	Ba^{2+}	TiO, VO, SO_2, PCl, FeC, S_2, SO_2H	2	For medium Ti and S
47	Ti	7.3	Zr^{2+}	NO_2, PO, SiO, CCl, SNH, SiOH, SN, N_2, NO_2H	10	Least interference

4.4 STATISTICAL ANALYSIS OF THE DATA

The statistical methods used in this study include correlation coefficients, regression analysis, and principal component analysis (PCA).

CORRELATION COEFFICIENT

Correlation coefficient (*r*) is a measure of the degree of linear relationship between two variables, usually labelled X and Y. The emphasis is on the

degree to which a linear model may describe the relationship between two variables. The correlation coefficient may take on any value between positive and negative one.

$$-1.00 \leq r \leq +1.00 \qquad (4.1)$$

The sign of the correlation coefficient (+, -) defines the direction of the relationship, either positive or negative. A positive correlation coefficient means that as the value of one variable increases, the value of the other variable increases; as one decreases the other decreases. A negative correlation coefficient indicates that as one variable increases, the other decreases, and vice-versa. The nearer r is to 1 or –1, the better the correlation and if r =0 then there is no correlation.

The Pearson's correlation coefficient is used for computing the correlation between two ratio scaled random variables. Pearson's correlation coefficient (r) is defined by:

$$r = \frac{n\sum xy - \sum x \sum y}{\sqrt{[n\sum x^2 - \sum (x)^2] * [n\sum y^2 - \sum (y)^2]}} \qquad (4.2)$$

where:

r = the correlation coefficient

x = the values of the independent variable

y = values of the dependent variable

n = number of paired data points

PRINCIPAL COMPONENT ANALYSIS (PCA)

PCA is a variance-orientated technique. The factor analysis technique (PCA analysis) is based on the calculation of factors, which are expressed by eigenvalues, as constituents of eigenvectors. Eigenvectors are correlated with specific combinations of emission sources of elements, which affect the

receptor (Seinfeld & Pandis, 1998). The PCA eigenvectors provide information about the contribution that each variable makes to a component.

It is a way of identifying patterns in data, and expressing the data in such a way as to highlight their similarities and differences. Since patterns in data can be hard to find in data of high dimension, where the luxury of graphical representation is not available, PCA is a powerful tool for analysing data. The other main advantage of PCA is that once you have found these patterns in the data, you can compress the data by reducing the number of dimensions, without much loss of information (Smith, 2002). The eigenvector with the highest eigenvalue is the principle component of the data set.

Principal component analysis (PCA) is a technique to reduce the dimensionality of a data set. PCA aims to determine few principal components (PC) that can explain as much of the total variance in the measured data as possible. The PCs are linear combinations of the observed variables, mass spectral peak intensities in the case of this study. After matrix calculations, a *loading* is determined that quantifies the correlation between each pair of observed variable and new PC (Haefliger, *et al.*, 2000).

The sum of the eigenvalues is the same as the number of variables. Indeed they will always add up to the number of variables if a correlation matrix, rather than a covariance matrix, is analysed. When a correlation matrix is used, each of the variables is standardised to have a mean of 0 and a variance of 1.0. Thus, the total variance to be partitioned between the components is equal to the number of variables.

The eigenvectors are termed component loadings and they are used to calculate the component scores.

.....

The site description, sampling and analysis procedures discussed in this chapter give a picture of what was actually done during the experimental part

of this study. The site description gives an indication of the activities that may influence the concentrations of particulate matter measured.

.....

CHAPTER 5

RESULTS ON THE LEVELS OF PARTICULATE MATTER

This chapter presents the results obtained from the three study sites within the Rustenburg area. Trends in the levels of PM10 within the area are established and the seasonal variations in the levels obtained from each site are discussed. The levels are also related to the domestic and industrial activities, as well as to the meteorology within the study area.

The data presented herein was obtained from the Tapered Element Oscillating Microbalance (TEOM), the methodology of which is discussed in Chapter 3. The experimental procedure is given in Chapter 4. The sampling of PM was performed at three different sites identified as Site A, B and C. The sampling period for seasonal variations lasted for 12 months i.e. from February 2004 to January 2005, during which three sampling sites within the Rustenburg area were covered. Sampling could not be performed simultaneously at the three sites since the TEOM had to be moved from one site to another.

5.1 PM10 AND METEOROLOGY

Meteorological observations are critical for analysing and predicting atmospheric dispersion of gases and particles. Depending upon which dispersion variables (e.g. transport, diffusion, stability, deposition, plume rise) are important for a particular problem, a corresponding suite of meteorological

parameters must be quantified through observation, modelling or a combination of both. These parameters can include wind speed and direction, temperature, humidity, precipitation type and intensity, mixing height, turbulence, and energy fluxes (Dabberdt *et al.,* 2004).

Table 5.1 shows the meteorology of the Rustenburg area for the entire study period. There seems to be little or no trend in the wind direction measured during the study, since for the year 2004, the winds were mainly NNW while for 2005 they were mainly SSW. This makes it difficult for one to determine accurately the sources of pollution within the area, since the directions stated below imply that Site A and B were downwind in 2004 and upwind in 2005. According to Figure 4.1, Site A was downwind to the smelters and human settlements in the area in 2004, while Site B was downwind to the central business district (urban area). The wind directions stated below suggest that the reverse of the situation above occurred in 2005.

There are arguments by Preston-Whyte and Tyson (1988) about whether or not relative humidity has more impact on the PM10 levels than temperature. The data on relative humidity in this study is insufficient and cannot be used to validate the statement made above. However, for the months of March to May 2004, a decrease in relative humidity (85, 80, and 76%) corresponds to a decrease in temperature, which also corresponds to a decrease in the levels of PM.

Results obtained by Anwari *et al.* (1992) indicate that temperature and mixing height most strongly influence gaseous concentrations like ozone, while moisture levels (particularly relative humidity) are the strongest predictors of PM concentrations in all the five cities examined. Meteorological variability typically accounts for 40–70% of ozone variability and 20–50% of PM variability.

Table 5.1: *Monthly average meteorological data for the Rustenburg area supplied by the South African Weather Services (SAWS)*

Season	Month	Temperature (°C)		Rainfall (ml)	Wind Speed (m/s)	Wind Direction (Degrees from true North)
		Min	Max			
Autumn	Mar -04	14.7	25.9	11.0	15.5	347 (NNW)
	Apr -04	12.4	25.4	27.4	16.3	337 (NNW)
Winter	May –04	7.0	24.3	0.2	8.7	337 (NNW)
	Jun –04	2.7	19.4	5.2	12.2	354 (NNW)
	Jul –04	1.0	19.6	0.0	13.3	349 (N)
Spring	Aug –04	6.5	23.8	1.6	15.7	349 (N)
	Sep –04	7.5	25.7	0.2	16.7	340 (NNW)
	Oct –04	12.5	28.8	39.4	9.4	176 (S)
Summer	Nov –04	15.3	31.5	38.2	10.2	165 (SSE)
	Dec –04	16.0	29.2	83	10.4	163 (SSE)
	Jan – 05	17.4	29.4	160	9.0	204 (SSW)
Autumn	Feb - 05	16.5	29.7	78.6	8.5	161 (SSE)
	Mar - 05	14.1	27.3	42.4	8.8	190 (S)
	Apr – 05	11.5	23.2	91	7.3	196 (SSW)
Winter	May - 05	6.4	23.5	0.8	6.7	188 (S)
	Jun – 05	4.4	22.6	0.0	6.8	205 (SSW)
	Jul - 05	2.8	22.0	0.0	6.0	164 (SSE)

5.1.1 PM10 AND METEOROLOGY AT SITE A

The meteorology of an area can change many times in one day. It is thus important to use daily PM10 mass concentrations in assessing the impact of meteorology on the PM10 levels. Figure 5.1 shows the daily PM10 levels, relative humidity, and temperature at Site A.

The relation between relative humidity and mass concentrations of PM10, though weakly portrayed, showed from 3 May to 10 May 2004 (Figure 5.1), that a decrease in relative humidity was linked with an increase in levels of PM10. PM10 contains hygroscopic components (sulphates, nitrates and sea-salt), which attract water (Al-Momani, 2003). Due to this uptake, particles in

the PM10 may become so large that they cannot be collected using a PM10 sampler. This normally causes concentration losses that account for a decrease in PM10 concentrations as relative humidity increases.

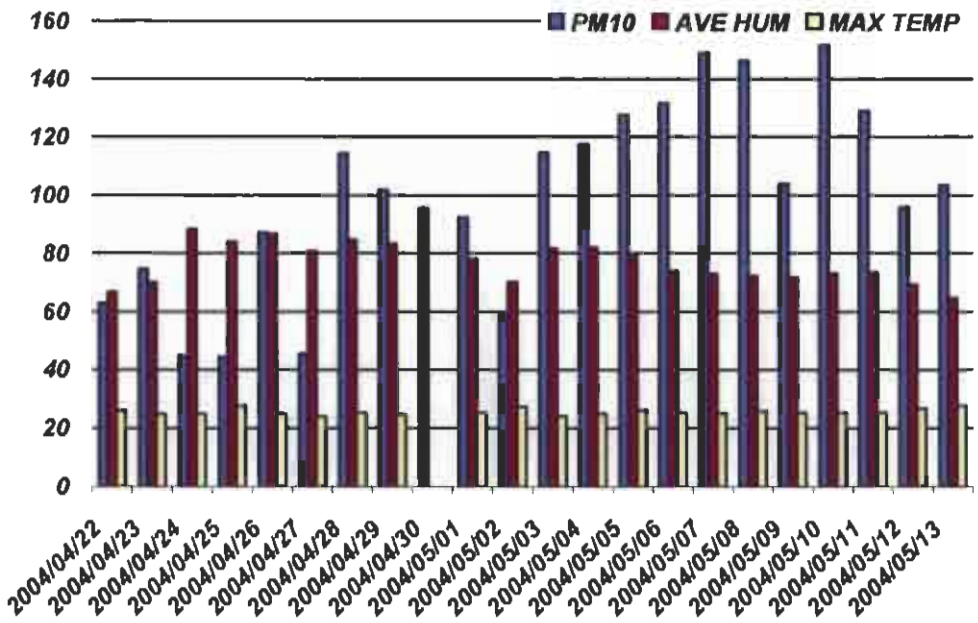

Figure 5.1: *PM10 mass concentrations, relative humidity and temperature at Site A*

The PM10 levels of 42 to 150 $\mu g.m^{-3}$ are within the range obtained as 10 – 220 $\mu g.m^{-3}$ for Oslo study sites, 20 – 230 $\mu g.m^{-3}$ for Helsinki study sites, 0 – 130 $\mu g.m^{-3}$ for London sites, and 10 – 380 $\mu g.m^{-3}$ for Milan. The pollution episodes in these study sites were found to relate to temperature (Nriagu, 1989). The levels observed in this study however, did not show a clear relation to temperature.

Over southern Africa as a whole, the winter nocturnal surface inversion has a depth of 400 – 600 m and strength of 5^0 – 7^0 C (Preston-Whyte & Tyson, 1988). Pollution released into a stable inversion layer is seldom able to rise through it and disperses slowly in clearly defined plumes.

Other contributory factors to the high levels of PM10 at Site A can be the wind speed and direction. The wind speed and direction for the months of April and

May 2004 were, on average, 16.3 $m.s^{-1}$ (337^0 from true north - NNW) and 8.7 $m.s^{-1}$ (337^0 from true north - NNW) respectively. The frequently changing wind direction during the month may be the cause of fluctuations in PM10 levels as shown in Figure 5.2.

Figure 5.2 shows the typical changes in wind direction that can occur almost every day in the Rustenburg area. The winds can practically come from about three different directions in one day, thus causing hourly fluctuations in the PM10 levels. The days 6 to 8 May 2004 were chosen as an example. The levels of inhalable particulate matter and the wind directions during these days were measured as 132 $\mu g.m^{-3}$ (SSE to NNW), 149 $\mu g.m^{-3}$ (NE and ENE), 146 $\mu g.m^{-3}$ (SE and ESE) and 104 $\mu g.m^{-3}$ (ESE to SW) respectively. These agree well with what is portrayed in a map showing the location of Site A within the Rustenburg municipality (Figure 4.1). The smelters within the vicinity of Site A are located to the North, North-East (NE) and North-West (NW) of the Site. This may be the reason for the highest levels when there are NE and ENE winds, as well as when the winds are mainly NNW.

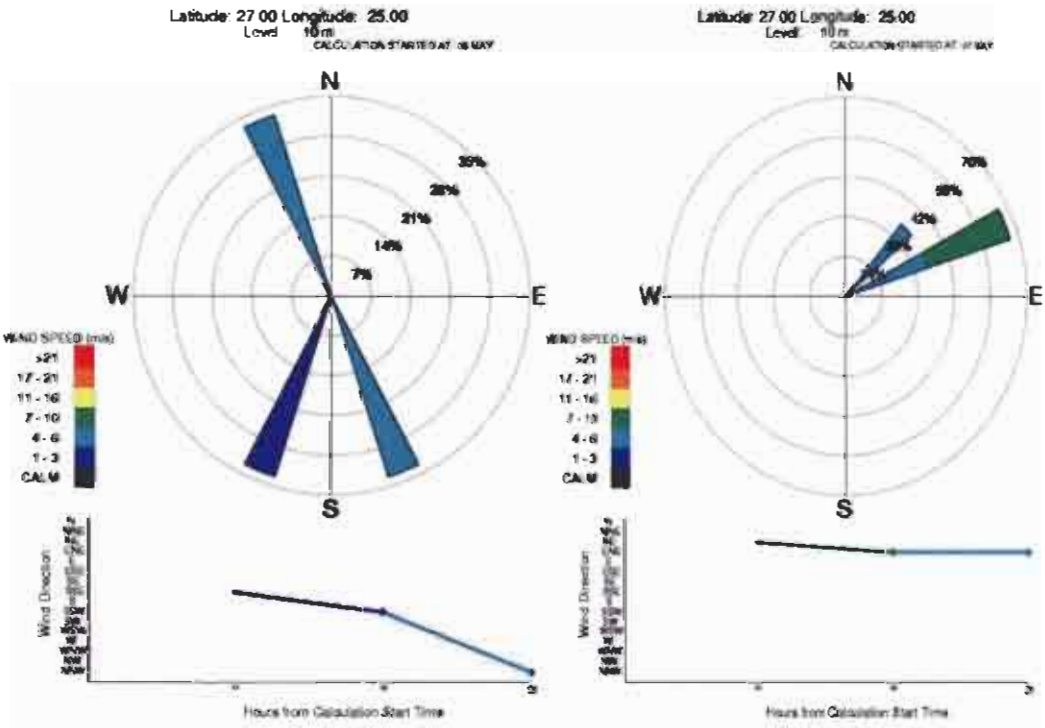

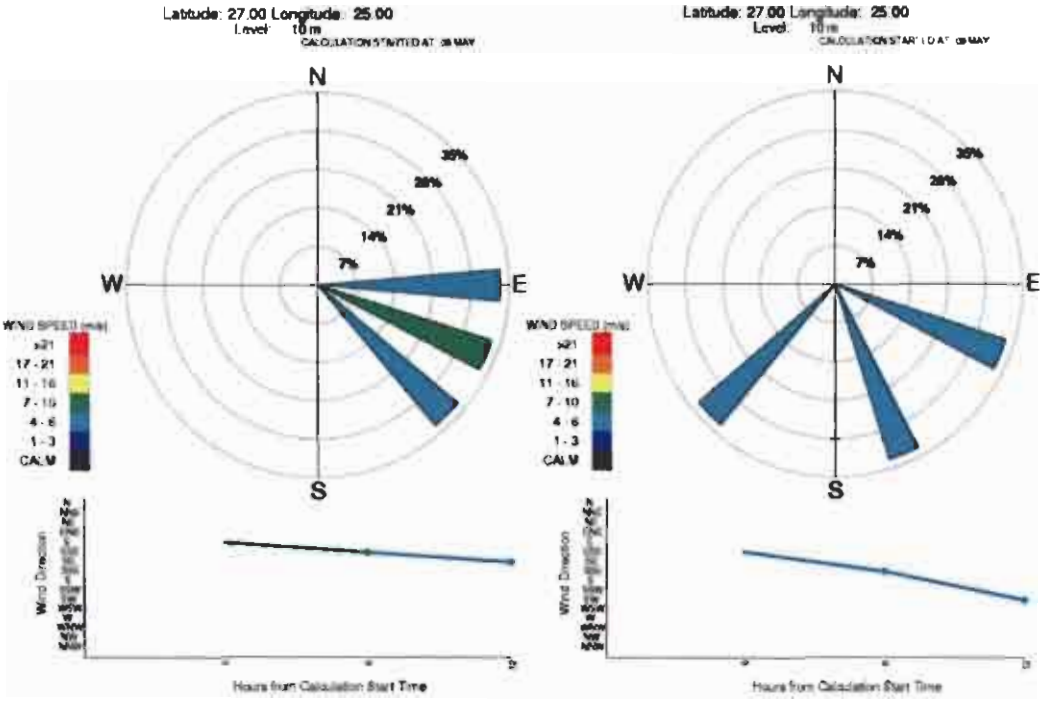

Figure 5.2: *Wind roses for the sampling days 6 - 9 May 2004 at Site A (NOOA, 2006)*

5.1.2 PM10 AND METEOROLOGY AT SITE B

Figure 5.3 shows a decrease in PM10 levels as wind speed increased. This decrease was not expected, but is in agreement with the fact that the diffusion of atmospheric pollutants into a greater volume of atmosphere reduces the concentration of a polluting material. This occurs most effectively under unstable conditions of free convection when the mixing layer is deep, which occurs frequently in summer during the day (Preston-Whyte & Tyson, 1988).

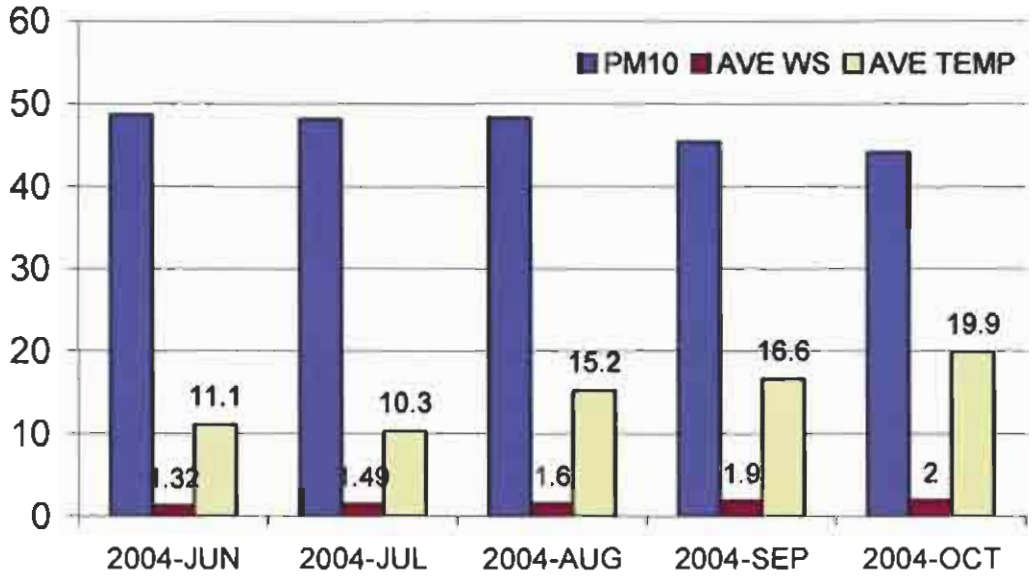

Figure 5.3 : *Monthly mass concentrations of PM10, temperature and wind speed at Site B*

This is also in agreement with a study conducted by Pirjola *et al.* (2006) where a typical daily pattern, maximum temperature in the afternoon accompanied by minimum relative humidity, was observed. As expected, higher wind speeds were associated with lower particle number concentration, however, the maximum concentrations were obtained with the wind speed around 1–2 ms^{-1}, indicating that besides dilution, a moderate plume rise can also be observed in these cases. Similar results near a ground-level highway have also been reported by Zhu *et al.* (2002b).

Figure 5.3 also shows an increase in the monthly PM10 levels as temperature decreased at Site B. The results for the monthly levels took an unusually different form compared to the daily levels in Figure 5.4, which shows an increase in the daily PM10 levels as the temperature increased. This can be linked to wind direction relative to the position of the sampling site. Wind direction determines the path followed by pollutants. Although the mean wind speed may remain approximately unchanged over a period of time, short-period direction and speed changes due to turbulence cause the plume to diffuse sideways (Preston-Whyte & Tyson, 1988).

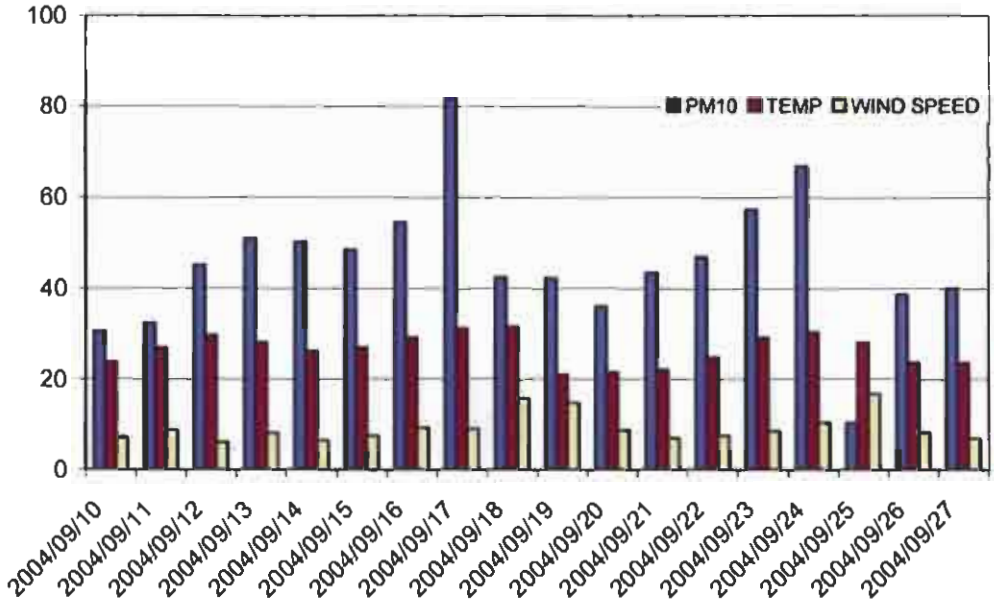

Figure 5.4: *Daily mass concentrations of PM10, temperature and wind speed* at Site B

An increase in PM10 levels as temperature and wind speed increased is evident in the given data set. The PM10 levels were below the 24-hour limit of 180 $\mu g.m^{-3}$ set as a South African guideline and the 150 $\mu g.m^{-3}$ set by the US EPA. In a similar study conducted by Chaulya (2004a), the average 24-hour PM10 concentrations ranged between 40.8 and 171.9 $\mu g.m^{-3}$.

The data on the 17th and 25th of September 2004 however, showed a different pattern. The highest value of PM10 (81.68 $\mu g.m^{-3}$), observed on 17 September corresponded to high temperature (31.2 ^{0}C) and low wind speed (8.9 $m.s^{-1}$). The lowest value of PM10 (10.3 $\mu g.m^{-3}$), observed on 25 September corresponded to high temperature (28.1 ^{0}C) and high wind speed (16.7 $m.s^{-1}$). These trends could not be explained since there was no rainfall as shown on Table 5.2 below, which could have been considered a contributory factor to the low levels on 25 September. There was practically no rainfall in September 2004, except for the 0.2 mm rainfall recorded on 27 September.

Table 5.2: *The daily rainfall at Rustenburg during 2004 (in mm) measured by the South African Weather Services (SAWS)*

Day	Jan	Feb	Mar	Apr	May	Jun	Jul	Aug	Sep	Oct	Nov	Dec
1												0.2
2												
3	2.2	0.6										5
4				0.2				1.6				
5			1.6	0.2								
6		0.8	0.2	0.2							0.4	26.2
7		2.6		1.2							2.8	1.2
8		3	0.2									11.2
9			0.8								0.4	
10												
11	1.6									32.8	14.2	1.2
12			0.4							3.8		
13		53.6								2.8		
14		9.2										0.2
15												
16												
17			0.4									
18	1.8	2										
19	42.2			25.6								8.4
20	74				0.2	3.4						
21	21.8					1.8					3.4	
22	18	7.4	0.2									
23		23.4										3.8
24		55.4	7.2									1.4
25		0.4										
26	0.8	17.2										0.8
27									0.2		7.8	11
28											1.2	12
29											7.4	
30											0.6	
31												0.4
Total	162.4	175.6	11	27.4	0.2	5.2	0	1.6	0.2	39.4	38.2	83

It is evident that comparisons between the monthly and daily variations of PM10 with wind speed and temperature are practically impossible. The fact that monthly levels are averages of the daily variations shows that the daily levels can be more reliable. The daily variations in wind speed and temperature are more reliable in explaining the PM10 concentrations.

5.1.3 PM10 AND METEOROLOGY AT SITE C

The monthly PM10 levels (Figure 5.5) also show an increase in PM as temperature and wind speed increased. In addition, Charron and Harrison (2003) have reported that particles above 30 nm decrease when the wind

speed increases, whilst the particles in the 11–30 nm range showed a lesser effect of dilution.

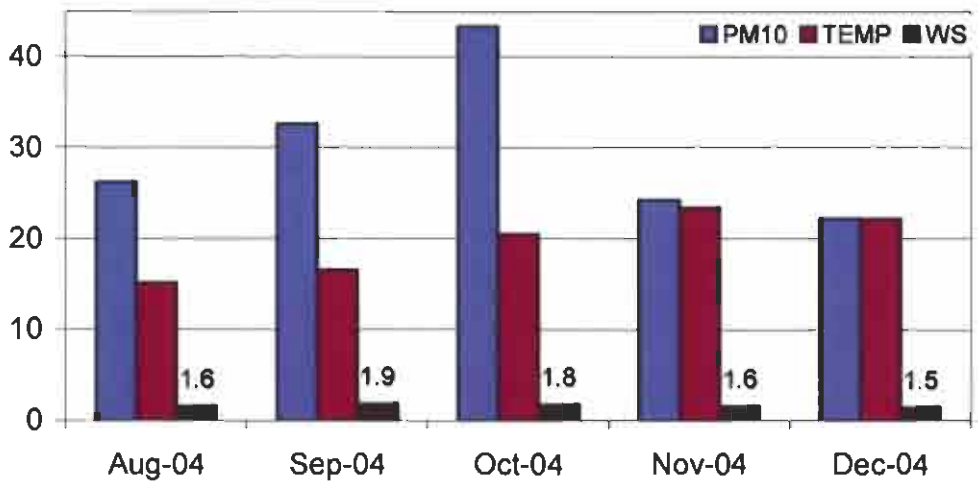

Figure 5.5: *Monthly PM10 concentrations and meteorology at Site C for the period August – December 2004*

Hussein *et al.* (2005) presented a "U-shape" relationship between the wind speed and particles larger than 100 nm (minimum in the particle concentration occurred with wind speed of around 5 $m.s^{-1}$, higher wind speed enhanced re-suspension) whereas for the ultrafine particles (<100 nm), the effect of dilution was clear, and the wind speed seldom exceeded 5 $m.s^{-1}$.

An increase in PM10 levels as temperature increases was also observed at Site C. The observation at Site C is similar to the one by Gadgil and Dhorde (2005) that suspended particulate matter (SPM) levels are higher during dry winter and summer seasons and are lower during the monsoon season. The latter occurs because of the rain washout of SPM. Higher SPM levels during winter and summer may be responsible for scattering the incoming solar radiation, consequently decreasing the amount reaching ground surface. This may in turn lead to a tendency of decreasing temperature during these seasons.

5.2 PM10 CONCENTRATIONS AND SEASONAL VARIATIONS

South Africa has clearly defined climatic seasons. Each of the seasons lasts for a period of approximately three months, and they are defined as Autumn (February to April), Winter (May to July), Spring (August to October) and Summer (November to January). Each season is characterised by a unique pattern of meteorological parameters, which govern the dispersion, transport and deposition of particulate matter. The discussions in this section are thus intended to establish the relationship between the seasons (in the form of months) and the concentration levels of particulate matter observed.

5.2.1 SEASONAL VARIATIONS AT SITE A

Site A, as described in Chapter 4, is located close (~2 km) to a ferro-chrome mine, and ~4 km away from an informal human settlement. The period of sampling of PM10 at this site covered mainly one season, autumn (February to April), even though some sampling was done at the beginning of winter (May and June). The beginning of winter (low temperatures) also encourages biomass burning and other types of fuel combustion within the area described. Figure 5.6 shows the average PM10 concentrations for the entire sampling period at Site A. Surprisingly, the lowest values were reported for the May–June period, when higher levels could have been expected.

The levels observed at Site A were generally very high (95 - 130 $\mu g.m^{-3}$) but comparable to the average concentrations obtained in a study by Mmolawa (2004), were PM levels between 248 $\mu g.m^{-3}$ and 320 $\mu g.m^{-3}$ were obtained for June and July in Gaborone, Botswana in 2002, which exceeded the monthly PM10 guideline of 200 $\mu g.m^{-3}$ set by the Botswana government.

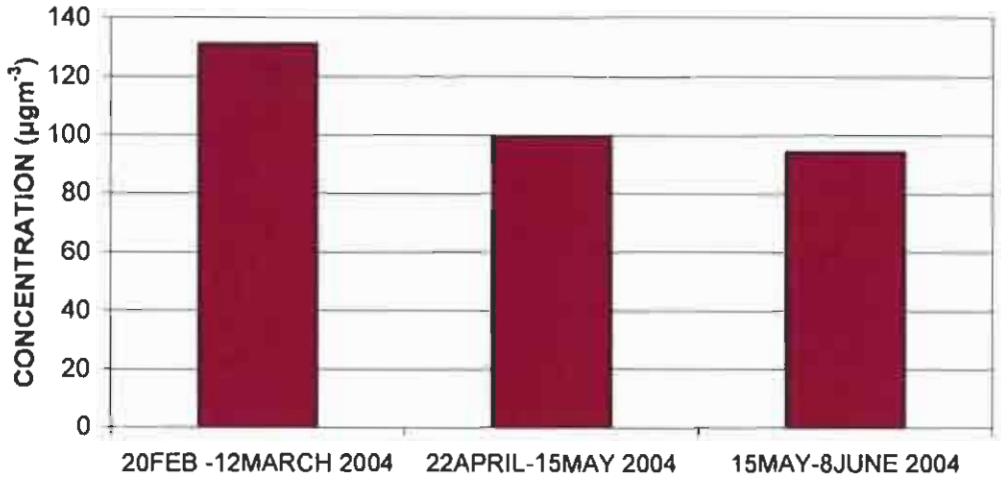

Figure 5.6: *PM10 mass concentrations at Site A*

The levels observed are the highest of the three sites. This may be due to the location (see Figure 4.1) of the site since it is located within a five-kilometer radius from the ferro-chrome smelter and from an informal settlement. Activities surrounding this site relate to resuspension of dust, fuel burning, and biomass burning. The levels are not surprising since there is no electricity at the informal settlement, and open cast mining activities are also prevalent.

5.2.2 SEASONAL VARIATIONS AT SITE B

Site B is located closer to the central business district (CBD) of the Rustenburg municipal area (~5 km), and further away from the platinum mine (~10 km). The sampling procedure for seasonal levels was done from June to December 2004. This covered the winter, spring and summer seasons.

Relatively high levels of PM10 were observed for the winter season (June and July). This could be expected since, according to Chow *et al.* (2003), the low wind speed and temperature in winter favors the accumulation of pollutants, while the high temperature in summer favors air convection and the dispersion of pollutants. In addition, the barer surface in winter would re-suspend more dust while more wet precipitation in summer would wash out more particles. The fact that most parts of the country experience dry winters may also

account for the high levels of particulate matter, since re-suspension of dust is favoured. Figure 5.7 shows a decrease in PM10 levels from winter to summer seasons at Site B.

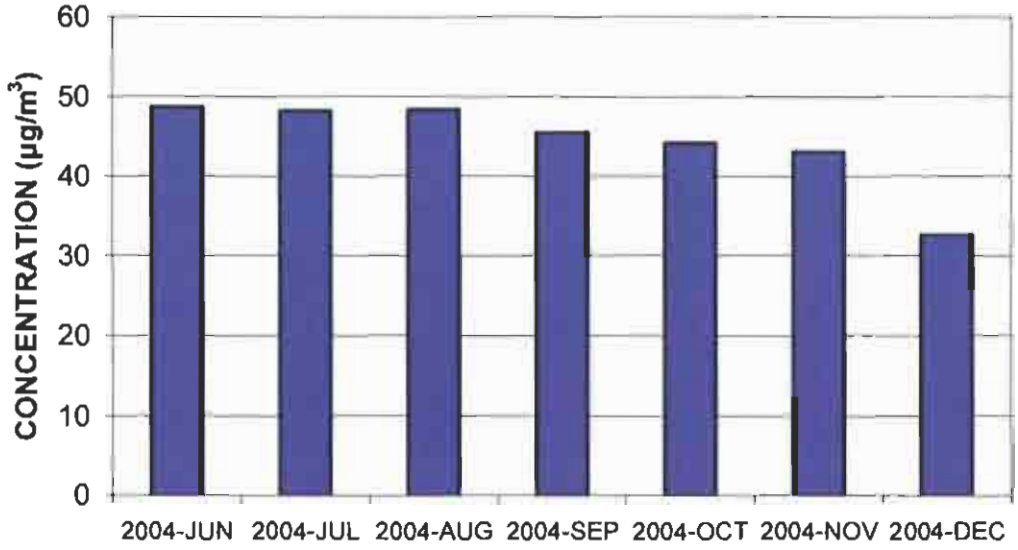

Figure 5.7: *Monthly mass concentrations of PM10 at Site B*

It could be expected that a peak in PM10 levels be measured during spring (October) mainly due to the high wind speeds associated with this season. The levels were however low but can be explained by the amount of rainfall as reported by SAWS in Table 5.1, which was 39.4 mm for October 2004, and was more or less the same as in November (38.2 mm). This month was characterised by high rainfall and low wind speed (see Table 5.1). The lowest levels of PM10 (32.63 $\mu g.m^{-3}$) measured during the month December (summer) can also be due to the high amount of rainfall (83.0 mm) measured during this month.

The average PM10 levels observed for winter, spring and summer are given as 48.48, 46.04 and 37.85 $\mu g.m^{-3}$ respectively. There was a decrease in PM10 levels from winter to summer. This can be explained by the fact that the climate of South Africa is characterised by summer rainfalls. Table 5.1 shows

a rainfall of 38.2 mm and 83 mm for November and December 2004, and 5.2 mm and 0 mm for June and July 2004, respectively.

The decrease in PM10 levels from winter to summer seasons at Site B is in agreement with a study where analysis of airborne particulate samples, to evaluate the PM concentration, showed a seasonal variation of the PM mean concentration that changed from 56 $\mu g.m^{-3}$ ±50% in the winter season to 41 $\mu g.m^{-3}$ ±30%, in the summer season (Marconi *et al.* 2003).

The winter (June and July) and summer (November and December) levels obtained for this study were very low compared to the mean PM10 concentrations reported at three sites in China, namely Beijing Normal University (BNU), Capital Steel Company (CS) and Yihai Garden (YH), were the levels 172.2(101.9) and 184.4(130.5), 170.0(66.7) and 287.7(155.7), 150.1(56.9) and 292.7(172.7) for summer and winter respectively, were observed (Sun *et al.*, 2004). The variation is unexpected since China has a mild (warm and wet) climate compared to the North-West province of South Africa, which forms part of the dry climate.

5.2.3 SEASONAL VARIATIONS AT SITE C

Site C is located more than 50 km away from the ferrochrome mine but closer (within 10 km radius) to a platinum smelter. The area is semi-remote with fewer roads and almost no urban activities. Figure 5.8 shows the monthly concentrations of the inhalable particulate matter at Site C.

The levels observed from August to October 2004 (26 to 43 $\mu g.m^{-3}$), and in January 2005 were within the average range observed by Querol *et al.* (2004) in different countries (Germany, Spain, Sweden, Austria, United Kingdom, and Netherlands) within the European Union, were the PM10 levels (annual mean) ranged from 28 to 42 $\mu g.m^{-3}$ at urban background, and from 37 to 53 $\mu g.m^{-3}$ at kerbside sites.

Site C had the lowest monthly levels of PM10 (22.2 to 47.4 $\mu g.m^{-3}$) compared to Site A and B. These are comparable to the 38.4 $\mu g.m^{-3}$ observed by Tolocka *et al.* (2001) during the months of January and February 1999 at Rubidoux site in the United States of America.

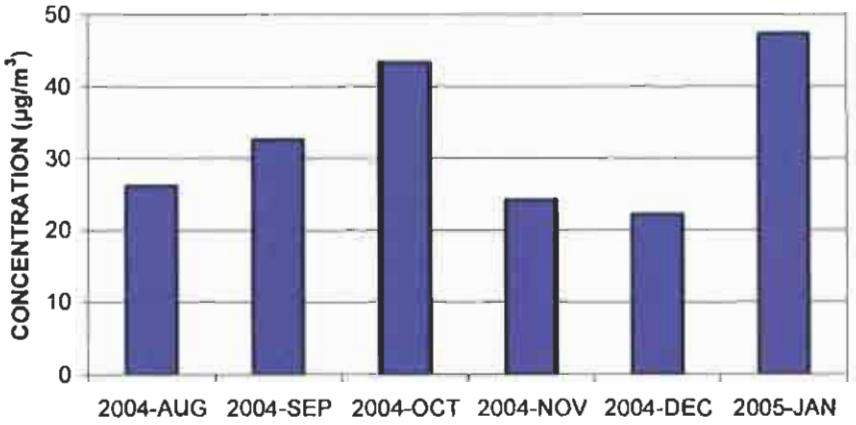

Figure 5.8: *Monthly mass concentrations of PM10 at Site C*

The PM10 levels for the spring season (August, September, and October) were relatively higher than the summer (November and December) levels at Site C.

A peak in PM10 levels was observed during the month of October (spring season), which agrees well with the fact that high wind speeds favor resuspension and transportation of atmospheric pollutants. The six-month average concentration at Site C was 33 $\mu g.m^{-3}$, which is the same as the annual average levels obtained in 1999 at the Goodwood site in Cape Town, South Africa (Granger, 2003). This agreement in results shows that the same level of pollution can result from urbanisation and industrialisation.

5.3 PM10 AND DOMESTIC AND INDUSTRIAL ACTIVITIES

The daily and hourly PM10 levels are vital in determining the contribution of domestic and industrial activities in the vicinity of the study area. The busiest

times of the day have high levels of PM, whilst the times when there are fewer anthropogenic activities have low levels linked to them. Weekdays are also expected to have higher levels than the weekends since there is less industrial activity during weekends.

5.3.1 PM10 AND DOMESTIC AND INDUSTRIAL ACTIVITIES AT SITE A

Figure 5.9 shows the PM10 levels during different time intervals of a typical day. It can be observed that the hourly PM10 levels were high mostly between 6h00 and 18h00, which shows a correlation between the activities at the sources (household and industrial) and the PM10 levels.

The high hourly levels observed at Site A during daytime are similar to the levels (e.g. 302 $\mu g.m^{-3}$) observed at the Branik site in the Czech Republic in 1999 (Fiala, 2000).

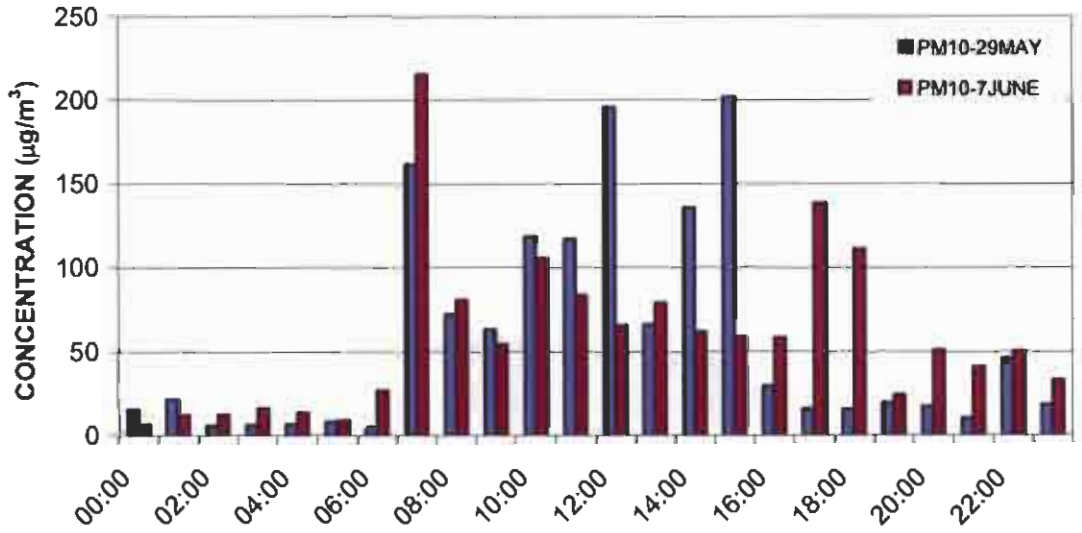

Figure 5.9: *Hourly PM10 levels at Site A on 29 May and 7 June 2004*

The peak average concentrations observed in the morning (8h00 – 9h00) and evening (8h00 – 19h00) hours on 7 June 2004 are in agreement with studies conducted by Munishi (2002) who observed peak concentrations of NO_2 and PM in the morning and evening hours. The guideline of 120 $\mu g.m^{-3}$ set by the WHO was exceeded twice during the day (7 June 2004). The levels are,

however, very low compared to the average concentrations ranging from 592 to 1, 211 $\mu g.m^{-3}$ observed by Msafiri (2004) at Dares Salaam.

It can be observed from Figure 5.9 that the concentration at 8h00 in the morning was 161.5 $\mu g.m^{-3}$ and the hourly afternoon concentrations were 195.8 $\mu g.m^{-3}$ at 12h00, 135.8 $\mu.gm^{-3}$ at 14h00, and 202.1 $\mu g.m^{-3}$ at 15h00 on 29 May 2004. These exceeded the hourly particulate matter guideline of 120 $\mu g.m^{-3}$ set by the WHO.

5.3.2 PM10 AND DOMESTIC AND INDUSTRIAL ACTIVITIES AT SITE C

The averaged hourly PM10 levels for 19 April to 10 May 2005 at Site C are given in Figure 5.10. The levels were very low compared to the ones at Site A, but still showed the effects of both the domestic and industrial activities.

The concentrations ranging from 13.1 to 14.7 $\mu g.m^{-3}$ observed at Site C were similar to the annual average of 13.9 $\mu g.m^{-3}$ obtained by Tolocka *et al.* 2001 at the Shenandoah National Park in the USA, during May 1998 to May 1999. For the Rustenburg area, Site C had the lowest hourly average levels and can be used as control (background) station.

The lowest hourly levels observed at Site C during 3 – 31 March 2005 ranged from 8.6 to 8.94 $\mu g.m^{-3}$. These were within the same range as the annual average of 9.2 $\mu g.m^{-3}$ observed at Meadview, USA (Solomon et al., 2000b) for the measurements done from May 1998 to May 1999.

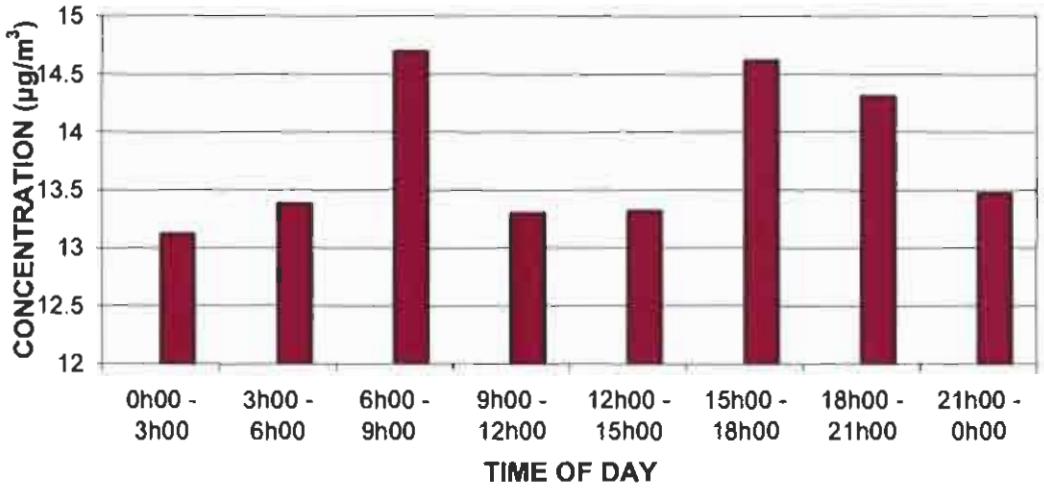

Figure 5.10: *Hourly PM10 levels at Site C from 3 to 31 March 2005*

The average level for the day at site C was 13.7 $\mu g.m^{-3}$, which is comparable to the levels measured by Heal *et al.* (2005) in Edinburgh, where the mean daily PM10 and PM2.5 for a year of measurement were 15.5 and 8.5 $\mu g.m^{-3}$. The comparison shows that the annual PM levels for areas characterised by different climatic conditions can be found to be similar. This implies that taking annual averages of daily levels can distort the relation between PM levels and meteorology, and PM levels and industrial activities.

The hourly levels for Site A as discussed in Section 5.3.1 were higher (6.5 – 215.7 $\mu g.m^{-3}$) than the hourly levels at Site C (13.1 – 14.7 $\mu g.m^{-3}$). This suggests that the anthropogenic activities in the Rustenburg area are linked with industry because Site A is closer to smelters than Site C. The PM10 and PM2.5 concentrations in Seoul of 47 and 79 $\mu g.m^{-3}$ respectively were found by Mishra *et al.* (2004a) to be twice as high as their Busan counterparts of 19 and 34 $\mu g.m^{-3}$ respectively. The higher particulate concentrations in Seoul were also found to reflect the relative dominance of anthropogenic sources (industry and traffic) compared to Busan. It is worth noting that the industrial activities in the vicinity of a sampling site plays a major role in determining the PM levels.

5.4 HEALTH IMPLICATIONS OF THE PM10 LEVELS

Various health hazards are associated with inhalable particulate matter. Some have been mentioned in Section 1.1 and 1.2, and selected types have been discussed in Section 2.1.1 of this report. Table 5.3 gives a summary of the trends of the PM10 levels within the three study sites in the Rustenburg municipality. The hourly, daily and monthly PM10 levels were higher at Site A than at any of the other study sites. The hourly and the 24-hourly PM10 standards of limitation have been exceeded several times during the study.

Table 5.3: Summary of the *PM10 levels (in $\mu g.m^{-3}$) at the three sites in Rustenburg*

SITE	Autumn (Feb'04-Apr'04) Mean (SD)	Winter (May'04-Jul'04) Mean (SD)	Spring (Aug'04-Oct'04) Mean (SD)	Summer (Nov'04-Jan'05) Mean (SD)	Monthly Range	Daily Range	Hourly Range
A	74.6	105.6	------	------	94.4 – 131.0	44.4 – 151.7	15.3 – 215.7
B	------	48.5	46.0	37.8	44.2 – 49.3	10.3 – 81.7	------
C	------	------	34.1	31.3	22.2 – 47.4	------	13.1 – 15.7

The data given in Table 5.3 can be evaluated against the air quality index given by Peters and Dockery, (2001) in Table 5.4. The index gives an indication of the health implications of various concentration levels. The numerical values in the air quality index described show that the hourly levels in Site A can range from moderate to very unhealthy, the daily levels from moderate to unhealthy, and the monthly levels from moderate to unhealthy for sensitive groups.

Both the monthly and hourly levels at Site C were good according to the air quality index table. This can also be explained by the fact that the sampling site is far from most sources of particulate matter. The wind direction in Rustenburg was mostly south easterly during the sampling, which shows in

Figure 4.2 that the wind was blowing away from the study site towards the smelter and the village. The daily levels at Site B range from good to moderate, while the monthly levels can be classified as good.

The good and moderate categories in Table 5.4 may not necessarily suggest that there are no health implications since according to Peters and Dockery (2001), the elevated risk of acute heart attack after short-term exposure to elevated levels of PM10 (even when PM10 levels are well below NAAQS standards), are 51% for an increase of 40 $\mu g.m^{-3}$ within 2 hours, and 66% for an increase of 30 $\mu g.m^{-3}$ within 24 hours.

Table 5.4: *Air quality index for inhalable particulate matter (Peters & Dockery, 2001)*

Air Quality Index Levels of Health Concern	Numerical Value	Meaning
Good	0-50	Air quality is considered satisfactory, and air pollution poses little or no risk.
Moderate	51-100	Air quality is acceptable; however, for some pollutants there may be a moderate health concern for a very small number of people who are unusually sensitive to air pollution.
Unhealthy for Sensitive Groups	101-150	Members of sensitive groups may experience health effects. The general public is not likely to be affected.
Unhealthy	151-200	Everyone may begin to experience health effects; members of sensitive groups may experience more serious health effects.
Very Unhealthy	201-300	Health alert: everyone may experience more serious health effects
Hazardous	> 300	Health warnings of emergency conditions. The entire population is more likely to be affected.

It has not been possible to identify a threshold for PM10 below which no health effects are observed. Serious health effects still occur at pollutant concentrations that are well below existing air quality guidelines and standards (Polyak & Johnson, 2005).

If it is assumed that the PM10 can contain 50% of PM2.5, then the health implications associated with PM2.5 may still be important in this study, and the standard of limitation set by the US EPA for daily PM2.5 concentration is

the standard of limitation set by the US EPA for daily PM2.5 concentration is assumed to be exceeded both at Site A and B during the study. Deposition of particles in the range of PM10 – PM2.5 occurs mainly through wall impact or sedimentation on the airways or bronchioles. According to Johnson (2004), for the PM2.5 – PM0.1 range, deposition is mainly through sedimentation into the respiratory bronchioles. Thus there is a possibility of experiencing more health problems than the ones anticipated in this study.

It is evident from the results discussed above that the levels of particulate matter depend on the meteorogical conditions, the time of day, activities around the sampling area, the distance from the source, as well as seasonal variations such as wet precipitation.

.....

Characterisation of the inhalable airborne particulates is becoming increasingly important to governments, regulators and researchers due to their potential impact on human health, trans-national migration and influence on climate forcing and global warming (Dockery et al., 1993). In the light of this, the next chapter focuses on chemical characterisation of particulate matter and apportionment of the source contributions within the Rustenburg area.

.....

CHAPTER 6

SEM/EDS RESULTS

In this chapter, the results obtained using Scanning Electron Microscopy coupled with Energy Dispersive Spectroscopy are presented. The oxides of the elements identified from each study site, the relationship between the concentration of the elements identified and particulate matter, as well as carbon are also discussed. Source apportionment of the toxic metals of particulate matter is also discussed.

6.1 OXIDES OF THE ELEMENTS IDENTIFIED

Aerosol measurements are the basic and useful indicators to reflect the general status of air pollution. Chemical characterisation of aerosols reveals the emitting sources of pollution from natural as well as anthropogenic activities.

Some of the data discussed in this section were obtained from analysis of teflon-coated borosilicate fiberglass filters, which were removed from the mass transducer component of the tapered element oscillating microbalance (TEOM), and the other data was obtained from Teflon ringed filters, which were removed from the exhaust of the TEOM. Quartz fiber filters were also used but did not give meaningful data. The composition observed gave the impression that there were no metals in the samples or that only C and F were deposited on the filter.

The filter samples of which PM10 levels were determined in Chapter 5, were analysed using SEM/EDS and the elements identified during the analysis are discussed below. The mineral composition of these samples may not be representative of the composition of the bulk dust from the specific region, but may be representative of the mineral part of the dust aerosol from these sources. This is mainly due to the fact that SEM/EDS gives data in the form of micrographs, which can be used to determine the elements or compounds present or the total sum of the oxides of a particular element.

Elements produced during combustion usually appear in the form of oxides such as magnesium oxide, aluminum oxide, silicon dioxide, calcium trioxide, titanium oxide, iron trioxide, phosphorus pentoxide, ammonium sulfate, copper oxide, zinc oxide, sodium chloride, potassium oxide, vanadium oxide, nickel oxide and manganese oxide (Miranda & Andrade, 2005). The terms metal and oxides of metals are used interchangeably throughout this chapter. The oxides of O mentioned hereafter, imply all the oxides that could not be explicitly identified by SEM/EDS.

6.1.1 OXIDES OF THE ELEMENTS IDENTIFIED AT SITE A

Table 6.1 gives the concentrations of the oxides of the elements identified at Site A. Sample 1 corresponds to the sampling period 20 February to 12 March (autumn), Sample 2 was obtained from 22 April to 15 May (autumn), and Sample 3 is linked to the 15 May to 8 June sampling period (winter). For all the samples described above, the data was obtained from analysis of teflon-coated borosilicate fiberglass filters.

Table 6.1: *Concentrations (in μg.m^{-3}) of oxides of the elements identified at Site A for autumn and winter 2004*

SAMPLE	PM10	Si	Fe	Al	Ca	Mg	K	Na	Ti	Cr	C	Cl	S	F	O
1	131.1	7.08	3.28	4.06	1.44	1.70	0.52	1.05	0.40	3.28	18.22	-	6.42	8.39	74.73
2	99.74	14.16	3.49	5.69	3.59	3.29	0.60	0.70	-	1.10	8.08	0.30	4.29	-	54.66
3	94.36	14.44	5.57	5.76	3.96	3.02	0.57	0.57	0.28	2.45	6.89	0.28	1.60	-	45.39
MEAN	**108.4**	**11.89**	**4.11**	**5.17**	**3.00**	**2.67**	**0.56**	**0.77**	**0.23**	**2.28**	**11.06**	**0.19**	**4.10**	**2.80**	**58.26**
SD	**11.46**	**2.41**	**0.73**	**0.56**	**0.79**	**0.49**	**0.02**	**0.14**	**0.12**	**0.64**	**3.59**	**0.10**	**1.39**	**2.80**	**8.66**

The oxides identified at this site are mainly of the elements Si, Fe, Al, Ca, Mg, K, Na, Ti, Cr, C, Cl, S, F and O. There was an increase in concentrations of crustal elements Si, Fe, Al, Ca, Na and Mg from the autumn to the winter season. The S and C concentrations also showed a decrease from autumn to winter. South Africa has dry winter seasons and the concentration of S shown in Table 6.1, at the beginning of winter (15 May to 8 June) was 1.6 μg.m^{-3}, 4.29 μg.m^{-3} (22 April to 15 May) and 6.4 μg.m^{-3} in autumn (20 February to 12 March). The rainfall reported by the South African Weather Services as given in Table 5.2 were 175.6, 11, 27.4, 0.2, and 5.2 for the months of February, March, April, May and June respectively. The levels of the oxides of sulphur are very important in a study that deals with toxic trace metals, because most of the metals occur in ambient air as sulphates.

The oxides of carbon identified were higher (18.22 μg.m^{-3}) for Sample 1 than for Sample 2 and 3 (8.08 and 6.89 μg.m^{-3}). There is more biological activity related to photosynthesis in summer and autumn than in winter, and this reduces the levels of carbon in the air. It is therefore expected that the oxides of carbon will be more in winter than in autumn. The high carbon content may also be linked to the high concentrations of Si, which were lowest for Sample 1. This, however, could not be explained. It may suggest that most of the particulate matter during the autumn and winter periods is linked to wind-blown dust from natural surfaces, roads, and smelters.

The potentially toxic metal of interest identified at Site A is Cr, with concentrations of 3.28, 1.1, and 2.45 μg.m^{-3} for the three samples analysed at

this site. This may have serious implications since for Sample 1 and 3; the limit of 1.5 $\mu g.m^{-3}$ for Cr, set by the Asia Pacific Centre for Environmental Law (APCEL) is exceeded. The limitation standard of 1000 $ng.m^{-3}$ (1 $\mu g.m^{-3}$) set by NIOSH was exceeded for the whole sampling period at this site. There are arguments about whether the standard for the levels of total Cr are relevant for air quality. The arguments are based on the fact that Cr exists mainly in two stable oxidation states 3+ and 6+, and the Cr^{6+} is carcinogenic while Cr^{3+} is not toxic. The two oxidation states may co-exist or may even be found to exist independently. It is therefore important also to determine the Cr^{6+} concentrations in the samples. The chemical determination of Cr^{6+} was not performed in this study.

MICROGRAPH OF PM10 SAMPLE FROM SITE A

The shape, size and colour of the particles can be used to identify the emission sources. The variable shapes and sizes of particles shown by these micrographs are predominantly irregular in shape.

Crustal material suspended by the wind and particles generated during the processing of soil, and industrial processing of minerals have irregular shapes indicative of the minerals being milled (Li *et al.*, 2000). Figure 6.1 gives the morphology of Sample 1, which was accumulated on the filter from 20 February to 2 March 2004.

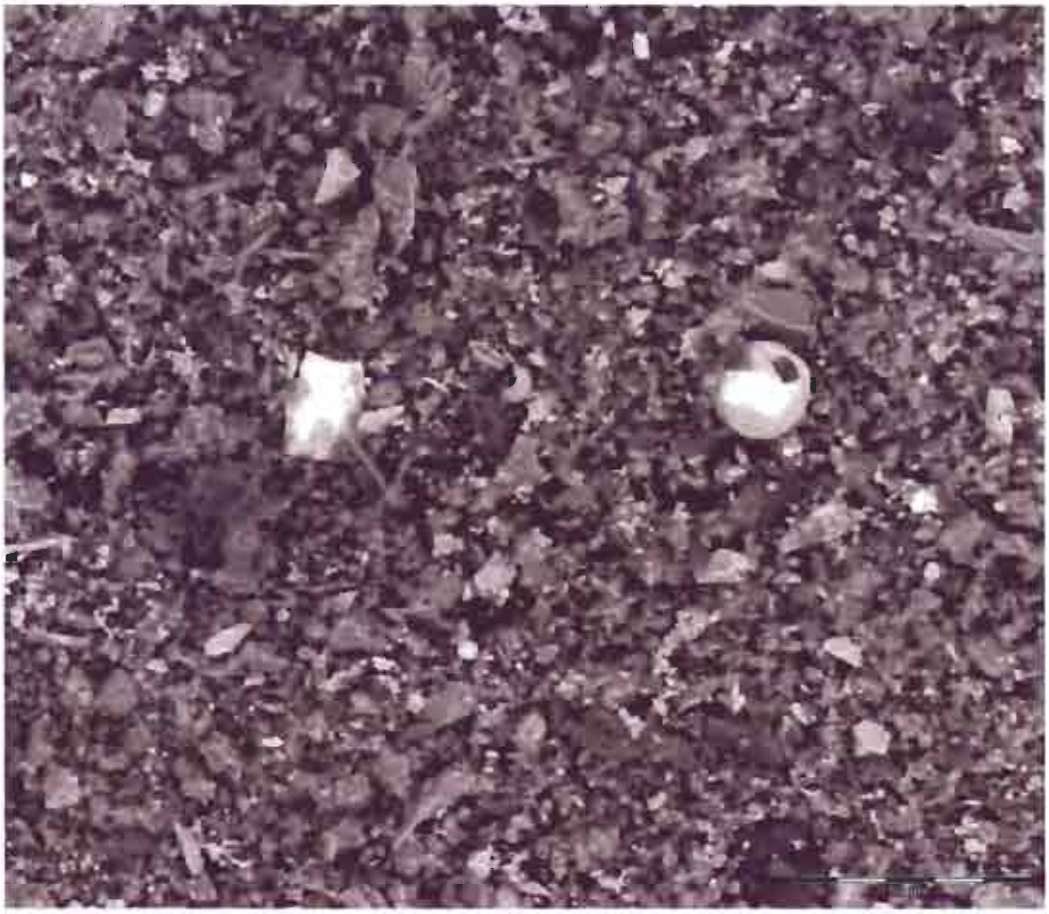

Figure 6.1: *Micrograph of Sample 1 at Site A*

The greyish particles are predominantly geological elements that include iron, silica and manganese (Herbst, 1984). This can be attributed to re-suspension of soil particles during wind episodes and emissions from industry during mineral processing. Angular fractured grains are produced as a result of mining and milling processes. The irregularly shaped particles may be linked to the results of anthropogenic abrading processes. The white particles that are predominantly chromium (Anwari *et al.*, 1992) and its oxides can be associated with the industrial emissions particularly from the ferrochrome smelter located > 15 km from the study area.

The ongoing industrial activities in the study area, which includes mechanical abrasion of soil during mineral processing will ultimately lead to re-suspension of soil particles that are predominantly irregular in shape.

Spherical particles shown in the micrograph are typically alumino-silicates, often with significant concentrations of iron that come from pyrites and other iron-containing minerals in coal (Anwari *et al.*, 1992). Smelting operations also generate spherical particles, including elements specific to the ores. This simply means that the ferrochrome smelter in the study area will emit Cr and Fe that are predominantly spherical in shape. Elemental analysis indicates that a large portion of the spherical particles contain elevated concentrations of carbon, oxygen, and silicon and lesser quantities of magnesium, sodium, aluminum, sulfur and calcium.

The fact that it is not possible to distinguish between total Cr and Cr(VI) using SEM/EDS is important since the toxicity of Cr is linked to Cr(VI). In a study conducted by Resane *et al.* (2005) in Rustenburg, the Cr(VI) was extracted from the filters with 0.1 M Na_2CO_3 and aliquots of these solutions were analysed for Cr(VI) by Electrothermal Atomic Absorption Spectrometry (ET AAS). The method yielded concentrations ranging from 1.9 to 15.9 ngm^{-3}. This may still have health implications since, according to Resane *et al.* (2005), US EPA estimates that 8 $ng.m^{-3}$ of soluble Cr(VI) species in air and 100 $ng.m^{-3}$ for particulate matter are associated with a 1 x 10^{-4} cancer risk.

6.1.2 OXIDES OF THE ELEMENTS IDENTIFIED AT SITE B

The elements identified at Site B are presented in Table 6.2, together with the PM10 levels determined in Chapter 5. The analysis for this site was also performed on the teflon-coated borosilicate fiberglass filters obtained from the mass transducer of the TEOM. These are the filters of which the PM10 concentrations were discussed in Chapter 5.

The number of metals identified in this site is higher than the metals at Site A. The concentrations of these metals are however, generally lower than at Site A. The elements identified at Site B include Si, Fe, Al, Ca, Mg, K, Na, Ti, Cr, C, Cl, S, F, V, Pb, and N.

Table 6.2: *Concentrations (in* μgm^{-3}*) of oxides of the elements identified at Site B for winter, spring and summer 2004*

Sample	PM10	Si	Fe	Al	Ca	Mg	K	Na	Ti	Cr	C	Cl	S	F	P	V	Pb	N	O
4	48.73	1.41	-	0.68	0.15	0.39	0.19	0.24	-	-	11.26	0.10	0.68	-	-	-	-	-	33.67
5	49.28	2.12	0.3	0.99	0.25	0.39	0.35	0.15	-	0.10	10.50	0.10	0.84	-	0.05	-	-	-	33.17
6	48.39	2.41	0.19	0.77	0.24	0.34	0.44	0.34	0.05	-	9.19	0.10	0.44	4.65	-	-	-	-	29.28
7	47.1	3.96	1.27	-	0.61	0.57	0.47	0.33	0.09	0.28	7.58	0.19	0.99	-	0.09	-	-	-	29.11
8	45.51	2.78	0.68	1.18	0.41	0.41	0.46	0.36	0.05	0.14	8.33	0.09	0.68	1.55	-	-	-	-	28.35
9	44.22	2.39	0.62	0.97	0.31	0.4	0.35	0.27	-	0.13	7.03	-	1.81	-	-	-	-	1.06	28.88
10	43.06	2.50	0.6	0.99	0.34	0.56	0.26	0.34	-	0.17	8.01	0.13	1.25	-	-	-	-	-	27.9
11	46.46	3.58	1.02	1.49	0.37	0.51	0.23	0.23	0.09	0.28	7.43	-	1.81	-	-	0.02	0.24	-	29.08
Mean	**46.52**	**2.64**	**0.59**	**0.88**	**0.34**	**0.45**	**0.34**	**0.28**	**0.04**	**0.14**	**8.67**	**0.09**	**1.06**	**0.78**	**0.02**	**0.00**	**0.03**	**0.13**	**29.93**
SD	**0.90**	**0.29**	**0.15**	**0.15**	**0.05**	**0.03**	**0.04**	**0.03**	**0.01**	**0.04**	**0.54**	**0.02**	**0.18**	**0.59**	**0.01**	**0.00**	**0.03**	**0.13**	**0.78**

For most samples, the oxides of Pb, V, N, P and F could not detected. The oxides linked with Cl were identified in almost all samples and P was identified in the winter (June – July) and Spring (August – September) samples. The occurence of oxides of P, Cl at Site B may suggest the presence of a Pb phosphate mineral (Pb-P-Ca and/or Cl) in the samples (Goldstein *et al.*, 2003).

The potentially toxic trace metals identified included Cr, V and Pb, though V and Pb could only be identified in summer. This could not be explained since it can be expected that the levels of Cr, V, and Pb are related mainly to mining and/or industrial activities and not meteorology. There was no clear trend in the levels of Cr within the study site. The levels ranged from 0.1 to 0.28 $\mu g.m^{-3}$ for Cr, and the concentrations of Pb and V were measured as 0.24 and 0.02 $\mu g.m^{-3}$ respectively.

The complex nature of particulate matter has always played a role in the monitoring of the toxic metals. PM has a high proportion of organic compounds. During summer, there are more biological activity like photosynthesis that reduces the carbon content (CO_2) of air. The ratio of C to

PM10 is thus expected to decrease from winter to summer. This may only be true for the CO_2 content and not all the carbon-containing compounds of PM. Figure 6.2 shows the relation and suggests that the oxides of carbon are linked with high levels of PM10.

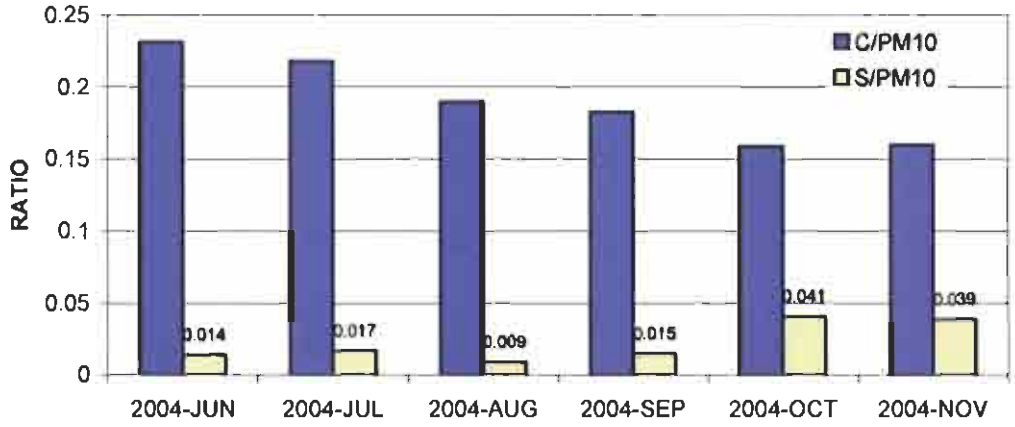

Figure 6.2: *The ratio of C to PM10 and S to PM10 at Site B*

A decrease in the C/PM10 ratio from winter to spring may also suggest that carbon compounds were emitted from both natural sources as well as domestic combustion activities. The rate at which carbon is used by plants decreases in winter thus contributing to the formation of ambient carbon compounds. There are more domestic combustion activities aimed at cooking and warming up the homes. These activities are responsible for the high C/PM10 ratios in winter.

Figure 6.2 also shows an inverse relationship between the C/PM10 and S/PM10 ratios measured at Site B. The S/PM10 was smaller than the C/PM10 ratio by an order of magnitude. The two were, however, fairly steady during the October-November period. An increase in the S/PM10 ratio from winter to spring is logical and may be linked to an increase in temperature and wind speed, which may also suggest an increase in the extent of the dispersal of both natural and anthropogenic pollutants.

The ratio of the metals of crustal origin (e.g. Fe, Si, Al) to PM10 is given in Figure 6.3.

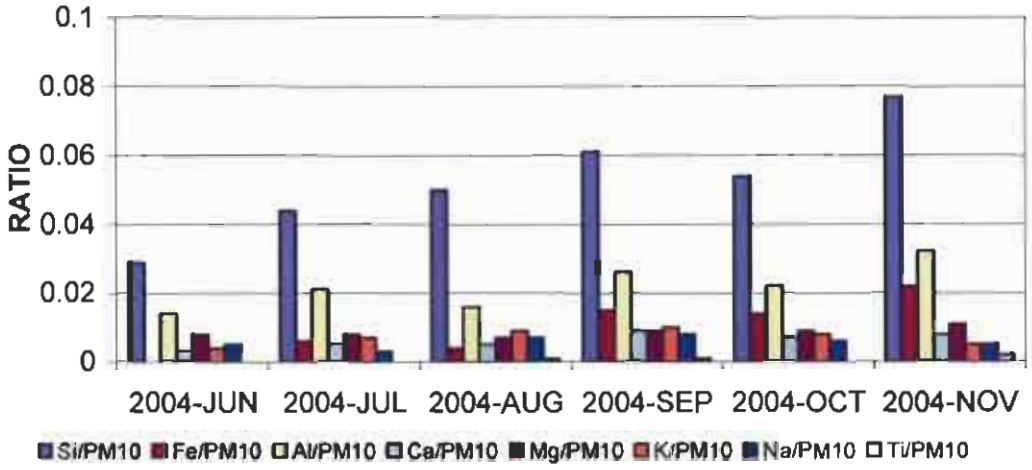

Figure 6.3: *The ratio of crustal metals to PM10 at Site B*

The ratio of Si/PM10, Fe/PM10 and Al/PM10 shows an increase from winter to spring. This was expected since the Si, Al and Fe are all related to crustal material and will thus increase with increase in wind speed and decrease with decrease (or absence) of rainfall.

The carbon-containing compounds form a large part of particulate matter. The ratio of levels of the metals measured in this site are related to C in Figure 6.4 and 6.5. It can be noted that the ratios of the toxic metals (Cr, Ni, V and Pb) to C are much lower (0 – 0.045) than the ratios for crustal elements to C (0 – 0.5). A peak is, however, observed for the ratios Cr/PM10 and Pb/PM10 in mid-spring (October). This is the time when there are major dispersals of pollutants including pollen, in the atmosphere.

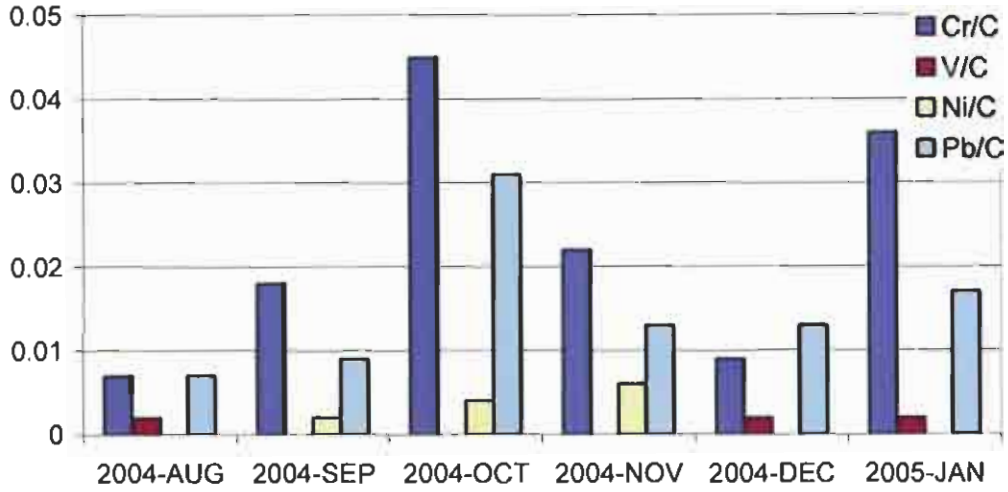

Figure 6.4: *The ratio of toxic metals to C at Site B*

There was an increase in the ratios of the crustal elements to carbon from winter to summer. This is due to a decrease in the carbon content since there is less biomass burning in the form of veld fires and domestic heating during summer. The ratios are however, highest for Si followed by Al, and then Fe. All the three metals mentioned above can be used as signatures for metals of crustal origin. Fe can, however, have originated from industrial sources because of the presence of ferrochrome smelters within Rustenburg.

Figure 6.5 also shows a decreasing order of ratios from Si/C, Al/C, Fe/C, Mg/C, K/C, Ca/C, Na/C, Ti/C during the months of September, October and November. This is interesting since it may imply that the ratios between the crustal elements themselves were roughly the same during these months.

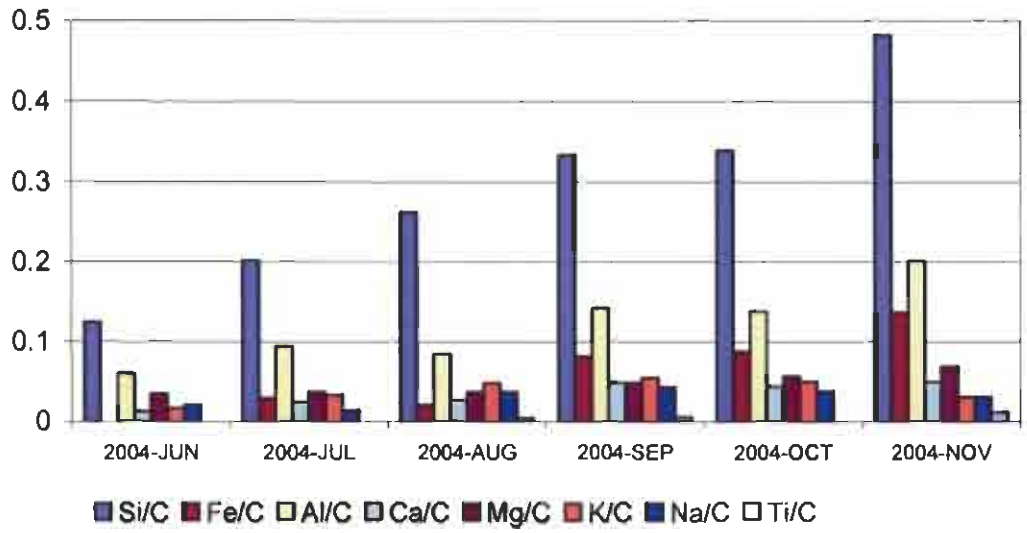

Figure 6.5: *The ratio of crustal metals to C at Site B*

6.1.3 OXIDES OF THE ELEMENTS IDENTIFIED AT SITE C

Two sets of data were collected at Site C, where both the monthly and hourly elemental compositions were determined. These are presented in Table 6.3 and 6.4 respectively. Teflon-coated borosilicate fiberglass filters from the mass transducer of the TEOM were used for monthly concentrations and 47mm Quartz fiber and Teflon filters, from the automatic cartridge collection unit (ACCU) of the TEOM were used for hourly concentrations. The flow rate for air entering the mass transducer is 3 $L.min^{-1}$ while the flow rate for the ACCU is 13.7 $L.min^{-1}$.

MONTHLY CONCENTRATIONS

The monthly concentrations of the elements identified at Site C are given in Table 6.3. Sample 13, 14, 15, 16, 17 and 18 were obtained during August, September, October, November, December 2004 and January 2005 respectively.

Table 6.3: *Concentrations (in µg.m^{-3}) of oxides of the elements identified at Site C for spring and summer 2004*

SAMPLE	PM10	Si	Fe	Al	Ca	Mg	K	Na	Ti	Cr	C	Cl	S	F	V	Ni	Pb	O
13	26.20	1.55	0.10	0.58	0.05	1.55	1.55	0.24	0.02	0.03	4.27	-	0.24	4.66	0.01	-	0.03	14.20
14	32.60	2.12	0.26	0.88	0.13	0.20	0.13	0.26	0.03	0.1	5.41	0.03	0.29	4.14	-	0.01	0.05	18.60
15	43.40	2.47	0.87	0.95	0.26	0.43	0.21	0.48	0.03	0.3	6.68	-	1.69	3.86	-	0.03	0.21	25.00
16	24.30	1.77	0.34	0.58	0.12	0.12	0.15	0.32	0.05	0.07	3.20	-	0.27	5.26	-	0.02	0.04	11.90
17	22.20	1.18	0.07	0.6	0.09	0.11	0.07	0.14	-	0.04	4.69	-	0.22	-	0.01	-	0.06	14.90
18	41.80	3.05	1.12	1.26	0.14	0.36	0.12	0.10	0.06	0.32	7.83	0.04	0.06	0.80	0.01	0.01	0.12	26.30
MEAN	**31.70**	**2.02**	**0.46**	**0.81**	**0.13**	**0.46**	**0.37**	**0.26**	**0.03**	**0.08**	**5.35**	**0.01**	**0.46**	**3.12**	**0.01**	**0.01**	**0.09**	**18.50**
SD	**8.310**	**0.27**	**0.18**	**0.12**	**0.02**	**0.19**	**0.20**	**0.05**	**0.01**	**0.06**	**0.78**	**0.01**	**0.22**	**0.84**	**0.00**	**0.00**	**0.02**	**2.530**

The following metals were identified at this site: Si, Fe, Al, Ca, Mg, K, Na, Ti, Cr, C, Cl, S, F, V, Ni, and Pb. More toxic metals (Cr, Ni, V and Pb) were identified at this site compared to Site A and B.

The S concentration is important because it includes the sulphates and most toxic trace metals exist in the atmosphere in the form of sulphates and/or nitrates. The S levels were relatively stable for August, September, November and December (Sample 13, 14, 16 and 17). A peak was observed in October (Sample 15) and an unusually low value was observed in January (Sample 18).There seems to be a propotionality correlation between S and Pb, and between S and Ni from August to December. The correlation also applies to Cr, but from August to November. It is uncertain what the cause of these correlations might be.

The oxides of Ni were measured mainly in spring (Sample 14 and 15) and ranged from 0.01 to 0.03 µg.m^{-3}. The levels of V were found to be lowest (0.01 µg.m^{-3}) for the months August, December and January (Sample 13, 17 and 18). Pb and Cr were identified throughout the sampling period, and their concentrations were measured as 0.03 to 0.21 µg.m^{-3} for Pb and 0.03 to 0.32 µg.m^{-3} for Cr. Figure 6.6 shows the ratios of the toxic metals to PM10.

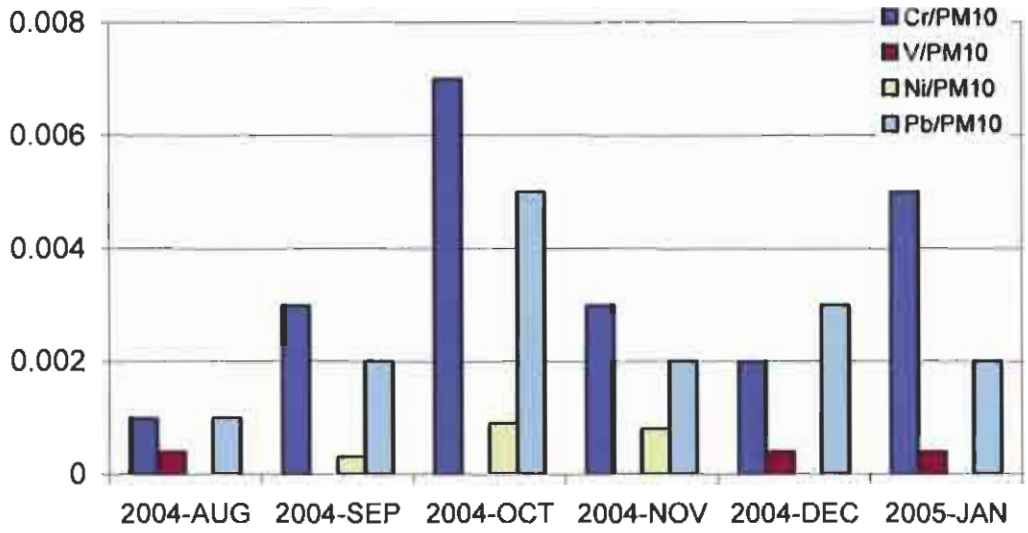

Figure 6.6: The ratio of potentially toxic metals to PM10 at Site C

The ratio of the potentially toxic metals to PM10 was very small (less than 0.001) for V and Ni. For Cr and Pb, the ratio was determined in the range from 0.001 to 0.007. The ratios are small but have a maximum in the month of October as one would expect. The maximum in the ratio is measured as a result of high PM10 levels and high potentially toxic metal concentrations observed in October as shown in Table 6.3.

The ratios of C and O to PM10 in Figure 6.7 showed a maximum in December (summer) and were fairly stable throughout the spring season. This was expected since, among all the elements identified in the PM10, O had the highest concentration followed by C. The F/PM10 ratio showed a maximum in November while the concentrations of S/PM10 were high in October (spring season) and low throughout summer. The high F/PM10 ratio could not be explained because teflon filters may be responsible for the F identified. The fact that South Africa is characterised by dry and windy spring seasons may account for the high S/PM10 ratio in October. The high rainfall which contributes to particle wash-out accounts for the low S/PM10 in summer.

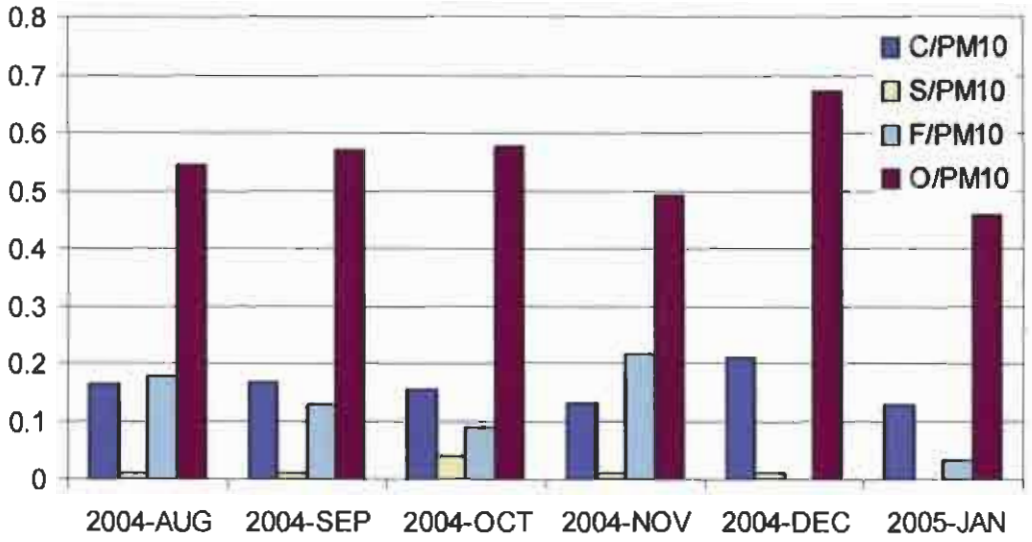

Figure 6.7: *The ratio of C, O, S and F to PM10 at Site C*

The correlation between carbon and the trace metals is also important since the carbon determined can form part of the elemental and organic carbon. The oxides of carbon may imply the presence of Cr in the form of chromium carbonate or even a gas. The carbon content can thus help give an indication of the main trace metals in the area. The r^2 values obtained for trace metals and carbon at Site C were low, except for C and Cr for which an r^2 value of 87% was obtained. The regression equation for C and Cr is given as:

$$C = 3.52 + 12.9\ Cr \qquad (6.1)$$

The graph giving the relationship between C and Cr is given in the Figure 6.8. The graph shows seven data points even though the sampling was done from August 2004 to January 2005. The occurrence of the seven data points is due to the fact that two samples were obtained for the month of August.

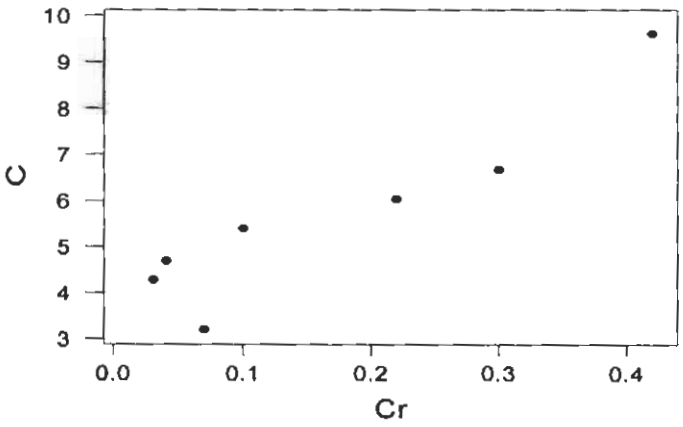

Figure 6.8: *Regression analysis graph for C and Cr obtained at Site C*

The Equation 6.1 implies that, in the absence of Cr, less C is observed, thus it is important to note the possibility of a large fraction of C existing with Cr in the particulate matter. The relation between C and Cr may not necessarily suggest Cr to be in the organic form, it may also imply the occurrence of Cr as a carbonate, or that the emission of Cr is associated with the use of carbon e.g. coal use in the furnace.

HOURLY CONCENTRATIONS

The hourly concentrations for 19 April to 10 May and 2 to 27 June determined on Teflon filters are given in Table 6.4. It can be noted that it was practically impossible to detect any toxic trace metals using the Quartz fiber filters and thus the results were discarded. With the Teflon filters though, only the crustal metals, carbon and sulphur were detected. The absence and the low concentrations of metals at Site C cannot be explained. It is worth noting that the flow rate of 13.67 $L.min^{-1}$ used during sampling, imply that a large volume of particulate matter is deposited on the filters. This however is not the case. The low concentrations might be due to the fact that Site C is less polluted compared to the other sites. The possibility of an error in the sampling equipment is also not ruled out.

It is important to note that each of the sample sets 41 to 48 and 57 to 64 correspond to the sampling periods 00h00 – 03h00, 03h00 – 06h00, 06h00 – 09h00, 09h00 – 12h00, 12h00 – 15h00, 15h00 – 18h00, 18h00 – 21h00, 21h00 – 00h00 respectively. Sample 41 for example, was obtained by continuous sampling from 19 April to 10 May but only during the 00h00 to 03h00 time period of each day.

The carbon content for the hourly samples is generally low compared to the monthly averages. This can be accounted for by the type of filter used, as well as the flow rate. Teflon has a high flouride content, which seems to either inhibit the identification of carbon, or to be inversely related to carbon.

Table 6.4: *Hourly-averaged concentrations (in $\mu g.m^{-3}$) of the elements identified at Site C*

19 APRIL – 10 MAY 2005										
SAMPLE	**PM10**	**Si**	**Fe**	**Mg**	**K**	**Na**	**C**	**S**	**F**	**O**
41	13.38	0.05	0.02	-	-	-	1.44	0.07	7.79	4.01
42	14.7	-	-	-	-	-	1.45	-	9.38	3.87
43	13.3	0.02	-	-	-	-	1.36	-	8.28	3.64
44	13.32	-	-	-	-	-	1.33	0.01	8.42	3.56
45	14.62	0.06	-	-	-	-	1.63	0.08	8.32	4.53
46	14.31	0.05	-	-	-	-	1.55	0.08	8.32	4.29
47	13.47	0.05	-	-	-	-	1.39	0.06	8.13	3.84
48	13.12	-	-	-	-	-	1.33	-	8.26	3.53
MEAN	**13.78**	**0.03**	**0.00**				**1.44**	**0.04**	**8.36**	**3.91**
SD	**0.61**	**0.01**	**0.00**				**0.04**	**0.01**	**0.16**	**0.13**
2 – 27 JUNE 2005										
57	11.4	0.15	0.06	0.05	0.04	0.02	1.41	0.18	5.25	4.25
58	11.1	-	-	-	-	-	1.11	0.01	7	2.98
59	11.77	-	-	-	-	-	1.17	0.01	7.46	3.13
60	11.4	-	-	-	-	-	1.15		7.2	3.05
61	11.79	0.05	-	-	0.03	-	1.33	0.12	6.47	3.79
62	11	0.05	-	-	0.03	-	1.17	0.1	6.33	3.33
63	12.26	0.1	0.05	0.04	0.04	0.01	1.47	0.15	6.12	4.29
64	12.22	0.04	-	-	-	-	1.25		7.57	3.36
MEAN	**11.62**	**0.05**	**0.01**	**0.01**	**0.02**	**0.00**	**1.26**	**0.07**	**6.68**	**3.52**
SD	**0.44**	**0.02**	**0.01**	**0.01**	**0.01**	**0.00**	**0.05**	**0.03**	**0.28**	**0.19**

Only a few oxides could be detected from the Teflon filters, and these were mainly the crustal elements and C, S and F. The metals of interest (Cr, Ni, V and Pb) were not detected.

MICROGRAPH OF HOURLY PM10 SAMPLE AT SITE C

The mineralogy of atmospheric particles may in some cases be more useful than their chemical composition with a view to establish their origin and their potential effects on human health, whether adverse (e.g. silicosis, asbestosis or lung cancer) or favourable (e.g. neutralization of acid aerosols). However, the mineralogy of particles is more difficult to determine than their chemical characterization in the case of a small sample, as it sometimes occurs in sedimentable and aerosol fractions (Anwari, 1992).

Other non-mineral particles detected by SEM in aerosol fractions included spherical and biological particles, as well as crystal aggregates. Spherical particles were of a spongy, smooth or rough texture. Spongy particles, in sizes from 7 to 35 mm, consisted mainly of S and Si accompanied by lower proportions of Al, Ca, P, Na, K, Cl, V or Fe. Smooth particles, in sizes from 2.5 to 6:5 mm, showed an Al-silicate and/or Ti composition. Finally, rough particles were either 1:5 mm in size and consisted mainly of Ti or 2mm in size and composed of S, Fe and Si (Anwari, 1992).

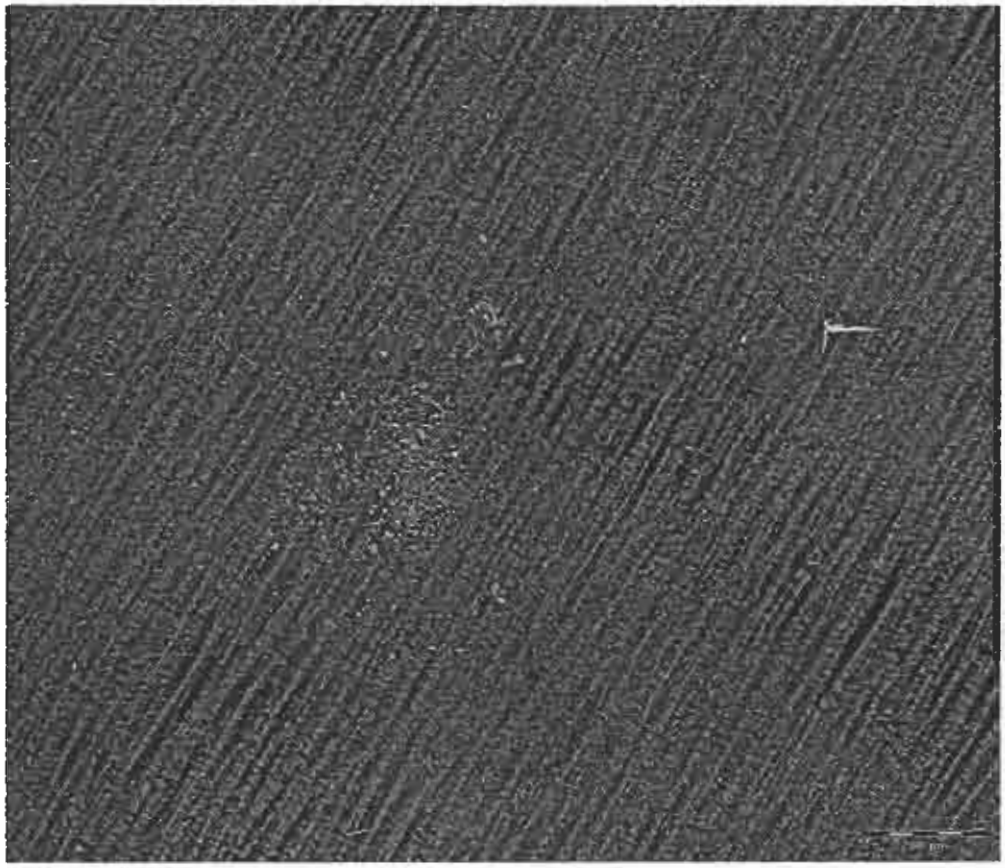

Figure 6.9: *A typical micrograph corresponding to the hourly average concentrations at Site C*

Low hourly concentrations were observed at Site C. This is evident in the micrograph given in Figure 6.9 were only a few bright spots (pollutants) were observed. The location of the site favors low levels of pollutants since it is far from the mine.

6.2 COMPARISON BETWEEN STUDY SITES

The fact that the levels of PM can vary significantly from one place to another based on the meteorolgy and distance from pollution sources, suggests the importance of comparing the concentration levels obtained at the three different sites used in this study. The composition of PM is also expected to vary from one site to another since the sites have different geographic locations, and are located closer to different potential sources of PM.

6.2.1 CONCENTRATION OF THE METAL OXIDES

The levels of oxides of Al, Ca, Si, Na, Cl, S, with Fe in almost all the monthly averaged samples, suggest the presence of aluminosilicates with traces of sulfate or sulfite, and chloride (Goldstein, 2003). For most of the samples, the content of oxides of sulphur is the fourth highest content. The presence of SO_x is not pleasant since it may be an indication of the presence of sulphur dioxide, sulphuric acids, ammonium sulfate, ammonium bisulfate, and the presence of nickel and other metal oxides, which may exist in the form of sulphate aerosols in the atmosphere.

The S concentrations of 1.5 $\mu g.m^{-3}$ at the Shenandoah National Park compare with the 1.6 $\mu g.m^{-3}$ observed at Site A during 15 May to 8 June 2004 and the 1.69 $\mu g.m^{-3}$ measured in October 2004 at Site C. The 0.68 $\mu g.m^{-3}$ measured at Site B in June and September 2004 compares with the 0.64 $\mu g.m^{-3}$ obtained by Solomon *et al.* (2000b) at the Rubidoux study site.

The concentrations of the oxides of crustal elements identified in this study are all relatively high compared to the levels obtained at four study sites (Atlanta, Rubidoux, Shenandoah National Park, and Meadview) between May 1998 and May 1999 in the USA by Solomon *et al.* (2000b). The Ca concentrations at Site C ranged from 0.05 to 0.14 $\mu g.m^{-3}$, whereas the Ca levels at the four sites in the US ranged from 0.03 to 0.16$\mu g.m^{-3}$. The 0.1 $\mu g.m^{-3}$ Fe measured at Site C in August 2004 compares with the 0.13 $\mu g.m^{-3}$ in August 1999 in Atlanta, while the 0.19 $\mu g.m^{-3}$ measured at Site B for July to August (Sample 6) compares with the 0.18 $\mu g.m^{-3}$ observed at Rubidoux for January to February 1999.

The levels of the oxides of Cr determined ranged from 1.1 to 3.28 $\mu g.m^{-3}$, 0.0 to 0.28, and 0.03 to 0.42 for Site A, B, and C respectively. This shows that the limit of 1000 $ng.m^{-3}$ (1 $\mu g.m^{-3}$) set by NIOSH was exceeded only at Site A.

The levels of Pb throughout the study ranged from 0.03 to 0.24 $\mu g.m^{-3}$. The 0.5 $\mu g.m^{-3}$ guideline set by the WHO was never exceeded during this study.

The levels are however, very high compared to the levels ranging from 0.0016 to 0.011 $\mu g.m^{-3}$ obtained from four study sites in the USA in 1999 Solomon *et al.* (2000b). The concentrations of Ni and V ranged from 0.01 to 0.02 $\mu g.m^{-3}$ and 0.01 to 0.03 $\mu g.m^{-3}$ respectively.

The regression analysis of carbon with Cr, Ni, V, and Pb at Site A and B yielded the r^2-values ranging from 3.7 to 31%. This suggests that the potentially toxic metals identified at Site C do not have a common source or region with carbon.

The high concentration of oxides of carbon for most samples is not unusual since it is linked to organic matter in the samples. The presence of oxides of carbon can also be linked to Pb-bearing particles that usually occur as Pb carbonate.

Table 6.5 gives a summary of the levels of the main metals and the standards or limits where available.

Table 6.5: *Monthly concentrations (in $\mu g.m^{-3}$) of metals in the Rustenburg area*

Metal		Site A	Site B	Site C	Standard or Limit
Cr	Range	1.1 – 3.8	0.1 – 0.28	0.03 – 0.32	1 $\mu g.m^{-3}$ – NIOSH
	Mean	2.28	0.14	0.08	1.5 $\mu g.m^{-3}$ - APCEL
	SD	0.64	0.04	0.06	
Ni	Range	------	------	0.01 – 0.03	No safe levels - WHO
	Mean			0.01	
	SD			0.00	
V	Range	------	0.00 – 0.02	0.00 – 0.01	1 $\mu g.m^{-3}$ - WHO
	Mean		0.00	0.01	
	SD		0.00	0.00	
Pb	Range	------	0.00 - 0.24	0.03 – 0.21	0.5 $\mu g.m^{-3}$ - WHO
	Mean		0.03	0.09	
	SD		0.03	0.02	

6.2.2 IDENTIFICATION AND APPORTIONMENT OF SOURCES

Correlation and regression analysis have been used by many researchers in health risk assessment and source apportionment studies. Table 6.6 gives the correlation matrix for all the elements identified during this study. A strong correlation between any two elements suggests that the two elements have a common source whereas the absence of correlation between any two elements may indicate that the two do not have a common source or source region.

The sources in this study were expected to be mainly due to anthropogenic activities like traffic, soil dust from scraping of the earth crust, and anthropogenic smelting. This is mainly due to the type of mining and industrial activities in the area as explained in Section 1.3 of this report.

CRUSTAL SOURCES AND SOIL DUST

According to Al-Momani (2003), crustal material is the only source of Al. It is therefore logical to use Al as a tracer for crustal material source. A strong correlation between Al and any other element suggests crustal material as a major source of that particular element. The r^2 values obtained from the regression analysis ranged from 0.8 to 1% for Al and V, 0.8 to 32% for Al and Pb, and 62 to 63% for Al and Cr, 0 and 1.4% for Al and Ni at Site C. This rules out the possibility of the same source for Al and the trace metals of concern, except for Al and Cr. The high r^2 value for Al and Cr at Site C presents the possibility of Cr being from a crustal source. This, however, does not rule out anthropogenic activities since they may cause resuspension of particulate matter.

The correlation between Fe and Cr (r = 0.88) is not surprising because there are ferrochrome mining and smeltering activities within the Rustenburg area. The crustal elements (Si, Fe, Al, Ca, Mg) identified in this study are highly correlated (r values between 0.90 to 0.97) with each other (Table 6.6). This shows that they are from a common source, i.e. soil dust.

Table 6.6: *Pearson's correlations between the elements identified in PM for the Rustenburg area*

	PM10	Si	Fe	Al	Ca	Mg	K	Na	Ti	Cr	C	Cl	S	F	P	V	Ni	Pb	N
Si	0.862																		
Fe	0.858	0.956																	
Al	0.895	0.971	0.947																
Ca	0.775	0.971	0.940	0.944															
Mg	0.820	0.947	0.893	0.935	0.936														
K	0.521	0.494	0.415	0.464	0.412	0.672													
Na	0.937	0.781	0.766	0.811	0.689	0.762	0.576												
Ti	0.778	0.612	0.769	0.668	0.559	0.562	0.347	0.747											
Cr	0.865	0.763	0.881	0.833	0.748	0.742	0.354	0.808	0.930										
C	0.870	0.559	0.543	0.603	0.405	0.509	0.478	0.814	0.633	0.622									
Cl	0.629	0.824	0.711	0.712	0.818	0.758	0.414	0.537	0.281	0.415	0.425								
S	0.891	0.697	0.702	0.767	0.637	0.696	0.405	0.897	0.693	0.818	0.734	0.387							
F	-0.491	-0.527	-0.409	-0.448	-0.392	-0.431	-0.395	-0.408	-0.117	-0.140	-0.593	-0.600	-0.249						
P	0.125	0.082	0.061	-0.081	0.030	0.022	0.178	0.082	0.065	-0.018	0.226	0.358	0.039	-0.318					
V	0.027	0.047	0.010	0.061	-0.064	0.069	0.273	0.009	0.077	-0.049	0.098	-0.118	0.028	-0.329	-0.082				
Ni	0.060	0.023	0.035	0.015	-0.073	-0.050	-0.055	0.188	0.018	-0.010	0.132	-0.162	0.008	-0.126	-0.082	-0.117			
Pb	0.110	0.078	0.080	0.083	-0.071	-0.006	0.022	0.131	0.092	-0.009	0.213	-0.172	0.088	-0.351	-0.104	0.639	0.599		
N	0.068	0.013	0.000	0.015	-0.012	-0.008	0.084	0.063	-0.076	-0.035	0.095	-0.091	0.144	-0.231	-0.042	-0.060	-0.059	-0.076	
O	0.983	0.799	0.774	0.828	0.682	0.749	0.532	0.920	0.714	0.781	0.938	0.602	0.863	-0.591	0.176	0.077	0.088	0.167	0.11

Resuspension of dust can be either due to traffic or scraping of the earth crust as an industrial anthropogenic activity. Figure 6.10 below shows the ratio of toxic metals to Al at Site B. All ratios of the potentially toxic metals are very small (0 – 0.3), which suggests that the toxic metals are not associated with crustal material (soil dust). A maximum in the ratios is however, observed for Cr, Ni and Pb in October 2004. The observation of a maximum can be the result of high wind speeds during the month of October. The ratio of Cr to Al is the highest followed by Pb/Al then Ni/Al. The results are similar to the Site C correlation results, which is interesting since there are not much smelting activities within the vicinity of Site C. This implies that for the Rustenburg area, the potentially toxic metals are not from soil dust.

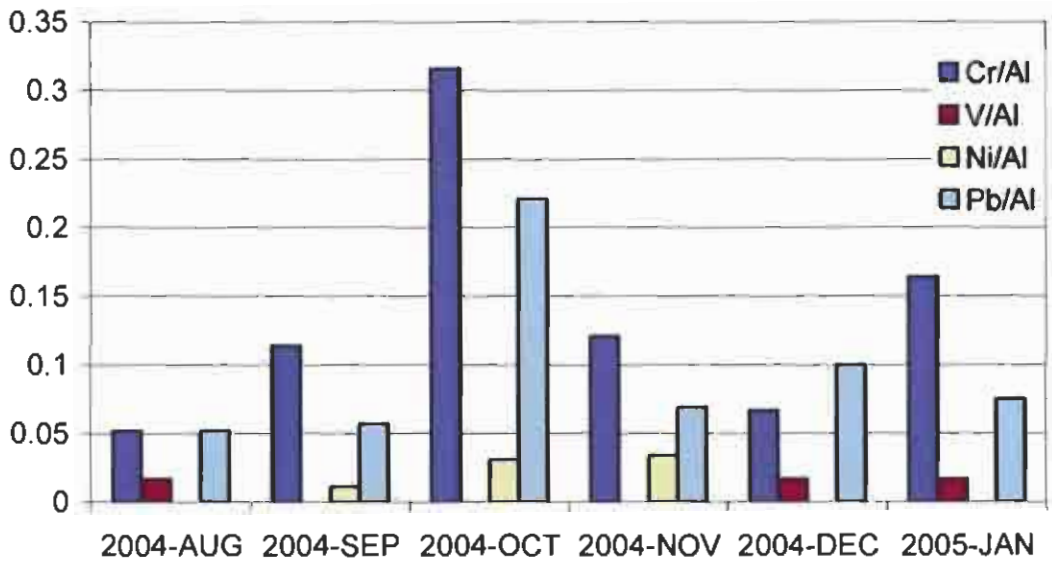

Figure 6.10: *The ratio of the potentially toxic metals to Al at Site B*

Metal smelting and fuel combustion are usually the source of non-crustal volatile metals in the atmosphere (Nriagu, 1989). According to Held *et al.* (1996), the elements Zn and Mn can be used as tracers for smelting sources, K can be used for biomass burning, Cl for sea salt, sulphate for anthropogenic sources, and Al, Si and Ti for soil dust. Zn, excess Mn, Cu and Ni are an unambiguous signal of anthropogenic smelting.

FUEL COMBUSTION

Potassium (K) has also been suggested by Held *et al.* (1996) as a tracer for biomass burning. The correlation between K and Si in this study is r^2 = 58%, 55% between K and Fe, and 55% between K and Ca. This suggests that biomass burning is not the major source of the elements identified in this study, since K and Si may be from the same source, and Si and Fe are tracers for a soil dust source.

The co-presence of both Pb and Zn and moderate correlations (between Pb and V) in Seoul (Mishra *et al.,* 2004b) was reported as indicators that the contribution from fuel combustion may be important. The small correlation observed between Pb and V (r^2 = 0.48), may suggest fuel combustion as one of the sources of particulates at these sites.

In a study conducted in an industrial area of Taejon, Korea, Pb was also found to be strongly correlated with crustal elements (Ba, Sb, Co, Fe, etc.) and fuel combustion (V). Strong correlations were also noticed among Pb, Fe, Zn, and Ti from a study conducted by Chow *et al.* (2003) in Los Angeles. The correlations observed during this study are however, very small r^2 = 0.8% for Pb and Ti, r^2 = 0.6% for Pb and Fe. This indicates that the Pb identified in this study cannot be of crustal origin, but is mainly due to fuel combustion (traffic).

The fact that the oxides of Cu, Mn and Zn could not be detected during this study makes it difficult to link the present elements to anthropogenic smelting unambiguously.

PRINCIPAL COMPONENT ANALYSIS OF SOURCES

Principal component analysis was also used to apportion the sources discussed above. The PCA results for Site A are given in Figure 6.11. The analysis yielded two factors, factor 1, which accounted for 84.4% of the variance and factor 2, which accounted for 15.6%.

Factor 1 contained Si, Al, Ca, Mg, K, Na, C, Cl, F and O, which suggests traffic and a soil dust source. The elements Si, Al, Ca, Mg, K and Na are indicative of a soil dust source while C and Cl are indicative of traffic. Elemental carbon (EC) was suggested by Ito *et al.* (2004), Ho *et al.* (2003) and Salvador *et al.* (2004) as an emission from vehicles. Cl was identified by Salvador *et al.* (2004) as an additive to petrol in the form of ethylene dihalide ($C_2H_4Cl_2$). The O is not used as a tracer or signature since it may be linked to carbon or any other element identified thus implying any oxide in the PM10 analysed.

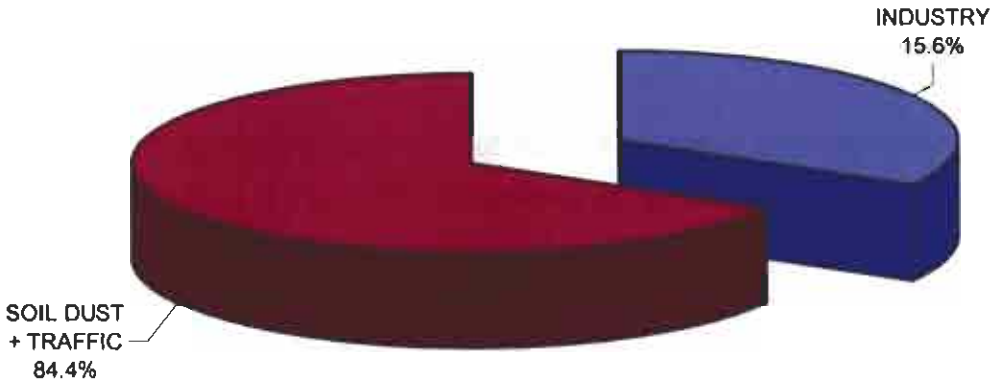

Figure 6.11: *PCA for Site A*

Factor 2 was composed of Fe, Ti, Cr and S, which imply that this source of PM10 is industry. The fact that Site A is closer to a ferrochrome mine justifies the presence of Fe and Cr as indicators for an industrial source. Ti may also suggest industrial activity relating to building and construction since it usually occurs in cement dust. The S in this factor indicates anthropogenic activities as a source of PM. The S may also indicate the presence of sulphates linked to Cr.

The PCA results for Site B are given in Figure 6.12.

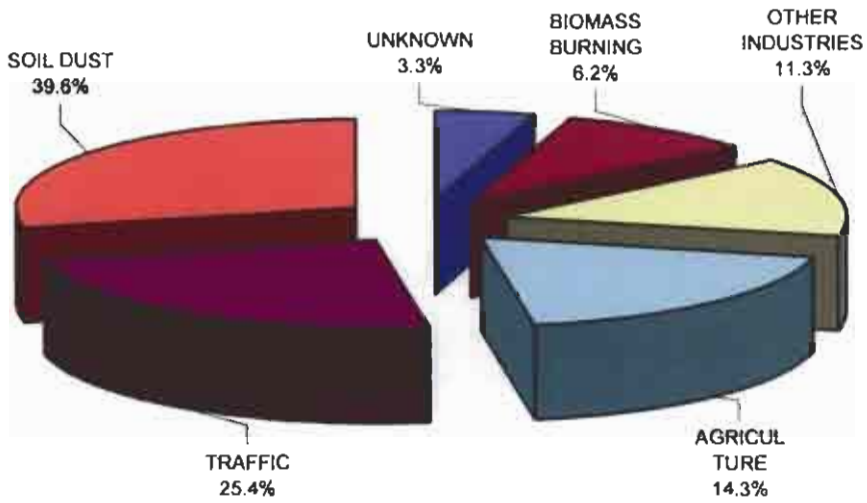

Figure 6.12: *PCA for Site B*

Five factors accounting for 96.7% of the PM analysed were identified at Site B. The remaining 3.3% of PM is labelled as an unknown source in Figure 6.12.

Factor 1, which explained 39.6% of the variance contained Si, Fe, Ca, Cr and C, and was associated with a soil dust source. Factor 2 (25.4%) contained Al, Cl, V, and Pb. This factor was linked to traffic. The third factor (14.3%) was apportioned as an agricultural source mainly because of the presence of P and Na, which may be from fertilizers and pesticides. The factor had loadings of Na, F, P and O. The fourth factor (11.3%) contained Ti and N, which are linked to industrial activities in the area. Ti can be linked to industrial building activities and N is associated with residual oil (Ito *et al.,* 2004). The factor was thus apportioned to other industries. Factor 5 which accounted for 6.2% of the PM analysed, was composed of Mg and K. The factor was linked to biomass burning.

Figure 6.13 gives the PCA for Site C. Five factors, which accounted for 98.4% of the PM were identified. The other 1.6% is the part with eigenvalues of less than one, which could not be apportioned and is labelled as 'unknown' in the figure.

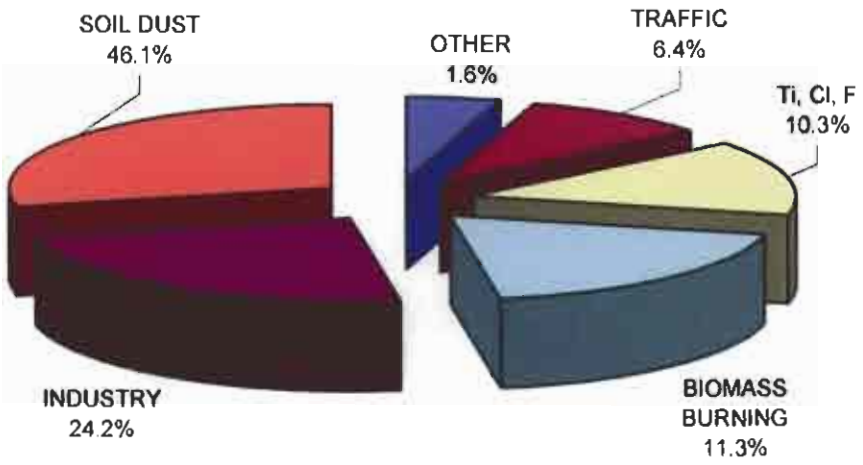

Figure 6.13: *PCA for Site C*

The first factor which accounted for 46.1% of the variance contained Si, Fe, Al, Cr, C and O. This is indicative of a soil dust. The occurrence of Cr is not surprising since it may have been deposited on the earth crust as a result of the long-term ferrochrome mining activities in the area. Factor 2, which formed 24.2% and contained Na and Ni, was linked to industrial activities. This is mainly because Ni is linked to residual oils and other anthropogenic activities.

The third factor accounted for 11.3% of the variance with loadings of Mg and K. The factor was linked to biomass burning. Factor 4, which formed 10.3% of the PM, contained Ti, Cl and F. The source of this factor could not be properly identified, mainly because of the presence of high loadings of F, which may also be from the filters used. The fifth factor (6.4%), which was linked to traffic, contained Ca, S, V and Pb, with high loadings of V.

Figure 6.14 gives the PCA results for the Rustenburg area (all three sites) from the monthly concentrations obtained throughout the study.

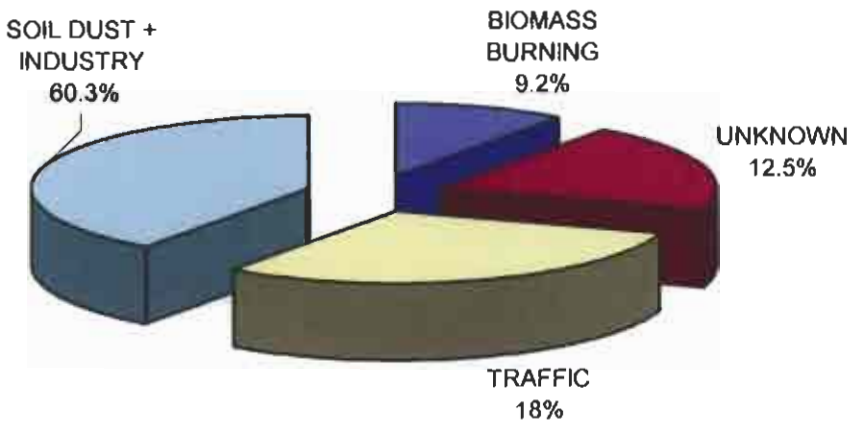

Figure 6.14: *PCA for the Rustenburg area using the results from Site A, B and C combined*

The PCA results for the three sites in Rustenburg, obtained from SEM/EDS concentrations showed that the sources, in decreasing order, within the area were largely soil dust and industry, traffic, biomass burning, and other sources. The three factors identified formed 60.3%, 18.0% and 9.2%, with loadings of Si, Fe, Al, Ca, Mg, Na, O, Cr and S; Ti, C, Cl and F; and K respectively. The factors accounted for 87.6% of the variance and the 12.4% is given as unknown in Figure 6.14 above.

6.3 HEALTH AND ENVIRONMENTAL IMPLICATIONS OF THE CONCENTRATION LEVELS

Airborne particulate matter is a mixture of thousands of different substances, diverse in such critical characteristics as their solubility, persistence in the atmosphere and in human tissue, reactivity, toxicity and carcinogenicity, as well as their chemical structure and elemental composition. Other metals, particularly iron (Fe), copper (Cu), and zinc (Zn), are of toxicological interest, since these transition metals may play a crucial role in the oxidative stress pathway, hypothesized by Gilliland *et al.* (1999) to be part of the causal explanation of many observed air pollution-related health effects.

The primary goal of air pollution research is aimed at identifying culprit agents of air pollution to understand and prevent adverse health outcomes. The SEM/EDS technique in this study revealed the presence of atmospheric particles of complex composition including S, Si, Al, Mg, Ca, Pb, Fe, Cr, Ni, V, and Pb among other elements. These particles can be harmful not only to human health, but also to the cultural heritage and the ecosystem as a whole. Therefore, it would be advisable to investigate further their potential hazards.

The WHO (2003) suggests that besides physical aspects such as particle number, size, or surface, the chemical composition of particles is likely to play a crucial role regarding the health implications of particulate matter. Various health effects of PM, from less serious to very serious ones, are associated with its specific chemical and physical (but mostly chemical) components (Sharma and Maloo, 2005).

Figure 6.15 shows a typical composition of an ordinary particle from traffic or fuel combustion source. Most of these particles contain carbon at their core, with toxics and carcinogenic substances attached to their surfaces.

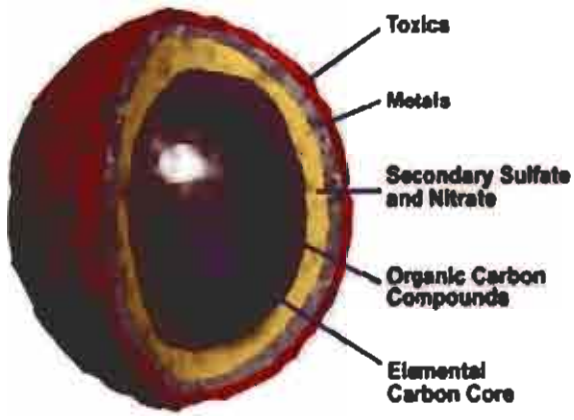

Figure 6.15: *Composition of a typical diesel particle (Schneider, 2005)*

The SEM/EDS method is thus very relevant to pollution studies since the scanning gives an indication of the toxics attached to the surface of the particle.

The following regression equations show a clear relationship between the levels of PM10 and the toxic trace metals of interest (Cr, Ni, V, and Pb) observed at Site C. The graphs corresponding to these equations are given in Figure 6.12 (a) – (b) below.

$$PM10 = 22.6 + 62.7\ Cr \quad (6.2)$$

$$PM10 = 22.3 + 123\ Pb \quad (6.3)$$

These correlations are important since they suggest an increase in the levels of toxic trace metals as the levels of PM10 increases.

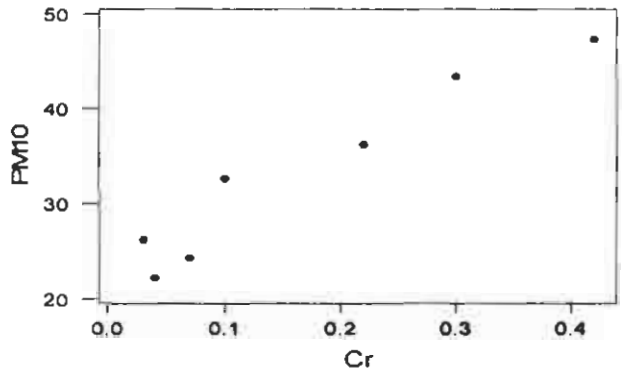

(a)

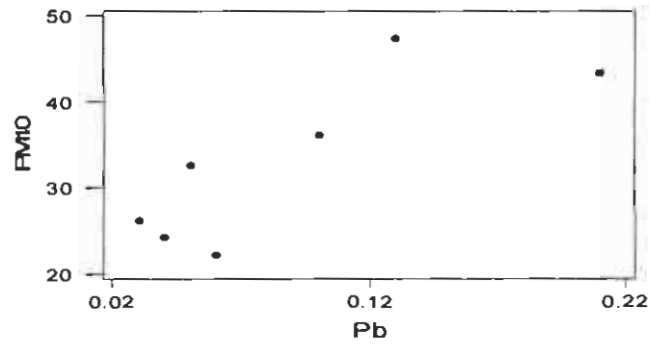

(b)

Figure 6.16: *Regression analysis graphs for (a) PM10 and Cr, (b) PM10 and Pb obtained from Site C*

This indicates the possibility of having high levels of trace metals at relatively low levels of PM10. Thus even when the standards set by the environmental protection agencies are not exceeded, the levels of the cancer-causing agents may still be hazardous to human health. The graph shows seven data points even though the sampling was done from August 2004 to January 2005. The occurrence of the seven data points is due to the fact that two samples were obtained for the month of August.

The SEM/EDS results presented in this chapter yielded some interesting information on the elemental and morphological composition of particulate matter. Some authors have also used this technique to examine particles in morphological and chemical terms, or elucidate their mineralogy (Esbert et al. 1996; Chabas and Lefevre, 2000). However, there are not many mineralogical analyses of atmospheric particles (Esteve et al., 1997; Querol et al., 1999; Queralt et al., 2004; Ekosse et al., 2004). It is thus imperative that other methods be used to ascertain and supplement the results obtained thus far. The next chapter presents data from chemical characterisation of the same samples using a different analytical method.

CHAPTER 7

INDUCTIVELY COUPLED PLASMA MASS SPECTROSCOPY RESULTS

In this chapter, the results obtained using Inductively Coupled Plasma Mass Spectroscopy (ICP-MS) are presented. Estimation and apportionment of sources of the elements identified is discussed. Trends in the concentration levels, comparison of the levels from the chosen study sites, and the health and environmental implications of the concentration levels are also discussed.

7.1 CONCENTRATION OF ELEMENTS

The results discussed in this section are concentrations at the three study sites within the Rustenburg area. The same filters analysed by SEM/EDS in Chapter 6, were taken for further analysis using ICP-MS. The results are thus presented in roughly the same manner as in Chapter 6, and the same meteorological conditions as given in Section 5.2 are applicable.

7.1.1 CONCENTRATION OF ELEMENTS AT SITE A

Site A has been identified thus far as the most polluted of the three sites in this study. Table 7.1 shows the metals identified using ICP-MS and their concentration levels. About 15 main metals were identified. Sample 1 and 2 were obtained during the autumn season (20 February – 12 March 2004 and 22 April – 15 May 2004), and Sample 3 was obtained during the beginning of winter (15 May – 8 June 2004).

Table 7.1: *Concentrations (in μg.m^{-3}) of the elements identified during autumn and winter at Site A*

Sample	PM10	Si	Fe	Al	Ca	Mg	K	Na	Ti	Cr	Ni	V	Pb	Cu	Zn	Mn
1	131.10	2.12	25.00	4.43	7.52	3.08	0.46	1.44	0.32	2.10	1.10	0.40	0.50	0.19	0.38	0.21
2	99.74	2.50	8.48	5.20	5.30	3.56	0.54	2.02	0.12	0.36	0.34	0.04	0.06	0.26	0.38	25
3	94.36	1.54	5.02	1.92	1.92	1.54	0.57	1.40	0.08	5.20	2.80	0.40	0.50	0.21	0.26	0.21
Mean	**108.40**	**2.05**	**12.83**	**3.85**	**4.91**	**2.73**	**0.52**	**1.62**	**0.17**	**2.55**	**1.41**	**0.28**	**0.35**	**0.22**	**0.34**	**8.47**
SD	**11.46**	**0.28**	**6.16**	**0.99**	**1.63**	**0.61**	**0.03**	**0.20**	**0.07**	**1.42**	**0.73**	**0.12**	**0.15**	**0.02**	**0.04**	**8.26**

The elements identified include Si, Fe, Al, Ca, Mg, K, Na, Ti, Cr, Ni, V, Pb, Cu, Zn, and Mn, and can still be categorised as crustal and potentially toxic trace metals. There are no clear relations between the toxic trace metal concentrations and the seasons or months of the year. K increases from autumn to winter and crustal elements Ti, Fe, Ca decrease from autumn to winter. This may be because of the increase in biomass burning during winter since K is a tracer for biomass burning.

It is worth noting that the different techniques used in this study show different sensitivities to different metals, thus the elements that could not be identified in Chapter 6 are Ti, Cu, Zn, and Mn. The levels of Mn were very high for Sample 2. This could not be explained. It can however be an analysis error because the value is three orders of magnitude higher than Sample 1 and 3 and thus clearly out of acceptable range. The Zn and Cu identified had a concentration range of 0.26 to 0.36 μg.m^{-3} and 0.19 to 0.26 μg.m^{-3} respectively.

Table 7.2 gives the correlation matrix for Site A. A surprising result is that for most elements, there is a negative correlation to the levels of PM10. This is a very important result as it suggests that the lowest level of PM10 can contain the highest level of potentially toxic elements. This can be very detrimental and requires that more focus be placed on setting standards of limitation for specific components of particulate matter within a specific area of concern rather than focusing only on values of PM.

A high correlation, (r = 0.98) was observed for Si and Al. This suggests that they were from the same source. The correlation between Al and Fe was however very low (r = 0.44), which may suggest that the two were not entirely from the same source. Some portion of Fe might be from anthropogenic sources since the site is characterised by ferrochrome smelters.

Table 7.2: *Correlation matrix for Site A*

	PM10	Si	Fe	Al	Ca	Mg	K	Na	Ti	Cr	Ni	V	Pb	Cu	Zn
Si	0.253														
Fe	1.000	0.279													
Al	0.420	0.984	0.444												
Ca	0.874	0.691	0.887	0.807											
Mg	0.417	0.985	0.441	1.000	0.806										
K	-0.991	-0.377	-0.995	-0.535	-0.930	-0.532									
Na	-0.324	0.833	-0.299	0.723	0.176	0.725	0.198								
Ti	1.000	0.272	1.000	0.438	0.884	0.435	-0.994	-0.305							
Cr	-0.292	-0.999	-0.318	-0.991	-0.720	-0.991	0.415	-0.810	-0.312						
Ni	-0.346	-0.995	-0.371	-0.997	-0.758	-0.997	0.465	-0.776	-0.365	0.998					
V	0.378	-0.800	0.353	-0.682	-0.119	-0.684	-0.254	-0.998	0.359	0.775	0.738				
Pb	0.378	-0.800	0.353	-0.682	-0.119	-0.684	-0.254	-0.998	0.359	0.775	0.738	1.000			
Cu	-0.620	0.602	-0.599	0.452	-0.161	0.455	0.512	0.943	-0.604	-0.569	-0.522	-0.961	-0.961		
Zn	0.613	0.920	0.634	0.974	0.919	0.974	-0.711	0.549	0.629	-0.935	-0.953	-0.500	-0.500	0.240	
Mn	-0.378	0.800	-0.353	0.682	0.119	0.684	0.254	0.998	-0.359	-0.775	-0.738	-1.000	-1.000	0.961	0.500

The V and Pb correlation of 1 suggests that the two were from the same source. This further suggests fuel combustion (traffic) as the source of these metals at Site A (Chow *et al.*, 2003; Mishra *et al.*, 2004b). The potential toxic trace metals had small correlations with Fe, Ti and K. This suggests that their origin was neither crustal nor biomass burning. Cr was highly correlated to Ni (r = 0.99), which implies that they had the same source. It can be suggested at this point that the potentially toxic trace metals at Site A are not from soil dust or biomass burning, but from some anthropogenic source.

Principal component analysis was used to identify and quantify the sources of particulate aerosols in this study. The PCA results at Site A, given in Figure 7.1 showed two factors that accounted for 100% of the variance.

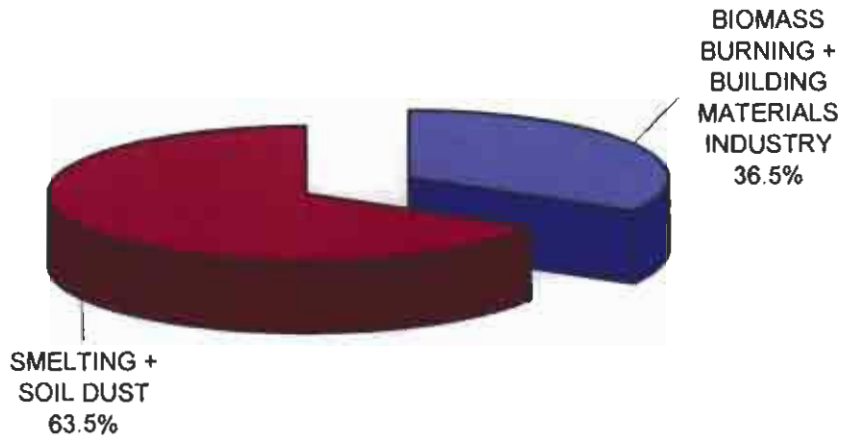

Figure 7.1: *PCA for Site A obtained from ICP-MS concentrations*

Factor 1, which accounted for 63.5% of the variance contained Si, Al, Mg, Cr and Ni which may indicate the presence of soil dust and anthropogenic smelting sources. The metal plating industry could be the dominant source for Ni in these aerosols (Nriagu & Pacyna, 1988). From the variations, it appears that Cr was dominantly crustal in nature while Ni, like Ba, has a mixed origin. Reheis *et al.* (2002) have also observed the mixed origin of Ni and Cr for the dust samples from the south-western United States.

The second factor accounted for 36.5% and had loadings of Fe, K and Ti. These are indicative of biomass burning (Held *et al.*, 1996), and building industrial activities (Zhang *et al.*, 2004).

7.1.2 CONCENTRATION OF ELEMENTS AT SITE B

Table 7.3 below shows the average monthly concentrations determined at Site B during the study. Sample 4 and 5 were obtained during winter (8 – 29 June 2004 and 29 June – 23 July 2004), Sample 6, 8 and 9 during spring (23 July – 19 August 2004, 10 – 28 September 2004 and 28 September – 26 October 2004) and Sample 10 and 11 were obtained during summer (26 October – 12 November 2004 and 12 – 23 November 2004). Sample 7 was lost after analysis using SEM/EDS; hence its data is not presented.

There seemed to be no clear trends for most of the elements identified as shown in Table 7.3, except for a trend observed during spring for Na, Pb, Mn and K in Sample 6,8 and 9. These show an increase in concentration as temperature increased as shown in Table 5.1, where the temperatures 23.8, 25.7 and 28.8^{0}C were measured for the months of August, September and October respectively.

The peak in the K-concentrations for Sample 4 and 9 may indicate activities related to biomass burning. This can be expected during winter (Sample 4) since there are more veld fires during this season. The peak in spring (Sample 9) may also indicate the effect of veld fires but from regional pollution, since the spring season is characterised by high wind speeds (15.7 m.s^{-1} in August, 16.7 m.s^{-1} in September and 9.4 m.s^{-1} in October 2004) as shown in Table 5.1.

Table 7.3: *Concentrations (in μg.m^{-3}) of the elements determined during winter, spring and summer at Site B*

Sample	PM10	Si	Fe	Al	Ca	Mg	K	Na	Ti	Cr	Ni	V	Pb	Cu	Zn	Mn
4	48.73	10.20	0.20	3.10	2.30	3.20	2.30	3.10	0.01	0.02	0.00	0.05	0.00	0.08	0.10	0.40
5	49.28	1.60	5.20	2.00	2.00	1.60	0.60	1.50	0.80	0.50	0.30	0.04	0.05	0.20	0.30	0.20
6	48.39	9.10	10.7	1.90	3.20	1.30	0.20	0.60	0.10	0.09	0.05	0.02	0.02	0.08	0.17	0.09
8	45.51	3.30	11.3	6.90	7.10	4.80	0.70	2.70	0.17	0.50	0.46	0.05	0.08	0.35	0.50	0.33
9	44.22	0.20	8.50	3.10	3.70	2.70	2.20	2.90	0.07	0.05	0.03	0.02	1.40	0.02	0.35	0.51
10	43.06	0.93	10.00	4.20	3.70	3.60	1.80	4.40	0.07	0.06	0.05	0.04	1.70	0.03	0.49	0.62
11	46.46		0.93	3.00	1.70	1.40	0.41	0.82	0.09	0.03	0.03	0.01	0.10	0.61	0.40	0.04
Mean	**46.52**	**4.22**	**6.69**	**3.46**	**3.39**	**2.66**	**1.17**	**2.29**	**0.19**	**0.18**	**0.13**	**0.03**	**0.48**	**0.20**	**0.33**	**0.31**
SD	**0.90**	**1.77**	**1.75**	**0.64**	**0.69**	**0.50**	**0.34**	**0.52**	**0.10**	**0.08**	**0.07**	**0.01**	**0.28**	**0.08**	**0.06**	**0.08**

The Cr and Ni concentrations were lowest for Sample 4 and 11. This is interesting since the wind directions corresponding to the samples were oppositely directed, that is, NNW in June and SSE in November 2004, and the average temperatures were also varied i.e. 19.4 and 31.5^{0}C for June and November respectively. The average wind speeds were however, roughly the same (12.2 and 10.2 m.s^{-1}) for June and November. The levels of Ca, Mn and V were also lowest for Sample 11.

The Pb concentrations show peaks for Sample 9 (1.4 μg.m^{-3}) and 10 (1.7 μg.m^{-3}). This may be due to the contribution from road dust, which could be expected to be higher when the wind speed is high. This was however, not the case since the wind speeds for Sample 9 and 10 were lower (9.4 and 10.2 m.s^{-1} for October and November) than for the samples obtained between June and September. The wind direction (S and SSE) corresponding to these samples can be responsible for the Pb levels, since they imply that the wind was blowing from the central business district, where there are more activities related to traffic, to Site B as shown in Figure 4.1.

Any two elements that have a correlation coefficient close to one (1) are said to be strongly correlated, and are thus expected to have a common source whereas a very small correlation (less than 0.5) between any two elements may indicate that the two do not have a common source or source region.

Table 7.4 gives a correlation matrix for the concentration of elements observed at Site B.

TABLE 7.4: *Correlation matrix for the monthly concentrations at Site B*

	PM10	Fe	Al	Ca	Mg	K	Na	Ti	Cr	Ni	V	Pb	Cu	Zn
Fe	-0.464													
Al	-0.529	0.391												
Ca	-0.460	0.725	0.878											
Mg	-0.516	0.354	0.902	0.802										
K	-0.383	-0.169	0.084	-0.020	0.443									
Na	-0.639	0.199	0.494	0.359	0.770	0.800								
Ti	0.466	-0.030	-0.269	-0.205	-0.304	-0.392	-0.294							
Cr	0.241	0.311	0.381	0.459	0.261	-0.441	-0.116	0.745						
Ni	0.084	0.391	0.598	0.650	0.440	-0.420	-0.036	0.547	0.964					
V	0.098	0.084	0.505	0.423	0.720	0.329	0.590	0.192	0.491	0.510				
Pb	-0.852	0.388	0.118	0.128	0.281	0.592	0.701	-0.284	-0.365	-0.329	-0.094			
Cu	0.109	-0.376	0.225	-0.039	-0.155	-0.598	-0.508	0.085	0.210	0.285	-0.299	-0.497		
Zn	-0.763	0.435	0.668	0.534	0.461	-0.121	0.339	0.022	0.316	0.445	0.007	0.469	0.355	
Mn	-0.665	0.289	0.374	0.333	0.677	0.844	0.967	-0.277	-0.162	-0.105	0.470	0.800	-0.647	0.284

In a study conducted by Pacyna (1998), the factor that explained most of the variance (60.5%) was heavily loaded with As, Zn, Pb, Ni, Cd, and Cu, representing the combined sources of industry and motor vehicle emission. The metallurgical processes could produce the largest emissions of Cu, Ni, and Zn in a study by Pacyna (1986) and Lee *et al.* (1999). The Pb identified at Site B had a negative and small correlation with Cr, Ni, V, and Cu with r-values of -0.37, -0.33, -0.09, -0.49 respectively. This clearly shows that the Pb identified is not linked to metallurgical and/or industrial activities but may be mainly from traffic. This may be supported by the fact that Site B is located closer to the Rustenburg Central Business District with main roads (see Figure 4.1).

Pb was also correlated to Mn by r = 0.80, Fe by 0.39, Zn by 0.47, K by 0.59. The high correlation to Mn however suggests some form of anthropogenic activity as one of the sources, which may also be linked to the industries closer to Site B. According to Zhu *et al.* (2004), the elements Mn, Fe, As and Br represent a combination of steel-mill source and automotive source. This may imply that the Pb identified in this site can still be linked to traffic (automotive source).

Figure 7.2 gives the PCA results for apportionment of the sources discussed above. The five factors identified accounted for 39.1, 29.6, 12.9, 10.0 and 7.2% for factor 1, 2, 3, 4 and 5 respectively. The remaining 1.2% is given as other in the figure.

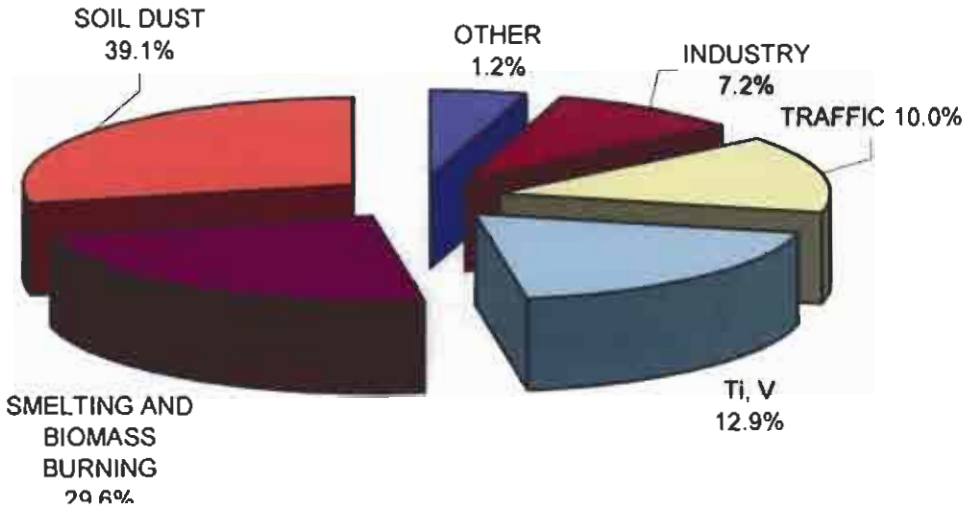

Figure 7.2: *PCA for Site B obtained from ICP-MS concentrations*

Factor 1 contained Mg, Mn, Al and Na, which suggests a soil dust source (Al-Momani, 2003; Heal *et al.*, 2005). Fe and Mn are both crustally (Heal *et al.*, 2005) and anthropogenically (Lingard *et al.*, 2005) derived and in urban areas can be attributed to soil, resuspended road dust, mechanical wear and combustion.

The second factor contained Ni, Cr, and K, and its sources were identified as smelting and biomass burning. Cr, Cu, Ni and Zn are principally anthropogenically derived, although they do occur naturally in low concentrations (Lingard *et al.*, 2005).

The third factor could not be properly identified because of the presence of V and Ti. According to Zhang *et al.*, 2004, a correlation between Ca and Ti may indicate the presence of building materials and activities as a source of metals in the area. These elements may indicate traffic and building or construction industry, or even road dust. The fourth factor was linked to a traffic source. The factor had loadings of Fe, Pb and Cu.

Factor 5 is linked to industrial activities like electrical, mechanical and building activities, since the factor contains Ca and Zn. According to Jiries *et al.* (2001) Zn and Cu may be derived from mechanical abrasion of vehicles, as they are

used in the production of the brass alloy itself and come from brake linings, oil leak sumps and cylinder head gaskets. The high concentration of copper found may be associated with electrical and mechanical working. This arises from the Zn-content of the tyre rubber, which is approximately 2% ZnO by weight (NAEI, 2002). The high minimum concentration for Zn at HS was believed to be the presence of a Zn-based paint used to waterproof and seal the building roof. The average concentrations of Cu at both OR and VL are similar, 26 and 29 $ng.m^{-3}$ respectively. The greatest maximum concentration of 105 $ng.m^{-3}$ was measured at VL. Elevated concentrations Cu at roadside sites are typically associated with brake pad wear (Var *et al.*, 2000).

7.1.3 CONCENTRATION OF ELEMENTS AT SITE C

PM concentration levels fluctuate from day to day and at different times of the day in response to the changing state of atmospheric stability, variations in mixing depth, and to the influence of mesoscale and microscale wind systems upon transport and dispersion of air pollution (Preston-Whyte & Tyson, 1988). The absence of surface inversion, which sometimes occurs during the day, promotes dispersion of air pollutants, which may still be prevented from diffusing freely upward by the presence of an elevated inversion. This type of inversion is always probable in southern Africa.

It is thus important that the chemical composition of PM10 be done also for the daily and hourly samples. The data in Table 7.5 is for the hourly samples from Site C. Each of the sample sets 41 to 48 and 57 to 64 corresponds to the sampling periods 00h00 – 03h00, 03h00 – 06h00, 06h00 – 09h00, 09h00 – 12h00, 12h00 – 15h00, 15h00 – 18h00, 18h00 – 21h00, 21h00 – 00h00 respectively. The Mn identified is fairly stable but shows a peak (0.06 $\mu g.m^{-3}$) at around 12h00 to 15h00. This suggests that Mn may be related to the anthropogenic activities near the site.

Table 7.5: *Hourly concentrations at Site C from 19 April to 2 June 2005*

19 APRIL – 10 MAY													
Sample	**PM10**	**Fe**	**Al**	**Ca**	**Mg**	**K**	**Na**	**Cr**	**Ni**	**Pb**	**Cu**	**Zn**	**Mn**
41	13.38	0.26	0.11	0.10	0.13	0.40	0.35	0.02	0.01	0.07	1.00	0.58	0.02
42	14.70	0.15	0.05	0.17	0.13	0.30	0.87	0.02	0.00	0.01	1.00	0.52	0.02
43	13.30	0.17	0.05	0.09	0.06	0.22	0.53	0.02	0.01	0.01	0.90	0.50	0.02
44	13.32	0.12	0.03	0.10	0.02	0.20	0.14	0.01	0.00	0.00	0.90	0.46	0.01
45	14.62	0.16	0.12	0.12	0.12	0.41	0.82	0.01	0.00	0.02	1.00	0.94	0.06
46	14.31	0.18	0.07	0.08	0.05	0.35	0.24	0.02	0.00	0.01	1.20	0.55	0.02
47	13.47	0.19	0.20	0.14	0.11	0.41	0.73	0.02	0.00	0.02	1.00	0.52	0.02
48	13.12	0.13	0.05	0.05	0.02	0.18	0.14	0.02	0.00	0.00	1.90	0.58	0.04
Mean	**13.78**	**0.17**	**0.09**	**0.11**	**0.08**	**0.31**	**0.48**	**0.02**	**0.003**	**0.02**	**1.11**	**0.58**	**0.03**
SD	**0.61**	**0.04**	**0.05**	**0.03**	**0.04**	**0.09**	**0.28**	**0.005**	**0.003**	**0.019**	**0.31**	**0.14**	**0.015**
10 MAY – 2 JUNE													
49	14.43	0.19	0.08	1.00	2.00	0.30	1.50	0.02	0.01	0.04	1.30	0.60	0.03
50	14.43	0.13	0.04	0.10	0.03	0.18	0.57	0.01	0.01	0.00	0.72	0.40	0.01
51	16.49	0.12	0.04	0.16	0.04	0.17	0.53	0.01	0.00	0.02	0.88	0.43	0.02
52	15.46	0.15	0.05	0.14	0.05	0.2	0.57	0.02	0.01	0.05	1.10	0.51	0.02
53	16.49	0.13	0.10	0.11	0.04	0.18	0.58	0.01	0.02	0.02	0.75	0.39	0.01
54	16.08	0.18	0.06	0.16	0.10	0.21	0.96	0.03	0.01	0.01	0.94	0.69	0.02
55	16.08	0.26	0.10	0.19	0.13	0.23	1.20	0.03	0.00	0.02	0.87	0.46	0.03
56	16.49	0.12	0.07	0.13	0.05	0.18	1.10	0.01	0.00	0.00	0.83	0.41	0.02
Mean	**15.74**	**0.16**	**0.07**	**0.25**	**0.31**	**0.21**	**0.88**	**0.02**	**0.008**	**0.02**	**0.92**	**0.49**	**0.02**
SD	**0.29**	**0.02**	**0.008**	**0.10**	**0.23**	**0.01**	**0.13**	**0.003**	**0.0002**	**0.005**	**0.06**	**0.04**	**0.003**

Table 7.6 below shows the correlation coefficients obtained from the hourly average concentrations from Site C. All the elements identified showed a negative and very small (r = 0.154 to 0.299) correlation with PM10 concentrations. The correlations between the crustal and trace metals, and between the trace metals themselves are very small. The highest correlation in this matrix is r = 0.99 for Ca and Mg, r = 0.71 for Al and K, and r = 0.69 for Cr and Fe.

Table 7.6: *Correlation matrix for the hourly concentrations at Site C for 19 April to 10 May 2005*

	PM10	Fe	Al	Ca	Mg	K	Na	Cr	Ni	Pb	Cu
Fe	-0.156										
Al	-0.112	0.492									
Ca	0.035	0.189	0.049								
Mg	-0.068	0.211	0.072	0.991							
K	-0.435	0.561	0.706	0.122	0.183						
Na	0.478	0.283	0.244	0.669	0.609	0.074					
Cr	-0.049	0.698	0.148	0.149	0.141	0.163	0.286				
Ni	0.165	0.047	-0.049	0.185	0.198	-0.222	0.062	0.000			
Pb	-0.039	0.593	0.320	0.308	0.323	0.436	0.116	0.224	0.376		
Cu	-0.454	-0.001	-0.065	0.186	0.254	0.097	-0.218	0.280	-0.259	0.024	
Zn	-0.217	0.234	0.271	0.120	0.170	0.591	0.136	0.183	-0.163	0.185	0.317

The correlations for 10 May to 2 June are higher than the ones presented in Table 7.6. There are more correlations between the crustal metals during this period (10 May to 2 June 2005). Also, the negative correlation between most metals and PM10 was observed.

The Pb in these results may be from an anthropogenic source since it has a correlation of 0.78 with Cu, and Cu has a correlation of 0.66 with Zn. Cr is highly correlated (r = 0.87) with Fe.

Table 7.7: *Correlation matrix for the hourly concentrations at Site C for 10 May to 2 June 2005*

	PM10	Fe	Al	Ca	Mg	K	Na	Cr	Ni	Pb	Cu
Fe	-0.130										
Al	0.258	0.545									
Ca	-0.568	0.318	0.227								
Mg	-0.593	0.296	0.232	0.998							
K	-0.546	0.649	0.388	0.913	0.907						
Na	-0.223	0.633	0.509	0.722	0.713	0.826					
Cr	-0.046	0.866	0.298	0.184	0.160	0.537	0.496				
Ni	-0.248	-0.209	0.207	0.084	0.127	0.059	-0.273	-0.114			
Pb	-0.245	0.250	0.099	0.476	0.457	0.509	0.090	0.273	0.228		
Cu	-0.440	0.327	0.021	0.816	0.799	0.816	0.552	0.401	0.018	0.780	
Zn	-0.232	0.422	-0.042	0.463	0.450	0.604	0.467	0.736	0.117	0.314	0.660

The second factor in Pacyna (1998) showed a composition of Fe, Mn, Mg, Ca, Ti, Al, and Na, which explained 17.8% of the total variance. This factor was clearly associated with the mineral aerosols that would be likely from the re-suspended road dust. The fact that K at Site C is highly correlated to Ca, and Mg with r-values of 0.91 and 0.9 respectively shows that K may not be due to biomass burning only but also from a resuspension of soil dust onto which K was probably deposited.

High correlations with Ca and Ti also suggest the presence of cement dust that may according to Zhu *et al.* (2004), come from building materials dust, hence linking the levels of particulate matter to anthropogenic activities relating to building materials and activities.

Pb has a correlation of 0.78 with Cu. This suggests that Pb is linked to anthropogenic activities that cause re-suspension of dust (Ti, Al), and also those that are caused by anthropogenic smelting. The correlation of Zn to Cu by r = 0.66, and to Cr by r = 0.74 confirms the contribution of anthropogenic smelting activities as a source of the metals at Site C.

Figure 7.3 gives the PCA results for the hourly concentrations at Site C. The results yielded four factors making up 89.3% of the PM10 analysed. The remaining 10.7% of PM10 is labelled as unknown in Figure 7.3.

The first factor, which accounts for 40% of the variance contained Al, Mg, K, Na and Pb, with high loadings of Mg and K. The composition of this factor suggests road or soil dust and biomass burning as the sources of PM10.

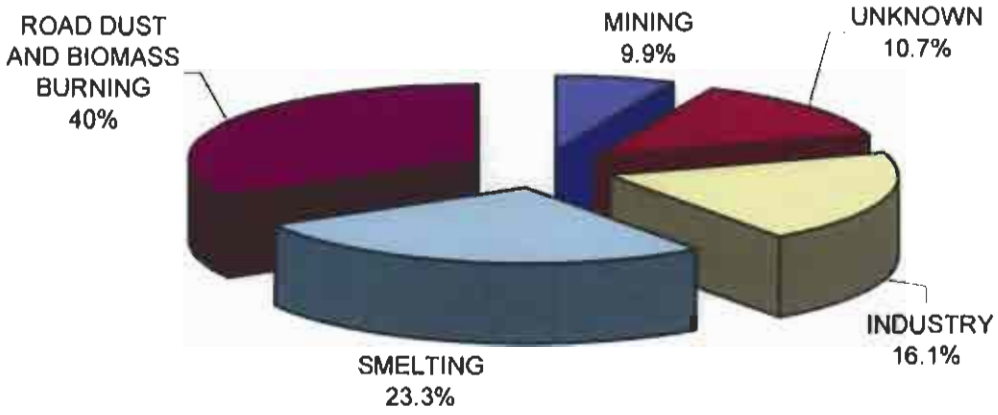

Figure 7.3: *PCA for 19 April to 10 May (sample 41 – 48)*

The second factor contained Mn, Zn and Ni, which suggests metal smelting as a source at Site C. The occurrence of Fe in this factor is not unusual since there are various ferrochrome smelting activities in the Rustenburg area. The third factor contained Ca only. This may be indicative of building material and activities in the area. The fourth factor contained Cr and Cu, which suggests anthropogenic activities related to mining of ferrochrome in the area.

Figure 7.4 gives the PCA results for hourly concentrations at Site C. Four factors forming 91.2% of the PM10 where identified while the remaining 8.8% could not be identified.

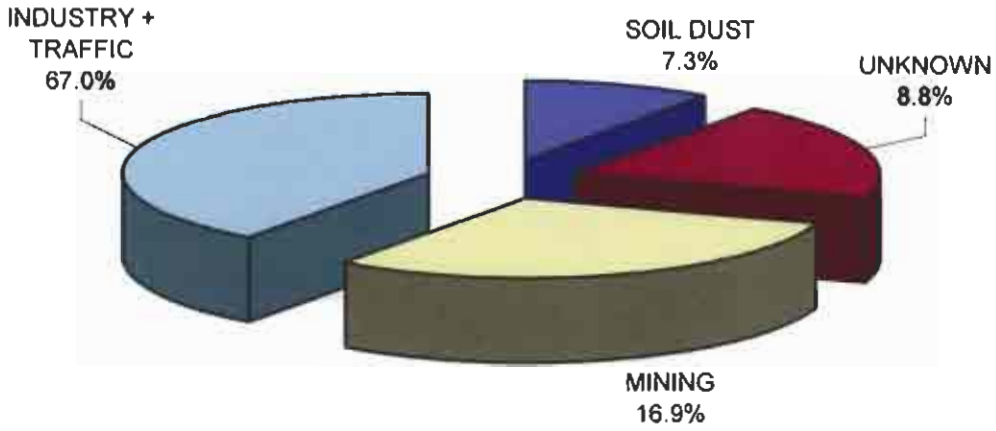

Figure 7.4: *PCA for Site C obtained from ICP-MS hourly concentrations*

Factor one, which accounted for 67% of the variance contained Fe, Ca, K, Ni, Pb and Cu. These may suggest traffic and other industrial activities like those related to building materials, and electrical and mechanical activities.

The second factor, which formed 16.9% of the variance, contained Al, Na, Cr, V, Zn and Mn. This factor suggests the mining industry as a source of PM. Cr and V are indicative of the commodities of the mining industry as in Table 1.1, while Zn and Mn are indicative of the metallurgical processes relating to mining.

The third factor accounting for 7.3% of the variance contained Mg and Ti with high loadings of Mg. This is indicative of a soil dust source.

It is worth noting that apportioning sources based on hourly concentrations can be complicated since there are sources that contribute to the PM at a particular time only. These are related to natural or anthropogenic activities that may occur in the vicinity of the sampler at a specific time. These cannot therefore, be used to give a complete picture of the sources within an area. The sources relating to monthly levels as given in Section 7.2 are thus preferred for consistency in the occurrence of events within the Rustenburg area.

7.2 COMPARISON OF CONCENTRATION LEVELS FROM THE THREE SITES

Some elements and their respective compounds like silicates and aluminum oxide are normally incompletely dissolved during extraction and dilution, or even escape the determination by evaporation. The mass concentration determined after digestion does not always represent the total mass concentration, instead only the portion that is determinable according to the distinct digestion for a given elemental composition will be analysed. The type of filters used at Site A and B is teflon-coated borosilicate fiberglass filters, while for Site C, 47 mm Teflon filters were used.

7.2.1 CONCENTRATION OF THE METALS IDENTIFIED

The concentrations of Cr, Ni, V, and Pb were relatively higher at Site A than at Site B. The spring Pb concentrations of 1.4 and 1.7 $\mu g.m^{-3}$ for Sample 9 and 10 respectively, determined in this study did exceed the WHO limit/guideline of 0.5 $\mu g.m^{-3}$. The levels at Site A were equal to 5 $\mu g.m^{-3}$ twice during autumn. This may be due to the location since this is closer to an informal human settlement and a Ferrochrome mine.

The Pb concentrations during this study ranged from 60 to 500 $ng.m^{-3}$, Ni from 50 to 2800 $ng.m^{-3}$, and V from 40 to 400 $ng.m^{-3}$. These are high compared to a similar study conduced by Fiala (2000) in the Czech republic at Sokolov and Všechlapy where ICP-MS concentrations of 3.5 to 3.7 $ng.m^{-3}$ and 15.8 to 57.8 $ng.m^{-3}$ were obtained for Ni and Pb respectively.

The occurrence of relatively high concentrations of Cr, Ni, V and Al in the autumn (March and April) and winter (May, June, and July) samples (Sample 1, 2, 3) is in agreement with a study by Begum *et al.* (2004), where out of the 14 metals observed the maximum concentrations were observed with the following patterns: (1) three during spring (Cu, Sr, and Zn), (2) five during summer (Bi, Cd, Cs, Pb, and Rb), and (3) six in fall season (Al, Ba, Co, Cr, Ni,

and V). The Cu and Zn levels shown in Figure 7.1(a) – (b) below were also relatively high during the spring season (August and September).

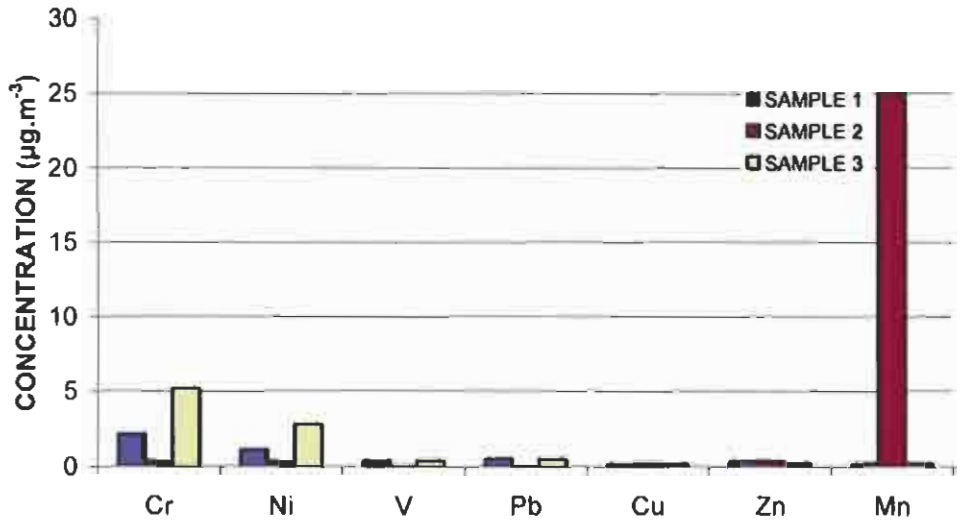

(a)

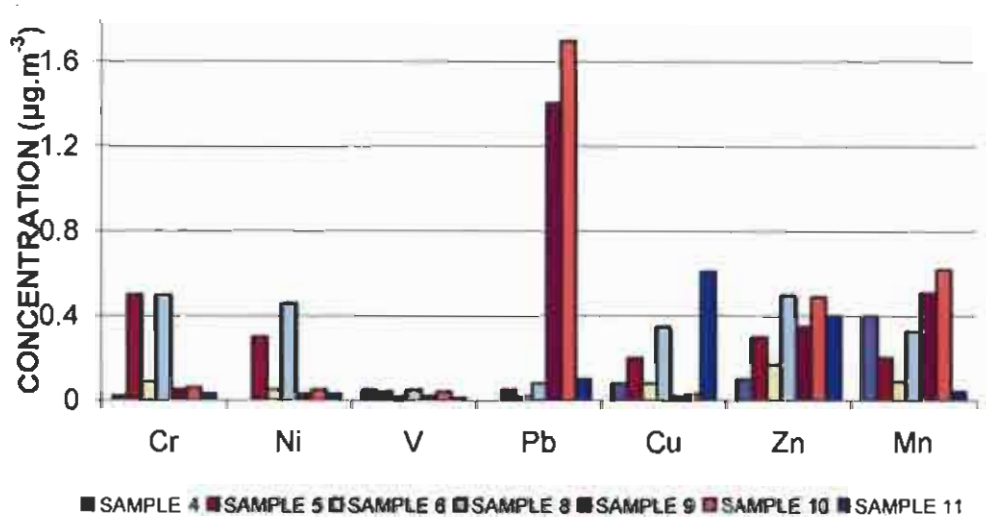

(b)

Figure 7.5: *Concentrations of toxic/trace metals identified at (a) Site A and (b) Site B*

The metals observed in this study all have health and environmental implications. Knowledge of the mean and the range of these in any given area

is very critical. Table 7.8 compares the mean concentration of toxic metals obtained from each study site to the available standards of limitation.

Table 7.8: *Summary of the concentrations of the potentially toxic trace metals in the Rustenburg area*

Metal ($\mu g.m^{-3}$)		Site A (Monthly)	Site B (Monthly)	Site C (Hourly)	Standard or Limit
Cr	Range	0.36 – 5.2	0.03 – 0.5	0.01 – 0.03	1 $\mu g.m^{-3}$ – NIOSH 1.5 $\mu g.m^{-3}$ - APCEL
	Mean	2.55	0.18	0.02	
	SD	1.42	0.08	0.00	
Ni	Range	0.34 – 2.8	0.03 – 0.46	0 – 0.02	No safe level - WHO
	Mean	1.41	0.13	0.01	
	SD	0.73	0.07	0.00	
V	Range	0.04 – 0.4	0.01 – 0.05	-------	1 $\mu g.m^{-3}$ - WHO
	Mean	0.28	0.03		
	SD	0.12	0.01		
Pb	Range	0.06 – 0.5	0.02 – 1.4	0 – 0.007	0.5 $\mu g.m^{-3}$ - WHO
	Mean	0.35	0.48	0.02	
	SD	0.15	0.28	0.01	

In general, the elements identified in order of decreasing abundance are: Fe, Ca, Al, Mg, Si, Na, K, Zn, Cr, Ni, Cu, Ti, Mn, Pb, and V. The trace metals of concern are found to be in decreasing order Cr, Ni, Pb, and V.

7.2.2 SOURCES OF METALS WITHIN THE RUSTENBURG AREA

The types of mining activities that take place in the Rustenburg area create an impression that the sources of toxic metals within the area are from anthropogenic origin. Correlation matrices for the monthly and hourly concentrations within the Rustenburg area are discussed in this section, with the main objective of determining whether the toxic metals are from soil dust (crustal source) or from an anthropogenic source. The anthropogenic sources

are discussed under the categories of metallurgical sources, traffic and other anthropogenic activities (other industrial activities).

Table 7.9 gives the correlation matrix obtained from the monthly concentrations (Site A and B) for the Rustenburg area. Cr was correlated to Al, Fe, Ti, and K by r-values that did not exceed 0.3. These correlations show that the Cr determined cannot be associated with crustal material (soil dust). There was however, a high correlation of Cr with Ni and V (r = 0.99 and 0.89), which shows that the Cr was linked to anthropogenic smelting.

The Pb in the monthly concentrations had no correlation with V (r = 0.04), Zn (r = 0.41) and Mn (r = –0.19). Correlation coefficients of 0.6 and 0.56 were however, obtained for Na and K respectively. The relation to V shows that the Pb may not be from a fuel combustion or traffic source. The relation to K could not be explained, mainly because K is a tracer for biomass burning.

Table 7.10 gives the correlation matrix derived from hourly concentrations in the Rustenburg area. The trace metals had a positive correlation with PM10. Cr had an r = 0.95, 0.98 and 0.69 correlation with Ni, V and Pb respectively. This shows that they were from the same source. The correlation of r = 0.83 to 0.9 for Cr, Ni, V and Pb with Fe may suggest a crustal source.

These results however, cannot be conclusive because the trace metals had 'unusual' correlations of r = 0.87 to 0.9 with Na, which cannot be explained.

Table 7.9: *Correlation matrix for monthly concentrations in Rustenburg*

	PM10	Fe	Al	Ca	Mg	K	Na	Ti	Cr	Ni	V	Pb	Cu	Zn
Fe	0.606													
Al	0.146	0.393												
Ca	0.473	0.824	0.820											
Mg	0.050	0.321	0.916	0.731										
K	-0.408	-0.277	0.011	-0.169	0.350									
Na	-0.313	-0.044	0.422	0.159	0.699	0.808								
Ti	0.078	0.161	-0.169	-0.004	-0.219	-0.345	-0.273							
Cr	0.607	0.155	-0.231	-0.039	-0.249	-0.311	-0.284	0.002						
Ni	0.608	0.156	-0.171	-0.001	-0.200	-0.334	-0.274	0.002	0.997					
V	0.805	0.493	-0.088	0.245	-0.105	-0.284	-0.252	0.053	0.889	0.874				
Pb	-0.123	0.214	0.021	0.039	0.190	0.567	0.651	-0.247	-0.002	-0.025	0.039			
Cu	0.052	-0.216	0.221	-0.014	-0.120	-0.570	-0.486	0.065	0.031	0.060	-0.032	-0.506		
Zn	0.036	0.361	0.682	0.520	0.509	-0.129	0.320	0.061	-0.108	-0.067	-0.051	0.414	0.349	
Mn	0.382	-0.002	0.360	0.244	0.277	-0.174	0.002	-0.101	-0.119	-0.076	-0.156	-0.199	0.098	0.135

Table 7.10: *Correlation matrix for the hourly concentrations in Rustenburg*

	PM10	Fe	Al	Ca	Mg	K	Na	Ti	Cr	Ni	V	Pb	Cu	Zn
Fe	0.272													
Al	-0.130	0.590												
Ca	0.323	0.911	0.569											
Mg	0.101	0.201	0.185	0.492										
K	0.048	0.918	0.684	0.860	0.209									
Na	0.616	0.746	0.222	0.685	0.259	0.557								
Ti	0.327	0.866	0.493	0.851	0.176	0.771	0.791							
Cr	0.526	0.873	0.301	0.779	0.166	0.654	0.914	0.845						
Ni	0.480	0.901	0.469	0.829	0.218	0.731	0.869	0.848	0.955					
V	0.524	0.878	0.314	0.816	0.162	0.661	0.866	0.885	0.985	0.945				
Pb	0.115	0.826	0.841	0.750	0.239	0.762	0.613	0.729	0.694	0.808	0.684			
Cu	-0.100	0.842	0.656	0.723	0.173	0.914	0.441	0.575	0.545	0.608	0.515	0.737		
Zn	-0.096	0.814	0.845	0.757	0.191	0.924	0.379	0.611	0.475	0.620	0.475	0.829	0.916	
Mn	-0.241	0.436	0.969	0.431	0.156	0.563	0.011	0.321	0.101	0.273	0.124	0.710	0.567	0.767

Soil Dust

According to Al-Momani (2003), crustal material is the only source of Al. It is therefore logical to use Al as a tracer for crustal material. A strong correlation between Al and any other element suggests crustal material as a major source of that particular element. A value near 1 for the ratio of an element to Al also suggests crustal material as a major source. The ratios of the elements to Al are given in Figure 7.6 (a) and (b).

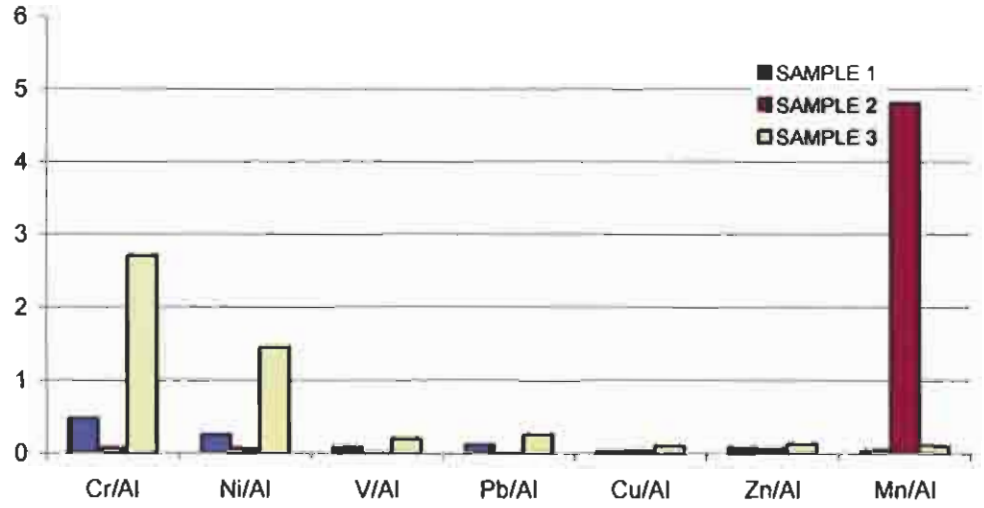

(a)

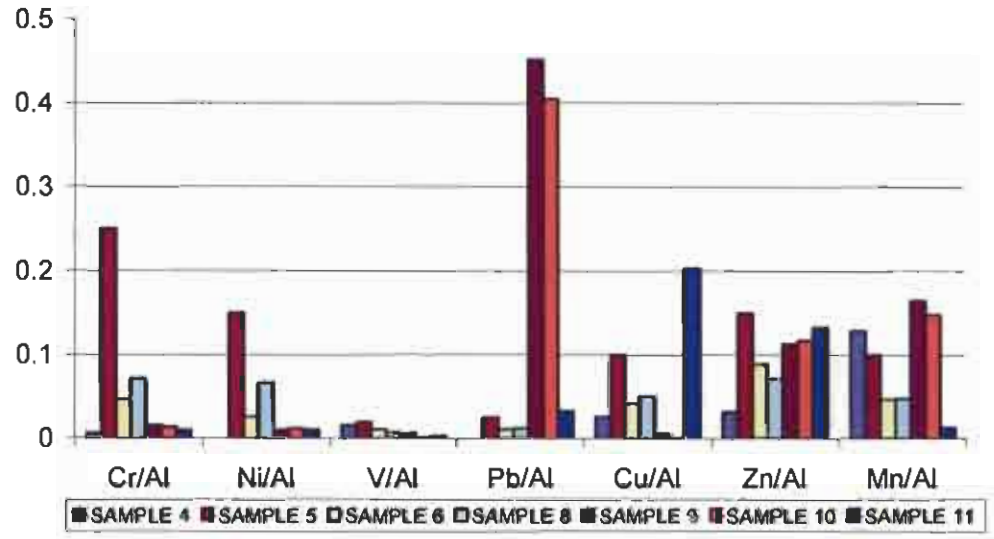

(b)

Figure 7.6: *The ratio of (a) crustal metals and (b) toxic/trace metals to aluminium*

The ratio of the concentration of Al to Cr was 3:2 at Site A and 4:0.3 at Site B, and the square of the correlation coefficient (r^2) between the two elements was 0.08. The values indicate a weak correlation and shows that the Cr determined in this study was not of crustal origin. Likewise, Ni, V and Pb had the ratios of 3:1 and 4:0.2, 4:0.3 and 4:0.04, 4:0.4 and 4:0.04, respectively. The r^2 values obtained were 0.05, 0.02 and 0.008 for Ni, V, and Pb respectively, which imply that these elements cannot be linked to crustal material source, but rather to metallurgical sources or fuel combustion (traffic).

Metallurgical Sources

The concentration ratios of K to Si were 0.5:2 and 1:6 for Site A and B respectively, and for K to Ti were 0.5:0.2, 1:0.3. This then, suggests that biomass burning is not the major source of the elements identified, since K and Si may be from the same source (soil dust), and Si and Ti are tracers for a soil dust source. Resuspension of dust can be either due to traffic or scraping of the earth crust as an industrial anthropogenic activity.

Metal smelting and fuel combustion are usually the source of non-crustal volatile metals in the atmosphere (Nriagu, 1989). According to Held *et al.* (1996), the elements Zn and Mn can be used as tracers for smelting sources, K can be used for biomass burning, Cl for sea salt, sulphate for anthropogenic sources, and Al, Si, Ti for soil dust. Zn, excess Mn, Cu and Ni are an unambiguous signal of anthropogenic smelting.

The average concentrations of Zn, Mn, Cu, and Ni observed from Site A were 0.34, 8.47, 0.22, and 1.41 $\mu g.m^{-3}$ respectively, while the concentrations observed for Site B were 0.27, 0.26, 0.18, and 0.20 $\mu g.m^{-3}$. The ratios of 0.26:0.27 (Mn:Zn), 0.26:0.2 (Mn:Ni), and 0.26:0.18 (Mn:Cu) at Site B suggest that the main source of elements at Site A was anthropogenic smelting.

The main source of Ni in the area may be anthropogenic smelting since there was an r = 0.99 and 0.95 correlation between Cr and Ni, for the monthly and hourly concentrations.

Traffic

The co-presence of both Pb and Zn and moderate correlations (between Pb and V) in Seoul (Mishra *et al.*, 2004b) indicates that the contribution from fuel combustion may still be important. The correlations observed in this study were r = 0.41 between Pb and Zn in the monthly concentrations and r = 0.83 in the hourly concentrations, which suggest fuel combustion as one of the sources of particulates. The Pb and V r value from hourly concentrations was 0.68.

According to Arslan (2001), zinc may come from lubricating oils, tyres of motor vehicles and zinc in carburetors. High correlation existed between Zn and Cu (r = 0.92). A reasonable correlation between Zn, Cu and Pb support the idea that vehicular traffic movement and industrial activities were the source of heavy metals in this area.

Other Anthropogenic Sources

According to Zhang *et al.*, 2004, a correlation between Ca and Ti may indicate the presence of building materials and activities as a source of metals in the area. The hourly concentrations showed an r value of 0.85 for Ca and Ti while the monthly concentrations had r = -0.004. These imply that not all of Rustenburg experiences contribution from building materials and activities, however Site C is the area that was mostly exposed to this source.

The correlations of Al, Ca, Si, Na, with Fe (r ranges from 0.59 to 0.91 for hourly concentrations and r between 0.04 and 0.82 for monthly concentrations) observed in this study suggests, according to Chong et al., the presence of aluminosilicates with traces of sulfate or sulfite, and chloride in the PM analysed.

The strong correlation between Cr and Ni (r = 0.99 and 0.96 for monthly and hourly concentrations) suggests, according to Mishra *et al.* (2004a), an

anthropogenic source of PM since the occurrence of Cr with Co or Ni indicates the anthropogenic origin of particulate aerosols.

According to Jiries *et al.* (2001), Zn and Cu may be derived from mechanical abrasion of vehicles, as they are used in the production of the brass alloy itself and come from brake linings, oil leak sumps and cylinder head gaskets. The high concentration of copper found may be associated with electrical and mechanical working.

Based on the correlations discussed, the sources of metals and/or particulate matter in the Rustenburg area can be divided into soil dust, metallurgical processes (mainly smelting), traffic, and other anthropogenic activities.

Figure 7.7 shows the principal component analysis (PCA) results for determination of the sources of particulate matter for the monthly concentrations obtained from Site A and B. The PCA yielded five (5) factors that explained 88.5% of the variance, and the remaining 11.5% of PM10 could not be explained by PCA. This may imply that the source for that portion is unknown. The first factor, which accounted for 29.6% was loaded with Mg, Na, and Al, and is associated with soil dust or crustal material. Factor 2, which formed 23.8% of the variance, may be indicative of industry mainly because of the high loadings of Ni and V. The Ni and V may imply that the type of industry discussed here is related to mining since according to Table 1.1, the Rustenburg area has many mining industries that produce Ni and V as major and for some, as minor commodities.

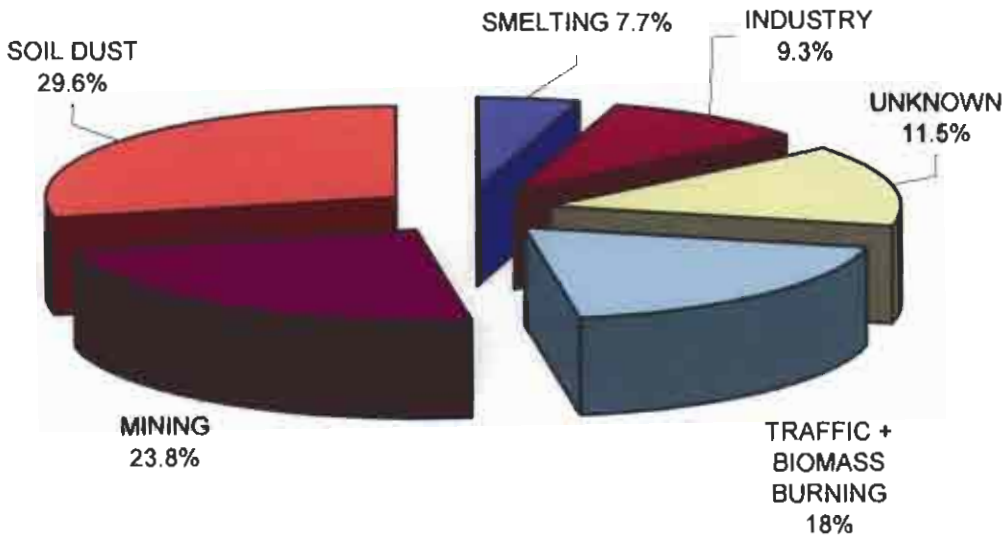

Figure 7.7: *PCA for ICP-MS monthly concentrations obtained from Site A and B (Sample 1 – 11)*

The third factor (18.0%) consisted of Pb and K, which is indicative of traffic and biomass burning. The presence of Cr in this factor, though in smaller amounts compared to Pb and K, is not surprising, since it may imply that the Cr which is on the earth crust due to long term deposition may be resuspended due to traffic and other earth scraping activities.

The fourth factor (9.3%) contained Ti and Fe. The presence of Fe and Ti may be indicative of an industrial source. The fact that Site A is closer to ferrochrome mining activities may contribute to the high loadings of Fe, while cement and other industrial building activities may also contribute to the presence of Ti.

Factor five consisted of Zn, Cu and Mn in order of decreasing abundance. These are all unambiguous tracers for smelting activities. The 7.7% of particulate matter in the Rustenburg area may thus be linked to smelting activities.

7.3 HEALTH AND ENVIRONMENTAL IMPLICATIONS OF THE CONCENTRATION LEVELS

The main trace metals of concern in this study were Cr, Ni, V and Pb. Nickel and chromium (VI) compounds have been classified as human carcinogens by International Applied Research on Cancer (IARC) (Group 1), manganese is neurotoxic (WHO, 2000), and iron has recently been linked to cardiovascular outcomes of PM exposures. The WHO has given guideline values of 0.25 and 25 $ng.m^{-3}$ for 10^{-5} excess cancer risk for Cr (VI) and Ni, respectively. Information on the speciation of chromium in ambient air is essential since, when inhaled, only hexavalent chromium is carcinogenic to humans. Based on the neurotoxic effects, a guideline value of 0.15 $\mu g.m^{-3}$ has been given for manganese in ambient air by the WHO.

The trace metals (Cr, Ni, Pb, V) form 6.3% of the metals determined in this study. This may seem comparatively small but has health implications for the exposed community since the limits allowed for Cr are 1 $\mu g.m^{-3}$ as set by NIOSH and the World Health Organisation (WHO), were exceeded at Site A (Table 7.1) where the Cr concentrations were 2100, 360, and 5200 $ng.m^{-3}$ for samples 1, 2 and 3, respectively.

According to Gatari *et al.* (2005), the WHO does not recommend any concentration level as safe for Ni.

Davis (1998) suggests that, in contrast to the non-physiological role of Pb, several human enzyme systems are either activated by or require Mn, and Mn plays an important role in metabolism, the nervous system and other key systems and functions. The Pb limit of 0.5 μgm^{-3} was exceeded only at Site B during this study.

Mergler *et al.* (1999) report that excessive Mn exposure in the workplace has led to development of a neurodegenerative syndrome resembling idiopathic Parkinson's disease, and subtle nervous system deficits, consistent with Mn activity in the brain, was observed in environmentally exposed adults.

In recent studies of children up to 6 years of age, Takser *et al.* (2003) suggests that environmental exposure to Mn in utero could affect early psychomotor development. The limit/guideline of 0.15 $\mu g.m^{-3}$ set by the WHO for Mn in general, was exceeded most of the time at Sites A and B during the study. This also has serious implications since the excess of Mn suggests smelting activities as sources of toxic trace metals.

The toxic level of vanadium to growing plants is about 10 ppm. Investigations by Bergman (2004) and Günes *et al.* (2004) showed that the usage of synthetic fertiliser with phosphorus increased vanadium content in soil. The mean vanadium content of most of the plants is between 1.32–10.01 ppm. The V levels in this study were lower than the limit of 1 $\mu g.m^{-3}$ set as a guideline by the WHO.

.....

In view of the quantity and quality of data that one can obtain from the results discussed in Chapter 5, 6 and 7, and considering the health and environmental implications of the metals identified, it is important that the effectiveness of the monitoring methods and procedures used in this study be evaluated. The next chapter is a comparative assessment of the methods and procedures used in this study.

.....

CHAPTER 8

A COMPARATIVE ASSESSMENT OF THE SAMPLING AND ANALYSIS METHODS

In this chapter, the strengths and shortcomings of the different methods used in this study are discussed. The efficiency of the type of filter media used, the frequency of sampling, the sampling period, the meteorology and the location of the sampling sites used are assessed. The efficiency and relevance of the methods used for determination of the metals during this study are also discussed.

8.1 EFFICIENCY OF THE SAMPLING METHODS AND PROCEDURES

The central concept in aerosol collection is the filtration of a representative sample of the aerosol from the gas phase, onto a suitable porous medium or filter. The transfer of the aerosol from a dispersed state in the air to a compact sample on the filter then facilitates the storage, transport, and sample preparation requisite for gravimetric, microscopic, microchemical, or other analytical techniques.

Sampling of PM was performed using a TEOM with different filter media namely teflon-coated borosilicate fiberglass filters, ringed teflon (teflon) filters and quartz filters. The teflon-coated borosilicate fiberglass filters were laced inside the mass transducer of the TEOM where the flow rate was measured as 3 $L.min^{-1}$. The ringed teflon filters and the quartz filters were placed in the Automatic Cartridge Collection Unit (ACCU) of the TEOM, where the flow rate was measured as 13.67 $L.min^{-1}$.

The TEOM was successful in continuous determination of the concentrations of PM10 for every hour of the day. The difficult part of the sampling procedure was moving the TEOM from one site to another since it required total dismantling before transportation, and calibration before taking measurements at the new location.

8.1.1 SAMPLING PERIOD

The sampling frequencies and sample durations needed to address the objectives of any air monitoring study has to be decided upon. More frequent samples, or samples taken at remote locations, may require a sequential sampling feature. Shorter sample durations may require a larger flow rate to obtain an adequate sample deposit for analysis.

Table 8.1 gives a summary of the important parameters of the sampling procedure. There was a direct relationship between the sampling period and the mass of PM accumulated on the filter. This relation holds for Site A and B only, the monthly accumulated mass at Site C did not show a trend. The hourly average mass of PM10 at Site C is lower (1309.4 µg) than the monthly samples (3100 µg) obtained over the same period (22 days) of sampling at the same site. This may suggest that the flow rate and the type of filter media also have an effect on the accumulated mass and hence the concentration of PM on the filter.

For most samples collected during this study, the elements identified by SEM/EDS and ICP-MS analysis comprise between 30 - 50% of the total mass accumulated on the filters. The fact that particulate matter can contain 30 - 50% of carbon (organic) species contributes to low masses of the inorganic species determined above and is a result of the one limiting factor of the ICP-MS analysis, which is the difficulty in assessing the efficiency of extracting the PM from different filters. This has been reported before by Li *et al.* (1996) who estimated an efficiency of 20–50% of PM removed from filters, and Gilmour *et al.* (1996) who estimated an efficiency of 10–30%. Attempts were made to assess the extraction efficiency by measurement of the extracted mass.

Some elements and their respective compounds like silicates and aluminum oxide are normally incompletely dissolved during extraction and dilution, or even escape the determination by evaporation. The mass concentration determined after digestion does not always represent the total mass concentration, instead only the portion that is determinable according to the distinct digestion for a given elemental composition will be analysed.

Table 8.1: *Sampling period, flow rate and filter media*

Site	Sample	Period (Days)	Flow Rate ($L.min^{-1}$)	Filter Media	Mass Of PM10 Accumulated (µg)	Concentration of PM10 ($\mu g.m^{-3}$)
A	2	22	3	Teflon-coated borosilicate fiber glass	9479.3	99.74
B	4	22	3	Teflon-coated borosilicate fiber glass	4631.3	48.73
	5	23			4896.5	49.28
	7	23			4680.0	47.10
C	14	22	3	Teflon-coated borosilicate fiber glass	3100.0	32.62
	15	23			4310.0	43.38
	41	22 (0:00 –3:00)	13.67	Ringed Teflon	158.9	13.38
	42	22 (3:00 – 6:00)			174.6	14.70
	43	22 (6:00 – 9:00)			158.0	13.30
	44	22 (9:00 – 2:00)			158.3	13.32
	45	22 (12:00 –15:00)			173.7	14.62
	46	22 (15:00 – 8:00)			170.0	14.31
	47	22 (18:00– 21:00)			160.0	13.47
	48	22 (21:00– :00)			155.9	13.12

8.1.2 FLOW RATE

The flow rate in any sampling procedure is important in determining the accumulation of material on the filters, as well as ensuring that all elements are kept on the filter. It can be expected that low flow rates are suitable for longer sampling periods and high flow rates are more applicable for short sampling periods. In this study sampling at a lower flow rate (3 $L.min^{-1}$)

yielded higher concentrations on the filters than the higher flow rate (13.67 $L.min^{-1}$) over the same period of sampling.

Table 8.1 also shows the sampling results at Site C for the 22 day sampling period, which yielded an accumulated mass of 1309.4 µg for the 13.67 $L.min^{-1}$ and 3100 µg for the 3 $L.min^{-1}$.

It is worth noting that flow rate alone cannot be used to explain differences in the accumulated mass and concentration on the filter media. The type of filter media used is also important.

8.1.3 FILTER MEDIA

The type of filter media is important both for the efficiency of sampling as well as the selected analysis method. Filter media are judged for specific applications according to Chow (1995a) and Lippmann (2001) based on their mechanical stability, chemical stability, particle or gas sampling efficiency, flow resistance, loading capacity, blank values, artifact formation, compatibility with analysis methods, cost, and availability. A sample from each batch (50 to 100 filters) must always be tested for contamination before sampling commences with that batch of filters. High and variable blank levels typically invalidate subsequent quantification of particle deposits using the particular batch of filters.

The most commonly used filter media for atmospheric particle and gas sampling are teflon membrane, quartz fiber, nylon membrane, cellulose fiber, teflon-coated glass fiber, etched polycarbonate membrane, and glass fiber. None of these materials is suitable for all purposes. The filter media used in this study are ringed-teflon membrane, quartz fiber and teflon-coated borosilicate fiberglass.

Table 8.2 shows the main elements identified using the different filter media. It is important that the results from quartz fiber filters for SEM/EDS had to be discarded since it just proved that quartz is not suited for determination of the

selected elements. For Site A, B and C, teflon-coated borosilicate fiberglass filters were used, but the hourly average concentrations at Site C were also sampled onto the ringed teflon and quartz filters.

Table 8.2: *Filter media and the main elements identified on them during the study*

Site	Filter Media	Elements Identified
A	Teflon-coated borosilicate fiber glass	**SEM/EDS:** Si, Fe, Al, Ca, Mg, K, Na, Ti, Cr, C, Cl, S, F, O
		ICP-MS: Si, Fe, Al, Ca, Mg, K, Na, Ti, Cr, Ni, V, Pb, Cu, Zn, Mn
B	Teflon-coated borosilicate fiber glass	**SEM/EDS:** Si, Fe, Al, Ca, Mg, K, Na, Ti, Cr, C, Cl, S, F, P, V, Pb, Ni, O
		ICP-MS: Si, Fe, Al, Ca, Mg, K, Na, Ti, Cr, Ni, V, Pb, Cu, Zn, Mn
C	Quartz	**SEM/EDS:** None
		ICP-MS: Si, Fe, Al, Ca, Mg, K, Na, Ti, Cr, Ni, V, Pb, Cu, Zn, Mn
	Ringed teflon	**SEM/EDS:** Si, Fe, Mg, K, Na, C, S, F, O
		ICP-MS: Fe, Al, Ca, Mg, K, Na, Cr, Ni, Pb, Cu, Zn, Mn
	Teflon-coated borosilicate fiber glass	**SEM/EDS:** Si, Fe, Al, Ca, Mg, K, Na, Ti, Cr, C, Cl, S, F, V, Pb, Ni, O

The main elements identified from the SEM/EDS analysis on ringed-teflon filters were Si, Fe, Mg, K, Na, C, S, F and O, and for ICP-MS, the following main elements were identified: Fe, Al, Ca, Mg, K, Na, Cr, Ni, Pb, Cu, Zn and Mn. Ringed-teflon membrane filters consist of a thin, porous polytetrafluoroethylene (PTFE) teflon sheet stretched across a polymethylpentane ring; the thin membrane collapses without the ring, and the filter cannot be accurately sectioned into smaller pieces. The white membrane

is nearly transparent and according to Campbell *et al.* (1995), has been used to estimate light absorption. PTFE teflon is very stable, absorbing negligible water or gases. It has inherently low contamination levels, but contamination has been found in some batches during acceptance testing. This filter type is commonly used for mass and elemental analyses. Although aerosol carbon has been inferred from hydrogen measurements by Kusko *et al.* (1989), carbon cannot be measured on Teflon membranes because of the high carbon content of the filters.

SEM/EDS analysis of the teflon-coated borosilicate fiberglass filters yielded Si, Fe, Al, Ca, Mg, K, Na, Ti, Cr, C, Cl, S, F, P, V, Pb, Ni and O while analysis using ICP-MS yielded Si, Fe, Al, Ca, Mg, K, Na, Ti, Cr, Ni, V, Pb, Cu, Zn and Mn. Teflon-coated glass fiber filters imbed Teflon slurry onto a loosely woven glass fiber mat. These filters meet requirements in all categories except blank element and carbon levels. Though a small amount of nitric acid absorption has been observed by Mueller *et al.* (1983), it is tolerable in most situations. Teflon-coated glass fiber filters overcome some of the inherent inadequacies of glass fiber filters by being inert to catalyzing chemical transformations as well as by being less moisture sensitive.

Quartz filters are commonly used in high-volume air sampling applications involving subsequent chemical analyses such as atomic absorption, ion chromatography, and carbon analysis, due to their low trace contamination levels as well as to their relative inertness and ability to be baked at high temperatures to remove trace organic contaminants. The main elements identified from ICP-MS analysis of these filters include Al, Cu, Pb, Ti, Zn, K, Fe, Cr, Ni, Mn, Ca, Mg, Na and V while for SEM/EDS analysis, the results had to be discarded because of poor quality.

For the two analysis methods, teflon-coated borosilicate fiberglass filters yielded better results since more metals could be detected compared to the quartz filters that yielded good results with one analysis (ICP-MS) method only. Fewer metals were determined from the analysis of ringed-teflon filters using both the SEM/EDS and ICP-MS. The efficiency of the filter media used

in this study can thus be given in a decreasing order as teflon-coated glass fiber filters, ringed-teflon filters, and quartz filters.

8.1.4 SITE SELECTION AND METEOROLOGY

The temporal and spatial distribution and transport pattern of aerosols in a region is closely related with the meteorological flow patterns (Chen *et al.*, 1997; Merrill & Kim, 2004). The location of the sampling sites used in this study is described in Chapter 4 and the meteorology is discussed in Chapter 5, 6 and 7. It is evident from the results obtained that Site A and B were the most suitable sites for this study. The location of Site C relative to the natural and anthropogenic sources and the prevailing meteorological conditions, did not give a true reflection of the levels in the area. This may be because the site has always been used by a certain industry for compliance monitoring and is thus positioned to suit the needs of that particular industry.

The scale of the transport of pollutants within a specific area depends, according to Carslaw and Beevers (2002) and Pacyna (1995), on the effective height of the emission source and the meteorological conditions, as well as on the size and chemical composition of particles. Site C used in this study is situated close to trees that may affect the concentration levels of the pollutants in the vicinity of the sampler. The site was also upwind of industrial sources for most of the time.

8.2 EFFICIENCY OF THE ANALYSIS METHODS AND PROCEDURES

The analysis procedures used during this study are discussed in Chapter 4 and the methodology is given in Chapter 3. The analysis methods used are SEM/EDS and ICP-MS. In general, the ICP-MS method proved to be more relevant for the analysis of the metals of interest in this study. The standard deviations obtained from this method were less than 30% for most of the metals identified. The method detection limit (MDL) was also low (0.2 to 1 $\mu g.L^{-1}$) for most metals. This suggests that the method is suited for trace elemental determinations.

Table 8.3 gives the standard deviations and method detection limits for the main elements measured during this study.

Table 8.3: *The mean, standard deviation and method detection limit (MDL) for the main metals identified during the study*

Metal	Method (MDL)	Site A MEAN (SD) (in $\mu g.m^{-3}$)	Site B MEAN (SD) (in $\mu g.m^{-3}$)	Site C Mean (SD) (in $\mu g.m^{-3}$)	
				Monthly	Hourly
Cr	ICP-MS (1 $\mu g.L^{-1}$)	2.55 (1.42)	0.18 (0.08)	-	0.2 (0.005)
	SEM/EDS	2.28 (0.64)	0.14 (0.04)	0.08 (0.06)	-
Ni	ICP-MS (0.3 $\mu g.L^{-1}$)	1.41 (0.73)	0.13 (0.07)	-	0.003(0.003)
	SEM/EDS	-	-	0.01 (0.00)	-
V	ICP-MS (0.2 $\mu g.L^{-1}$)	0.28 (0.12)	0.03 (0.01)	-	-
	SEM/EDS	-	0.00 (0.00)	0.01 (0.00)	-
Pb	ICP-MS (0.1 $\mu g.L^{-1}$)	0.35 (0.15)	0.48 (0.28)	-	0.02 (0.019)
	SEM/EDS	-	0.03 (0.03)	0.09 (0.02)	-
Cu	ICP-MS (0.2 $\mu g.L^{-1}$)	0.22 (0.02)	0.20 (0.08)	-	1.11 (0.31)
	SEM/EDS	-	-	-	-
Zn	ICP-MS (0.2 $\mu g.L^{-1}$)	0.34 (0.04)	0.33 (0.06)	-	0.58 (0.14)
	SEM/EDS	-	-	-	-
Mn	ICP-MS (0.1 $\mu g.L^{-1}$)	8.47 (8.26)	0.31 (0.08)	-	0.03 (0.015)
	SEM/EDS	-	-	-	-
Ti	ICP-MS (0.2 $\mu g.L^{-1}$)	0.17 (0.07)	0.19 (0.10)	-	-
	SEM/EDS	0.23 (0.12)	0.04 (0.01)	0.03 (0.01)	-
Ca	ICP-MS (100 $\mu g.L^{-1}$)	4.91 (1.63)	3.39 (0.69)	-	0.11 (0.03)
	SEM/EDS	3.00 (0.79)	0.34 (0.05)	0.13 (0.02)	-
Fe	ICP-MS (50 $\mu g.L^{-1}$)	12.83 (6.16)	6.69 (1.75)	-	0.017 (0.04)
	SEM/EDS	4.11 (0.73)	0.59 (0.15)	0.46 (0.18)	0.01 (0.01)
Si	ICP-MS (100 $\mu g.L^{-1}$)	2.05 (0.28)	4.22 (1.77)	-	-
	SEM/EDS	11.89 (2.41)	2.64 (0.29)	2.02 (0.27)	0.05 (0.02)
Al	ICP-MS (0.7 $\mu g.L^{-1}$)	3.85 (0.99)	3.46 (0.64)	-	0.09 (0.05)
	SEM/EDS	5.17 (0.56)	0.88 (0.15)	0.81 (0.12)	-
S	ICP-MS			-	-
	SEM/EDS	4.10 (1.39)	1.06 (0.18)	0.46 (0.22)	0.07 (0.03)

Detection limits and analytical precision vary widely with analytical protocol, instrumental response, blank contamination, interferences, matrix composition, and isotope abundance, but range from <100 ppb to <1 ppt in aqueous solution. Analytical precision is typically ~2%, of one standard deviation.

The method detection limits for SEM/EDS are not easy to determine since they depend on different factors such as size and density of the sample, resolution of the detector and the working voltage. In this study, the spectrum range of 0 – 20 keV was maintained throughout, and quant-optimisation of the system was done with Ni to standardise the system. On each filter, the fault boundaries (weight % sigma) were observed to be ranging from ±0.05 to 0.3.

It is also evident from Table 8.2 that more metals were identified using ICP-MS. The SEM/EDS method cannot be considered irrelevant since it enables one to determine the oxides of the carbon-containing compounds.

The efficiency of the methods in determining the potential toxic metals (Cr, Ni, V and Pb) of PM can be assessed based on the mean and standard deviations (refer to Table 8.4) obtained for each metal.

Table 8.4: *Percentage of the ratio of the standard deviation to the mean for the ICP-MS and SEM/EDS methods*

SITE	Cr	Ni	V	Pb
ICP-MS				
A	55.7	51.8	42.9	42.9
B	44.4	53.9	33.3	58.3
C	0	0	-	50.0
SEM/EDS				
A	28.1	-	-	-
B	28.6	-	-	100
C	75.0	0.0	0.0	22.2

ICP-MS generally has a high SD to mean ratios for Ni and Pb. The lower (50% or less) ratio may imply better results or concentrations obtained using a particular method.

.....

Given the economic and social needs of the North-West province, one realises that the province needs to be stricter in monitoring of air pollutants, but cannot do away with industries that are the main contributors to the levels of air pollution in the province. The people's way of life also cannot be easily influenced. The pressure that the provincial and local governments have, concerning implementation of the Air Quality Management Act, which is mainly to ensure that people live in a hazardous-free environment, leads to inclusion of some recommendations to the air quality authorities within the province, on what needs to be considered when monitoring the levels of toxic metals of particulate matter within the province. The conclusion and recommendations of this study are also given in the next chapter.

.....

CHAPTER 9

CONCLUSION AND RECOMMENDATIONS

This chapter gives a summary of the findings from this study. The suggestions and recommendations regarding monitoring of toxic metals of air particulate matter are presented. Achievement of the objectives set is assessed, and areas that still need attention in this field of research are also discussed.

9.1 CONCLUSION

The study was successful in determining the concentration levels of air particulate matter PM10 using the Tapered element Oscillating Microbalance (TEOM). The hourly concentration levels of PM10 ranged from 13.12 to 215.7 $\mu g.m^{-3}$, the daily levels from 10.3 to 151.7 $\mu g.m^{-3}$ and the monthly levels from 22.2 to 131.0 $\mu g.m^{-3}$.

The physical and chemical composition of the samples collected was determined using Scanning Electron Microscopy coupled with Energy Dispersive Spectrometry (SEM-EDS). The concentrations of the trace metals of concern were in the range of 0.03 – 3.8 $\mu g.m^{-3}$ for Cr, 0.01 – 0.03 $\mu g.m^{-3}$ for Ni, 0.00 – 0.02 $\mu g.m^{-3}$ for V and 0.00 – 0.24 $\mu g.m^{-3}$ for Pb. The study has shown that Scanning Electron Microscopy coupled with Energy Dispersive Spectrometry can be used as a tool to characterise particulate matter. The characterisation of PM10 samples yields information that can help epidemiologists and toxicologists understand the causes of respiratory illnesses. The ability to perform non-destructive analysis of individual particles by SEM/EDS is indispensable in the characterisation of PM10 samples because it allows the same sample to be chemically speciated by other spectroscopic methods. In some cases, the SEM/EDS analysis may not

provide conclusive analysis as in the distinction between sulfate and sulfite or Cr(III) and Cr(VI) in the particles, however, the ambiguity of the chemical composition can be resolved using other analytical techniques such as inductively coupled plasma mass spectroscopy and atomic absorption spectroscopy.

The determination of the elemental composition of the collected samples was also achieved using Inductively Coupled Plasma Mass Spectroscopy (ICP-MS). The monthly concentrations of the potentially toxic trace metals of particulate matter were measured in the range of 0.03 – 5.2 $\mu g.m^{-3}$ for Cr, 0.03 – 2.8 $\mu g.m^{-3}$ for Ni, 0.01 – 0.05 $\mu g.m^{-3}$ for V and 0.02 – 0.5 $\mu g.m^{-3}$ for Pb. ICP-MS was shown to be a relevant characterization tool for particulate aerosols. The technique provides valuable information which, when properly analysed, contributes significantly to studies on seasonal variations and source apportionment, and ultimately to exposure assessment studies. A large number of metals can be identified using ICP-MS.

It is however, suggested that determination of elemental composition of PM using ICP-MS for the purpose of identifying and quantifying major source contributions, be coupled with chemical speciation of ammonium, sulfate, nitrate, organic carbon, and elemental carbon. This is necessary because atmospheric particulate aerosols, in general, consist of sulphates, nitrates, sea-salt, mineral dust, organics and carbonaceous components.

Apportionment of the sources of toxic metals using correlation and regression, and principal component analysis (PCA) was also achieved. Sources of metals of particulate matter within the Rustenburg area were successfully apportioned in order of decreasing abundance as soil dust, mining industry, traffic and biomass burning, unknown sources, other industries, and smelting.

The study has also shown, from correlations between PM and trace metals that the limits of PM set by protection agencies and other authorities do not necessarily help to reduce the levels of trace metals and their health effects.

The sampling system was discussed and important factors to be considered during sampling were highlighted. This study has also shown the importance of meteorology in monitoring the air pollutants.

Chemical speciation was shown to be essential for establishing more specific relationships between particle concentrations and measures of public health. Chemical speciation also facilitates understanding of PM temporal and spatial variations, source/receptor relationships, and the effectiveness of emission reduction strategies.

9.2 RECOMMENDATIONS

The results obtained during this study justify a recommendation that the monitoring system and procedure of air particulate matter in the North West province, and South Africa at large, should not be based only on determining the hourly, daily and annual levels of particulate matter for compliance with air quality standards. The system should also include the determination of the chemical and physical properties of atmospheric pollutants, estimation of the emitting sources for chemical constituents of suspended particulate matter, and evaluation of adverse health effects on the exposed community as well as assessment of the impacts on the environment at large.

The approved sampling and analysis methods for the province should be comprehensive to both the polluter and the air pollution authorities, and specific and relevant to the type of pollutants within the province. A sampling system for the province should not only cater for compliance with mass-based air quality standards, but should also be applicable to sampling for chemical characterization. A sampling system that serves one objective does not necessarily meet the needs of other objectives. It is therefore important that the type of filters used should be suitable for the type of pollutant to be analysed.

The analysis procedures should be clearly defined to justify enforcement of standards. Accredited laboratories should be used for analysis of particulate matter in the province.

The province should set its air quality standards in line with the national standards, but most importantly, specific to the criteria pollutants within the province. The province should have a comprehensive method of source apportionment to be used in order to justify law enforcement. Source apportionment relates elemental, mineral, or chemical components in an aerosol sample to those same components in the sources of the aerosol.

Tackling individual pollutants in isolation could even be counterproductive if it leads to increases in another pollutant component. This was shown from discussions of correlation coefficients for each sampling site. The effect on the pollution mix as a whole must always be considered in designing interventions.

Finally, one important way to ensure that health issues are routinely taken on board in air quality decisions is to require that all stakeholders be subjected to adequate health impact assessments (HIAs). Impact assessment is worthless if it is not used to guide the process of policy-making, thus an analysis of stakeholders and their contribution to air quality issues can help in deciding when and how to make assessments.

.....

"We all have the right to an environment that is not harmful to health and well-being. This means that we also have the right to clean air. .....Now it is time for us to become air quality managers." Honorable Rejoice T Mabudafhasi, Deputy Minister of Environmental Affairs and Tourism Of South Africa (September 2004)

.....

REFERENCES

AL-MOMANI, I.F. 2003. Trace elements in atmospheric precipitation at Northern Jordan measured by ICP-MS: acidity and possible sources., *Atmospheric Environment*, 37: 4507–4515.

ANWARI, M.A., TUNCEL, G. & ATMAN, Q.Y. Journal of Environment and Analytical Chemistry 47, 227-237, 1992.

ARSLAN, H. 2001. Heavy metals in street dust in Bursa, Turkey. *Journal of Trace and Microprobe Techniques,* 19 (3): 439–445.

ASIA PACIFIC CENTRE FOR ENVIRONMENTAL LAW (APCEL), National University o Singapore, http://www.nus.edu.sg Accessed on 8 February 2006.

BARON, A.P. & WILLEKE, K. (Eds). 2001. Aerosol measurement: Principles, Techniques, and Applications. 2nd. Edition, Canada: John Wiley & Sons. 1131p.

BEGUM, B.A., KIM, E., BISWAS, S.K. & HOPKE, P.K. 2004. Investigation of sources of Atmospheric aerosol at urban and semi-urban areas in Bangladesh. *Atmospheric Environment*, 38: 3025–3038.

BERGMAN, W. 2004. Nutritional Disorders of Plants. New York: Gustav Fischer.

BERNABÉ, J.M., CARRETERO, M.I. & GALÁN, E. 2005. Mineralogy and origin of atmospheric particles in the industrial area of Huelva (SW Spain). *Atmospheric Environment*, 39: 6777–6789.

BRADFORD, T. & COOK, M.N. Inductively Coupled Plasma. http://www.cee.vt/edu/ Accessed on 20 December 2004.

BRIMBLECOMBE, P. 1996. Air Composition and Chemistry, 2nd edition, Cambridge: Cambridge University Press.

CAMPBELL, D.S., COPELAND, S. & CAHILL, T.A. 1995. Measurement of aerosol absorption coefficient from Teflon filters using integrating plate and integrating sphere techniques. *Aerosol Science and Technology*, 22: 287 – 292.

CARSLAW, D.C. & BEEVERS, S.D. 2002. Dispersion modeling considerations for transient emissions from elevated point sources. *Atmospheric Environment*, 36: 3021–3029.

CENTER FOR ENVIRONMENTAL RESEARCH INFORMATION SELECTION. 1999. Preparation and Extraction of Filter Material, Compendium Method IO - 3.1. June.

CHABAS, A. & LEFEVRE, R.A. 2000. Chemistry and microscopy of atmospheric particulates at Delos (Cyclades-Greece). *Atmospheric Environment*, 34: 225–238.

CHAN, C.Y., XU, X.D., LI, Y.S., WONG, K.H., DING, G.A., CHAN, L.Y. & CHENG, X.H. 2005. Characteristics of vertical profiles and sources of PM2.5, P M10 and carbonaceous species in Beijing. *Atmospheric Environment*, 39: 5113–5124.

CHARRON, A. & HARRISON, R.M. 2003. Primary particle formation from vehicle emissions during exhaust dilution in the roadside atmosphere. *Atmospheric Environment,* 37: 4109–4119.

CHAULYA, S.K. 2005. Assessment and management of air quality for an opencast coal mining area. *Journal of Environmental Management,* 70: 1–14.

CHEN, L.L., CARMICHAEL, G.R., HONG, M.S., UEDA, H., SHIM, S., SONG, C.H., KIM, Y.P., ARIMOTO, R., PROSPERO, J., SAVOIE, D., MURANO, K., PARK, J.K., LEE, H.G. & KANG, C. 1997. Influences of continental outflow events on the aerosol composition at Cheju Island, South Korea. *Journal of Geophysical Research*, 102 (D23): 28551–28574.

CHONG, N., SIVARAMAKRISHNA, K., WELLS, M. & JONES, K. 2002. Characterization of Inhalable particulate matter in ambient air by Scanning Electron Microscopy and Energy-Dispersive X-ray Analysis. *Electronic Journal of Environmental, Agricultural and Food Chemistry*, 1(3): 145 – 164.

CHOW, J.C. 1995a. Critical review: Measurement methods to determine compliance with ambient air quality standards for suspended particles. *JAWMA*. 45: 320 – 382.

CHOW, J.C., WATSON, J.G., ASHBAUGHB, L.L. & MAGLIANO, K.L. 2003. Similarities and differences in PM10 chemical source profiles for geological dust from the San Joaquin Valley, California. *Atmospheric Environment,* 37: 1317–1340.

CHUNG, A., CHANG, D.P.Y., KLEEMAN, M.J., PERRY, K.D., CAHILL, T.A., DUTCHER, D., MCDOUGALL, E.M. & STROUD, K. 2001. Comparison of real-time instruments used to monitor airborne particulate matter. *Journal of the Air & Waste Management Association*, 51: 109-120, January.

DABBERDT, W.F., FREDERICK, G.L., HARDESTY, R.M., LEE, W.C. & UNDERWOOD, K. 2004. Advances in meteorological instrumentation for air quality and emergency response. *Meteorology and Atmospheric Physics*, 87: 57–88.

DAVIS, J.M. 1998. Methylcyclopentadienyl manganese tricarbonyl: health risk uncertainties and research directions. *Environmental Health Perspectives* 106: 191.

DEPARTMENT OF HEALTH AND AGEING. 2005. Concise International Assessment Documents. Australia. http://www.nicnas.gov.au/international Accessed on 30 September 2005.

DIRECTORATE OF CORPORATE AND ENVIRONMENTAL SERVICES. 2000. Review and Assessment of Air Quality in Charnwood. October.

DOLAZALEK, H., REITER, R. & KRÖLING, P. 1985. Basic comments on the physics, occurrence in the atmosphere, and possible biological effects of air ions. *International Journal Biometeorology*, 29: 207 – 242.

DOCKERY, D.W., POPE, C.A., XU, X., SPENGLER, J.D., WARE, J.H., FAY, M.E., FERRIS, B.G. & SPEIZER, F.E. 1993. *New England Journal of Medicine*, 329: 1753.

EKOSSE, G., VAN DEN HEEVER, D.J., DE JAGER, L. & TOTOLO, O. 2004. Environmental chemistry and mineralogy of particulate air matter around Selebi Phikwe nickel–copper plant, Botswana. *Minerals Engineering*, 17: 349–353.

ENVIRONMENTAL HEALTH CRITERIA. 1988. Geneva: WHO. http://www.inchem.org/documents Accessed on 8 January 2006.

ESBERT, R.M., DÝÁZPACHE, F., ALONSO, F.J., ORDAZ, J. & GROSSI, C.M. 1996. Solid particles of atmospheric pollution found on the Hontoria limestone of Burgos Cathedral (Spain). (*In* Riederer, J. ed. Proceedings of the Eighth International Congress on Deterioration and Conservation of Stone. Berlin, Germany. 393–399. 1996.)

ESTEVE, V., RIUS, J., OCHANDO, L.E. & AMIGO, J.M. 1997. Quantitative X-ray diffraction phase analysis of coarse airborne particulate collected by cascade impactor sampling. *Atmospheric Environment*, 31: 3963–3967.

EUROPEAN ENVIRONMENT AGENCY. 1996. Air Quality in Europe, - A Pilot Report, Topic Report no: 25/1996.

FIALA, J. 2000. Air pollution on the territory of the Czech Republic in Graphical Yearbook, CHMI, 1999.

FUCHS, N.A. & SUTUGIN, A.G. 1971. Highly dispersed aerosols. *In*: Topics in current aerosol research (part 2). *eds.* Hidy GM and Brock JR. New York: Pergamon. 1971.

GADGIL, A. & DHORDE, A. 2005.Temperature trends in twentieth century at Pune, India. *Atmospheric Environment*, 39: 6550–6556.

GATARI, M., WAGNER, A. & BOMAN, J. 2005. Elemental composition of tropospheric aerosols in Hanoi, Vietnam and Nairobi, Kenya. *Science of the Total Environment*, 341: 241– 249.

GILLILAND, F.D., McCONNELL, R., PETERS, J. & GONG, H.J. 1999. A theoretical basis for investigating ambient air pollution and children's respiratory health. *Environmental Health Perspectives*, 107(3): 403–407.

GILMOUR, P.S., BROWN, D.M., LINDSAY, T.G., BESWICK, P.H., MACNEE, W. & DONALDSON, K. 1996. Adverse health effects of PM10 particles: involvement of iron in generation of hydroxyl radical. *Occupational and Environmental Medicine*, 53: 817–822.

GOLDSTEIN, J., NEWBURY, D., JOY, D., LYMAN, C., ECHLIN, P., LIFSHIN, E., SAWYER, L. & MICHAEL, J. 2003. Scanning Electron Microscopy and X-Ray Microanalysis. 3rd Edition. New York: Kluwer Academic Publishers.

GRANGER, S. 2003. State of the environment report of Cape Town 2002, http://www.capetown.gov.za/airqual August 2005.

GULFLINK. 2002. Environmental Exposure Report Particulate Matter. http://www.gulflink.osd.mil/pm/pm_s05.htm Accessed on 4 June 2005.

GÜNES A., ALPASLAN M., & INA LA. 2004. Plant nutrition and fertilizer. Ankara University. Agriculture Publication No. 1539, Ankara, Turkey.

HAEFLIGER, O.P., BUCHELI, T.D. & ZENOBI, R. 2000. Laser Mass Spectrometric Analysis of Organic Atmospheric Aerosols. *Environmental Science & Technology*, 34 (11): 2184-2189.

HAMERI, K. Properties of aerosols
http://www.atm.helsinki.fi/~khameri/aeroprop.pdf Accessed on 16 December 2004.

HEAL, M.R., HIBBS, L.R., AGIUS, R.M. & BEVERLAND, I.J. 2005. Interpretation of variations in fine, coarse and black smoke particulate matter concentrations in a northern European city. *Atmospheric Environment*, 39: 3711–3718.

HECKMANN BUILDING PRODUCTS. 2000. Material Safety Data Sheets (MSDS). Chicago. June. http://www.heckmannbuildingprods.com/msds.htm Accessed on 10 August 2005.

HELD, G., ANNEGARN, H.J., TURNER, C.R., SCHEIFINGER, H. & SNYMAN, G.M. 1996. Atmospheric particulates, aerosols and visibility. *In*: Held G, Gore BJ, Surridge AD, Tosen GR, Turner CR, and Walmsley RD. *eds.* Air pollution and its impacts on the South African Highveld, Environmental Scientific Association, Cleveland. 144p.

HERBST JA., 1984. Control 84: Mineral/Metallurgical processing. New York: American Institute of Mining, Metallurgical, and Petroleum Engineers, Inc.

HIDY, G.M. 1984. Aerosols: An Industrial and Environmental Science. Academic Press, 757.

HIDY, G.M. & BROCK, J.R. 1970. The Dynamics of aerocolloidal systems, Oxford: Oxfordshire Pergamon Press.

HINDS, WC. 1999. Aerosol Technology: Properties, behavior, and measurement of airborne particles. 2nd edition. New York: John Wiley & Sons.

HINDS, W.C., KENNEDY, N.J. & TATYAN, K. 1998. Inhalability of large particles for mouth and nose breathing. Journal of Aerosol Science, 29: S277-S278.

HO, K.F., LEE, S.C., CHOW, J.C. & WATSON, J.G. 2003. Characterization of PM10 And PM2.5 source profiles for fugitive dust in Hong Kong. *Atmospheric Environment*, 37: 1023 – 1032.

HOPPEL, W.A., FITZGERALD, J.W., FRICK, G.M., LARSON, R.E. & MACK, E.J. 1990. Aerosol size distributions and optical properties found in the marine boundary layer over the Atlantic ocean, *Journal of Geophysical Research*, 95: 3659 – 3686.

HUSSEIN, T., HÄMERI, K., AALTO, P.P., PAATERO, P. & KULMALA, M. 2005. Modal structure and spatial-temporal variations of urban and suburban aerosols in Helsinki—Finland. *Atmospheric Environment*, 39: 1655–1668.

IPCC. 2001. The Third Assessment Report of Working Group I of the Intergovernmental Panel on Climate Change: Technical Summary, Lead Authors, Albritton DL (USA), Meira Filho LG (Brazil), Shanghai, 17–20, January.

ITO, K., XUE, N. & THURSTON, G. 2004. Spatial variation of PM2.5 chemical species and source apportioned mass concentrations in New York City. *Atmospheric Environment*, 38: 5269 – 5282.

JIRIES A, 2001. Chemical composition of dew in Amman, Jordan. *Atmospheric Research*, 57: 261–268.

JOHNSON, R.L. 2004. Relative Effects of Air Pollution on Lungs and Heart. *Circulation*, 109: 5-7.

KHLYSTOV A. 2001. Quality Assurance Project Plan for Pittsburgh Air Quality Study (PAQS). Department of Chemical Engineering. Carnegie Mellon University, February.

KOCH, D.L. & COHEN, C. 2000. Turbulent Coagulation of Aerosol Particles. (*In* Proceedings of the Fifth Microgravity Fluid Physics and Transport Phenomena Conference held in the NASA Glenn Research Center, Cleveland, CP-2000-210470, 1365 – 1367. August.)

KUKKONEN, J., POHJOLA, M., SOKHI, R.S., LUHANA, L., KITWIROON, N., FRAGKOU, L., RANTAMAKI, M., BERGE, E., ØDEGAARD, V., SLØRDAL, L.H., DENBY, B. & FINARDI, S. 2005. Analysis and evaluation of selected local-scale PM10 air pollution episodes in four European cities: Helsinki, London, Milan and Oslo. *Atmospheric Environment,* 39: 2759-2773.

KULMALA, M., HÄMERI, K., AALTO, P., MÄKELÄ, J.M., PIRJOLA, L., NILSSON, E.D., BUZORIUS, G., RANNIK, U., DAL MASO, M., SEIDL, W., HOFFMANN, T., JANSSON, R., HANSSON, H.C., VIISANEN, Y., LAAKSONEN, A. & O'DOWD, C.D. 2001a. Overview of the international project on biogenic aerosol formation in the boreal forest (BIOFOR). *Tellus,* 53B: 324 – 343.

KULMALA, M., PIRJOLA, L. & MÄKELÄ J.M. 2000a. Stable sulphate clusters as a source of new atmospheric particles. *Nature*, 404: 66 – 69.

KULMALA, M., RANNIK, Ü., PIRJOLA, L., DAL MASO, M., KARIMÄKI, J., ASMI, A., JÄPPINEN, A., KARHU, V., KORHONEN, H., MALVIKKO, S.P., PUUSTINEN, A., RAITTILA, J., ROMAKKANIEMI, S., SUNI, T., YLI-KOIVISTO, A., PAATERO, J., HARI, P. & VESALA, T. 2000b. Characterization of atmospheric trace gas and aerosol concentration at forest sites in southern and northern Finland using back trajectories. *Boreal Environment Research,* 5: 315 – 336.

KULMALA, M., TOIVONEN, A., MÄKELÄ, J.M. & LAAKSONEN, A. 1998a. Analysis of the growth of nucleation mode particles observed in boreal forest. *Tellus,* 50B: 449 – 462.

KUSKO, B.H., CAHILL, T.A., ELDRED, R.A., MATSUDA, Y. & MIYAKE, H. 1989. Nondestructive analysis of total nonvolatile carbon by Forward Alpha Scattering Technique (FAST). *Aerosol Science and Technology*, 10: 390 – 396.

LAAKSO, L., GRÖNHOLM, T., RANNIK, Ü., KOSMALE, M., FIEDLER, V., VEHKAMÄKI, H. & KULMALA, M. 2003. Ultrafine particle scavenging coefficients calculated from 6 years field measurements. *Atmospheric Environment,* 37: 3605 – 3613.

LEE, E., CHAN, C.K. & PAATERO, P. 1999. Application of positive matrix factorization in source apportionment of particulate pollutants in Hong Kong. *Atmospheric Environment,* 33: 3201–3212.

LEE, SW., HE, I., HERAGE, T., YOUNG, B., RAZBIN, V., KELLY, E. & POMALIS, R. 2002. Fuel sulfur effects on particulate emissions from fuel oil combustion systems under accelerated laboratory conditions, REPORT CETC 02-09(CF). March.

LEHTINEN, K.E.G. & KULMALA, M. 2003. A model for particle formation and growth in the atmosphere with molecular resolution size. *Atmospheric Chemistry and Physics,* 3: 251 – 257.

LENTS, J.M., NIKKILA, R.M. 2003. South African Air Quality Related Findings and Recommendations. Refinery Managers Environmental Forum (RMEF). http://www.rmef.co.za Accessed on 20 April 2006.

LI, W-W., BANG, J.J., CHIANELLI, R.R., YACAMAN, M.J. & ORTIZ, R. 2000. Characterization of Airborne Particulate Matter in the Paso del Norte Air Quality Basin: Morphology and Chemistry. January.

LI, X.Y., GILMOUR, P.S., DONALDSON, K. & MACNEE, W. 1996. Free radical activity and pro-inflammatory effects of particulate air pollution (PM10) in-vivo and in-vitro. *Thorax*, 51: 1216–1222.

LINGARD, J.J.N., TOMLIN, A.S., CLARKE, A.G., HEALEY, K., HAY, A.W.M., WILD, C.P. & ROUTLEDGE, M.N. 2005. A study of trace metal concentration of urban airborne particulate matter and its role in free radical activity as measured by plasmid strand break assay. *Atmospheric Environment*, 39: 2377–2384.

LIPPMANN, M. 2001. Filters and filter holders. (*In* Cohen, B.S. McCammon, C.S. Jr. Cincinnati, O.H. eds. Air Sampling Instruments for Evaluation of Atmospheric Contaminants. American Conference of Government Industrial Hygienists, p. 281-314.)

LOS ALAMOS NATIONAL LABORATORY. 2003. Non-Radioactive Air Constituents in Los Alamos County, RRES-MAQ Worldview. http://www.lanl.gov Accessed on 30 January 2006.

MÄKELÄ, J.M., AALTO, P., JOKINEN, V., POHJA, T., NISSINEN, A., PALMROTH, S., MARKKANEN, T., SEITSONEN, K., LIHAVAINEN, H. & KULMALA, M. 1997. Observation of ultrafine aerosol particle formation and growth in boreal forest. *Geophysical Research Letters,* 24: 1219 – 1222.

MÄKELÄ, J.M., DAL MASO, M., PIRJOLA, L., KERONEN, P., LAAKSO, L., KULMALA, M. & LAAKSONEN, A. 2000. Characteristics of the atmospheric particle formation events observed at a boreal forest site in southern Finland. *Boreal Environment Research, 5*: 299 – 313.

MAR, T.F., NORRIS, G.A., KOENIG, J.Q. & LARSON, T.V. 2000. Associations between Air Pollution and Mortality in Phoenix, 1995-1997. *Environmental Health Perspectives*, 108 (4): April.

MARCONI, A., GATTANI, G., CUSANO, M.C. & FERDINANDI, M. 2003. Two years fine and ultrafine particles measurements in Rome, Italy 2nd AIRNET Annual Conference / NERAM International Colloquium 'Strategies for Clean Air and Health', November 2003.

MASON, E.A. & McDANIEL, E.W. 1988. Transport Properties of Ions in Gases. New York: Wiley. 560.

MERGLER, D., BALDWIN, M., BELANGER, S., LARRIBE, F., BEUTER, A., BOWLER, R., PANISSET, M., EDWARDS, R., DE GEOFFROY, A.,

SASSINE, M.P. & HUDNELL, K. 1999. Manganese neurotoxicity, a continuum of dysfunction: results from a community based study. *Neurotoxicology*, 20: 327.

MERRILL, J.T. & KIM, J. 2004. Meteorological events and transport patterns in ACE-Asia. *Journal of Geophysical Research*, 109: D19S18.

MESZAROS, E. 1981. Atmospheric Chemistry: Fundamental Aspects. Amsterdam: Elsevier Scientific. 90 – 160.

MINISTRY OF WATER, LAND AND AIR PROTECTION. 2002. Environmental Indicator: Air Quality Impacts from Inhalable Particulates and Ozone. British Columbia.

MIRANDA, R.M. & ANDRADE, M.F. 2005. Physicochemical characteristics of atmospheric aerosol during winter in the Saõ Paulo Metropolitan area in Brazil. *Atmospheric Environment*, 39: 6188–6193.

MISHRA, V.K., KIM, K. KANG, C. & CHOI, K.C. 2004a. Wintertime sources and distribution of airborne lead in Korea, *Atmospheric Environment,* 38: 2653–2664.

MISHRA, V.K., KIM, K. HONG, S. & LEE, K. 2004b. Aerosol composition and its sources at the King Sejong Station, Antarctic peninsula. *Atmospheric Environment*, 38: 4069–4084.

MMOLAWA, M.D. 2002. Urban air pollution in Botswana. (*In*: Better air quality in the cities of Africa. 2004. 117 – 122.)

MORAWSKA, L. 2004. Environmental Aerosol Physics, International Laboratory for Air Quality and Health, Queensland University of Technology, Australia. http://www.src.qut.edu.au Accessed on 16 November 2004.

MSAFIRI, J.M. 2004. The contribution of vehicles to air pollution in the city of Dar es Salaam. (*In* Better air quality in the cities of Africa. 86 – 97. 2004.)

MUELLER, P.K., HIDY, G.M., BASKETT, R.L., FUNG, K.K., HENRY, R.C., LAVERY, T.F., NORDI, N.J., LLOYD, A.C., THRASHER, J.W., WARREN, K.K. & WATSON, J.G. 1983. Sulfate Regional Experiment, (SURE): Report of findings, Technical Report no. EA-1901(1). Prepared by electric power institute. Palo Alto. CA, p.352.

MULLER, E. & MANGOLD, S. 2002. Air Quality. (*In* Mangold, S. Kalule-Sabiti, M. & Walmsley, J. Eds. State of the Environment Report of the North West Province.)

MUNISHI, S. 2002. Road traffic air pollution in Dar es Salaam, BSc (Env Eng) thesis. UCLAS. Tanzania. (*In* Better air quality in the cities of Africa, 2004.)

MYERS, R. 1998. Revision of Emission Factors for AP-42 Section 11.9 Western Surface Coal Mining, MRI Project no: 4604-02, September.

NOAA Air Resources Laboratory, http://www.arl.noaa.gov/ready/hysplit4.html Accessed on 8 February 2006.

NRIAGU, J.O. 1989. A global assessment of natural sources of atmospheric trace metals. *Nature*, 338: 47–49.

NRIAGU, J.O. & PACYNA, J.M. 1988. Quantitative assessment of worldwide contamination of air, water and soils by trace metals. *Nature,* 320: 735–738.

NSDL, 2006. The national science discovery, Data discovery of aerosols, http://www.newmediastudio.org/DataDiscovery/Aero_Ed_Center/ Accessed on 6 September 2006.

NTP, 1994. National Toxicology Program Draft Report on the toxicology and carcinogenicity of nickel sulphate in F344/N rats by inhalation, Springfield VA, Publication No. 94-3370.

PACYNA, J. 1995. Sources, particle size distribution and transport. (*In* Kouimtzis T, Samara C eds. The Handbook of Environmental Chemistry. Airborne Particulate Matter, 4 (Part D). Berlin: Springer.)

PACYNA, J.M. 1986. In: Nriagu JO, Davidson CI (Eds.), Toxic Metals in the Atmosphere. New York: Wiley. 635p.

PACYNA, J.M. 1998. Source inventories for atmospheric trace metals. (*In* Harrison, R.M. van Grieken, R.E., eds. Atmospheric Particles. IUPAC Series on Analytical and Physical Chemistry of Environmental Systems, Chichester, UK: Wiley. p. 385–423. 1998.)

PAOLETTI, L., DE BERARDIS, B. & DIOCIAIUTI, M. 2002. Physico-chemical characterisation of the inhalable particulate matter (PM_{10}) in an urban area: an analysis of the seasonal trend. *The Science of the Total Environment,* 292: 265–275.

PETERS, A. & DOCKERY, D.W. 2001. Increased Air Pollution and the Triggering of Myocardial Infarction. *Circulation*, 103: 2810-2815.

PINTO, J.P. & LESTER, D.G. 1998. Approaches to monitoring of air pollutants and evaluation of health impacts produced by biomass burning: Health

Guidelines for Vegetation Fire Events. October http://www.etcentre.org/publication accessed on 10 May 2003.

PIRJOLA, L., KULMALA, M., WILCK, M., BISCHOFF, A., STRATMANN, F. & OTTO, E. 1999. Formation of sulphuric acid aerosol and cloud condensation nuclei: An expression for significant nucleation and model comparison, *Journal of Aerosol Science*, 30: 1079 – 1094.

PIRJOLA, L., PAASONEN, P., PFEIFFER, D., HUSSEIN, T., HÄMERI, K., KOSKENTALO, T., VIRTANEN, A., RÖNKKÖ, R.E., KESKINEN, J., PAKKANEN, T.A. & HILLAMO, R.E. 2006. Dispersion of particles and trace gases nearby a city highway: Mobile laboratory measurements in Finland. *Atmospheric Environment*, 40: 867–879.

PLANET EARTH SCIENCE. What are aerosols? http://www.planearthsci.com/products/aerosols/ California. Accessed on 10 December 2003

POLYAK, L.M. & JOHNSON, H.L. 2005. Health Effects of Particulate Matter, US Army Center for Health Promotion and Preventive Medicine.

PRESTON-WHYTE RA, & TYSON PD, 1988. The atmosphere and weather of Southern Africa, New York: Oxford University Press. 366p.

PROVINCIAL HEALTH OFFICE. 1993. Health Effects Of Wood Smoke. A Report of the Provincial Health Officer of British Columbia (250/952-0876).

QUERALT, I., SANFELIU, T., GOMEZ, E. & ALVAREZ, C. 2001. X-ray diffraction analysis of atmospheric dust using low background supports. *Journal of Aerosol Science*, 32: 453–459.

QUEROL, X., ALASTUEY, A., RUIZ, C.R., ARTINANO, B., HANSSON, H.C., HARRISON, R.M., BURINGH, E., BRINK, H.M., LUTZ, M., BRUCKMANN, P., STRAEHL, P. & SCHNEIDER, J. 2004. Speciation and origin of PM10 and PM2.5 in selected European cities. *Atmospheric Environment,* 38: 6547–6555.

QUEROL, X., ALASTUEY, A., LOPEZ-SOLER, A., MANTILLA, E. & PLANA, F. 1999. Mineralogy of atmospheric particles around a large coal-repower station. *Atmospheric Environment*, 30: 3557–3572.

RAES, F. J & JANSSENS, A. 1985. Ion-induced aerosol formation in a H_2O-H_2SO_4 system: Extension of classical theory and search for experimental evidence. *Journal of Aerosol Science,* 16: 217 – 227.

RAJAKOPAL, K. 2005. Investigation on respirable particulates and trace elements with source identification in air environment of Korba: Executive Summary, New Delhi. http://static.terin.org/reports/rep08 Accessed on 6 August 2005.

REHEIS, M.C., BUDAHN, J.R. & LAMOTHE, P.J. 2002. Geochemical evidence for diversity of dust sources in the southwestern United States. *Geochimica Cosmochimica Acta*, 66, 1569–1587.

RESANE, T.T.V. 2004. Total hexavalent chromium in air samples, MSc Thesis, University of the Witwatersrand.

ROUESSAC, F. & ROUESSAC, A. 2000. Chemical Analysis: Modern Instrumental Methods and Techniques. England: John Wiley & Sons. P. 438.

RUPPRECHT & PATASHNICK 2002. TEOM Series 1400a Ambient Particulate (PM_{10}) monitor (AB Serial numbers), Operating manual, Revision B, R&P part number 42-003347. Albany: Rupprecht and Patashnick Co. March.

SALVADOR, P., ARTIÑANO, B., ALONSO, D.G., QUEROL, X. & ALASTUEY, A. 2004. Identification and characterisation of sources of PM10 in Madrid (Spain) by statistical methods. *Atmospheric Environment*, 38: 435 – 447.

SATEESH, S.K. 2002. Aerosols and Climate. *Resonance*. 48 – 59. April.

SCHLECHT, P.C & O'CONNOR, P.F. 2004. eds. NIOSH manual of analytical methods. 4th edition. Accessed on 12 September 2005. http://www.cdc.gov/niosh/nmam/nmampub.html/

SCHNEIDER, C.G. 2005. Diesel and Health in America: The Lingering Threat; Clean Air Task Force, February.

SEINFELD, J.H. & PANDIS, S.M. 1998. Atmospheric chemistry and Physics: From air pollution to climate change. New York: John Wiley & Sons. P. 1360.

SHARMA, M. & MALOO, S. 2005. Assessment of ambient air PM10 and PM2.5 and characterization of PM10 in the city of Kanpur, India. *Atmospheric Environment*, 39: 6015–6026.

SKOOG, D.A., HOLLER, J.F. & NIEMAN, A.T. 1998. Principles of Instrumental Analysis. 5th Edition. United States of America: Brookes Cole. P. 969.

SMITH, L.I. 2002. A tutorial on Principal Components Analysis, February 26, 2002. http://csnet.otago.ac.nz/cosc453/student_tutorials/ Accessed on 4 September 2006.

SUN, Y., ZHUANG, G., WANG, Y., HAN, L., GUO, J., DAN, M., ZHANG, W., WANG, Z. & HAO, Z. 2004. The air-borne particulate pollution in Beijing: concentration, composition, distribution and sources. *Atmospheric Environment, 38*: 5991–6004.

TAKSER, L., MERGLER, D., HELLIER, G., SAHUQUILLO, J. & HUEL, G. 2003. Manganese, monoamine metabolite levels at birth, and child psychomotor development. *Neurotoxicology*, 24: 667.

TAMMET, H. 1998a. (*In* Raton, B. & Arbor, A. CRC Handbook of Chemistry and Physics 14. 79th Edition. London: CRC Press. 32 – 34.)

TOLOCKA, M.P., SOLOMON, P., MITCHELL, W., GEMMILL, D., WEINER, R.W., HOMOLYA, J., NATARAJAN, S. & VANDERPOOL, R.W. 2001. East vs. West in the US: Chemical characteristics of PM2.5 during the winter of 1999. *Aerosol Science and Technology,* 34. 88 – 96.

UNIVERSITY OF HELSINKI. Atmospheric ions and electricity. http://www.atm.helsinki.fi/aerosol/ions/html October 2004.

UPSTATE MEDICAL UNIVERSITY. Particle analysis by computer controlled Scanning Electron Microscopy and Energy Dispersive X-ray Analysis, http://www.upstate.edu/pathenvi/basics/bas4.html Accessed on 16 December 2003.

USEPA. 1996a. Particulate Matter: An Introduction. United States Environmental Protection Agency (USEPA) Report.

USEPA. 1996b. Particulate Matter Research Program Strategy, US Environment Protection Agency, NHEERL MS-97-019. October.

VAR, F., NARITA, Y., & TANAKA, S. 2000. The concentration, trend and seasonal variation of metal in the atmosphere in 16 Japanese cities shown by the results of national air surveillance network (NASN) from 1974 to 1996. *Atmospheric Environment*, 34: 2755–2770.

VAUGHAN, M.A. & HORLICK, G. 1986. Oxide, Hydroxide, and Doubly Charged Analyte Species in Inductively Coupled Plasma/Mass Spectrometry. Applied Spectroscopy, 40 (4).

VILJOEN, M.J. & REIMOLD, W.U. 1999. An Introduction to South Africa's Geological and Mining Heritage. Randburg: Mintek in association with Geological Society of South Africa. 193p.

VINCENT, J.H. 1989. Aerosol Sampling: Science and Practice. Chichester: Wiley. P. 416.

VINCENT, J.H., MARK, D., MILLER, B.H., ARMBRUSTER, L. & OGDEN, J.L. 1990, Aerosol inhalability at high speeds. *Journal of Aerosol Science.* 21: 577 – 586.

WATSON JG & CHOW JC. 2001. Source characterisation of major emission sources in the Imperial and Mexicali Valleys along the US/Mexico border, *The Science of the total environment,* 276:1 – 3, August.

WHO (World Health Organisation). 2003. Health Aspects of Air Pollution with Particulate Matter, Ozone and Nitrogen Dioxide. Bonn 98.

WISE, E.K. & COMRIE, A.C. 2004. Meteorologically adjusted urban air quality trends in the Southwestern United States, *Atmospheric Environment,* 39: 2969–2980.

WORLD RESOURCES INSTITUTE. 1999. Urban Air: Health Effects of Particulates, Sulfur Dioxide, and Ozone. http://www.wri.org Accessed on 12 April 2004.

YU, F. & TURCO, R.P. 2000. Ultrafine aerosol formation via ion-mediated nucleation. *Geophysical Research Letters,* 27: 883 – 886.

ZHANG, R., ZIFA, W. & ZHU, G. 2004. Study on the chemical composition of atmospheric aerosols in air pollution control period by PIXE method in Beijing, China. (*In* 10^{TH} International Conference on Particle Induced X-ray Emission and its Analytical Applications PIXE 2004 held in Portoroz, Slovenia on 4 – 8 June 2004.)

ZHU, G., WANG, X. & ZHANG, R. 2004. Source identification of atmospheric aerosols collected at the suburb of Beijing by using PIXE. (*In* 10th International Conference on Particle Induced X-ray Emission and its Analytical Applications PIXE 2004 held in Portoroz, Slovenia on 4 – 8 June 2004.)

ZHU, Y., HINDS, W.C., KIM, S. & SIOUTAS, C. 2002. Concentration and size distribution of ultrafine particles near a major highway. *Journal of Air and Waste Management Association*, 52: 174–185.